Core-Collapse Supernovae

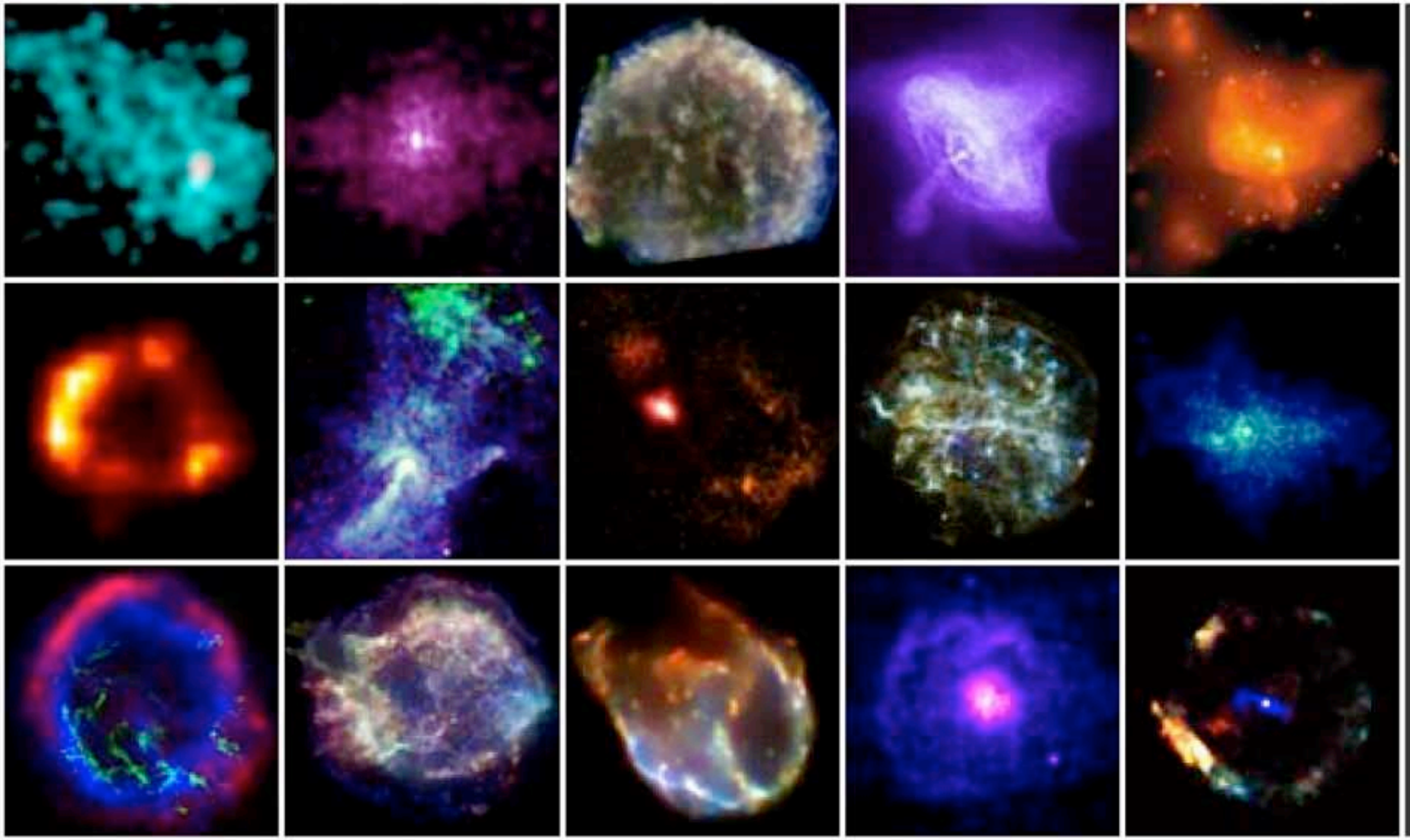

W. Raphael Hix

ORNL Physics Division and UTK Department of Physics & Astronomy

Supernova!

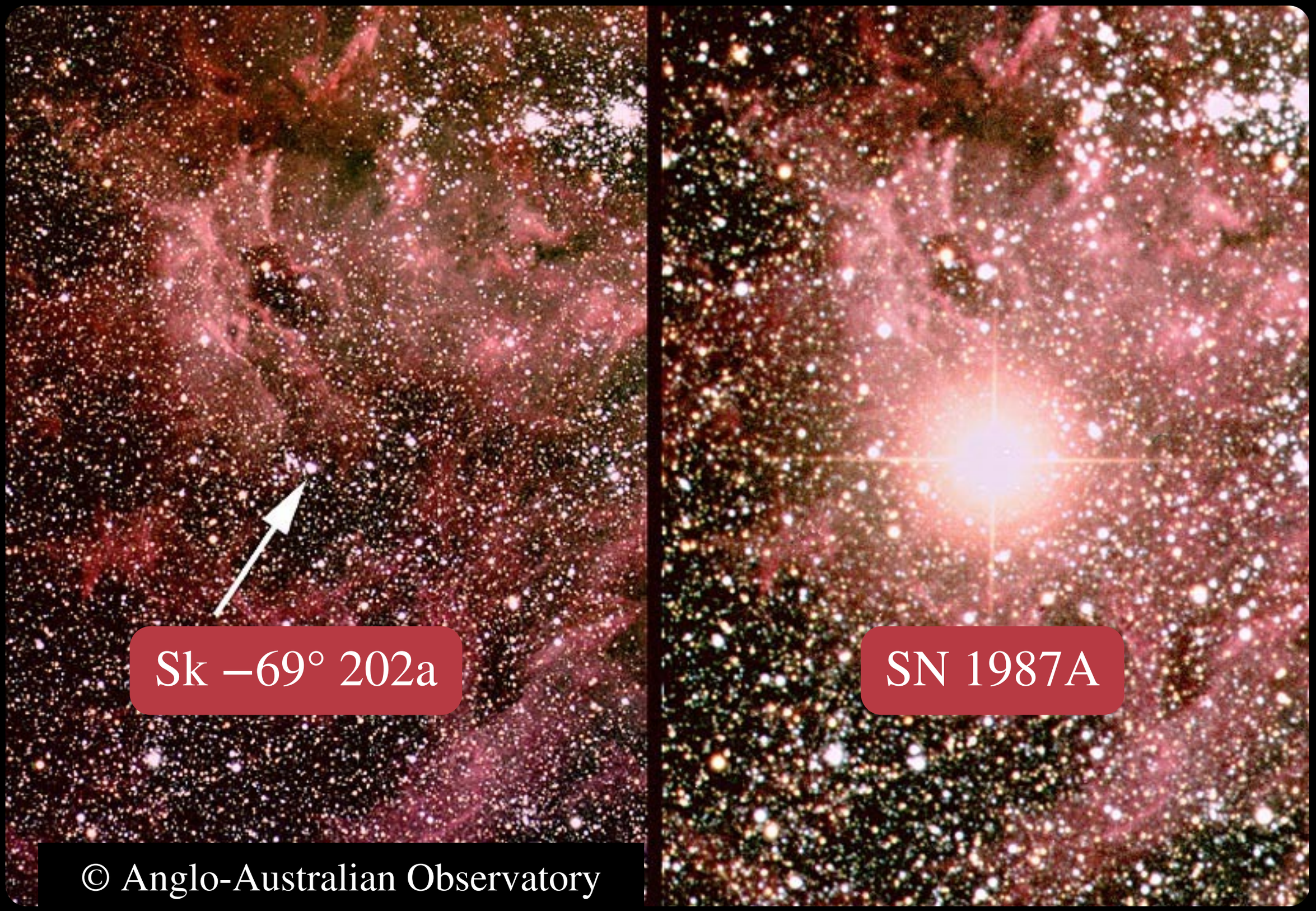

Historical Supernovae

Name	Year
RX J1713.7-3946	393
G327.6+14.6	1006
Crab Nebula	1054
3C 58	1181
Tycho	1572
Kepler	1604
Cassiopeia A	1668
G1.9+0.3A	1870
S Andromedae	1885
Shelton	1987

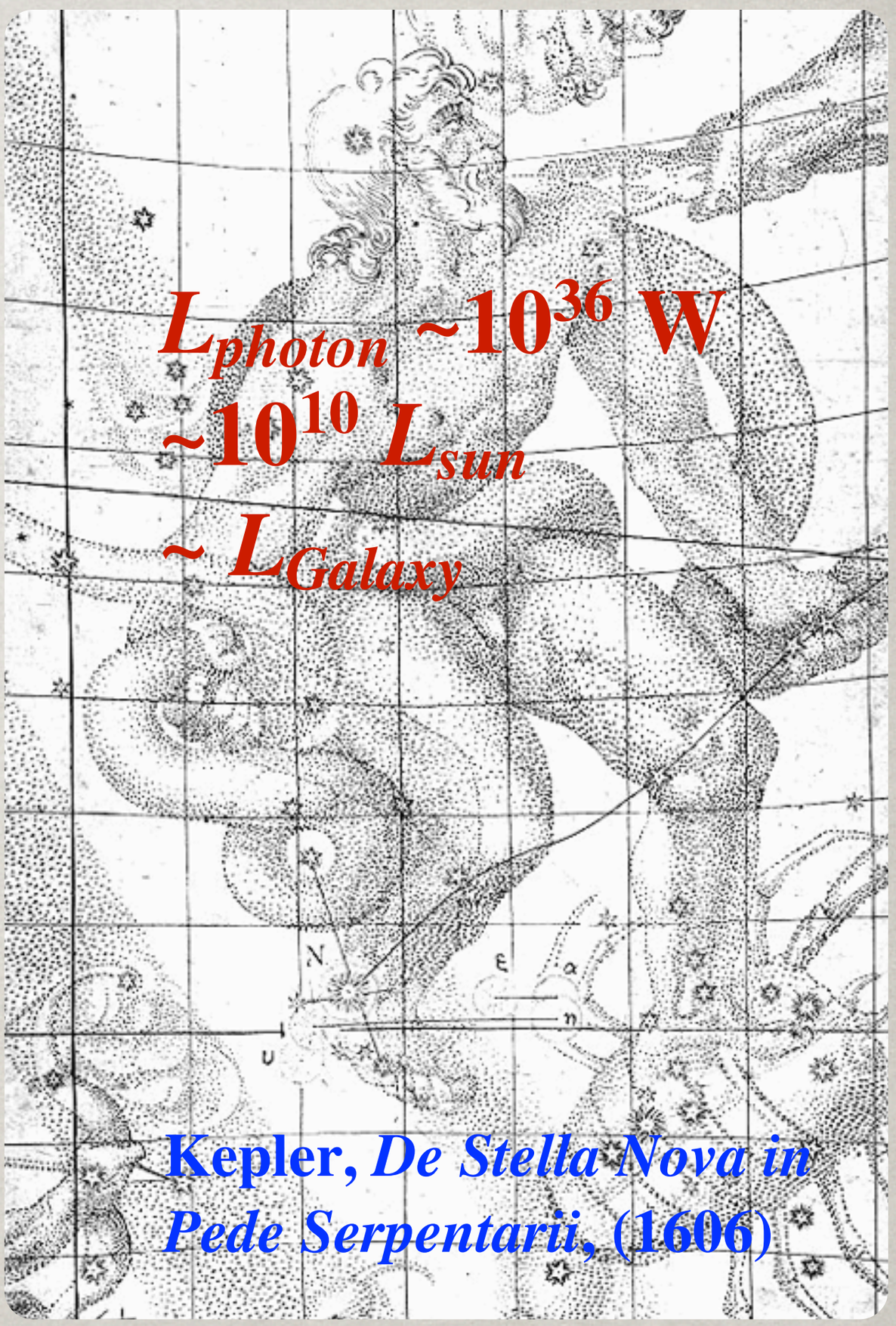

Kepler, *De Stella Nova in Pede Serpentarii*, (1606)

Supernova Taxonomy

Observationally, there are 2 types (7 subtypes) based on their spectra and light curves.

Physically, there are ~~2~~ ~~3~~ 4 mechanisms,

thermonuclear (white dwarf)

core collapse (massive star)

collapsar or magnetar (very massive star),

pair instability (very, very massive star)

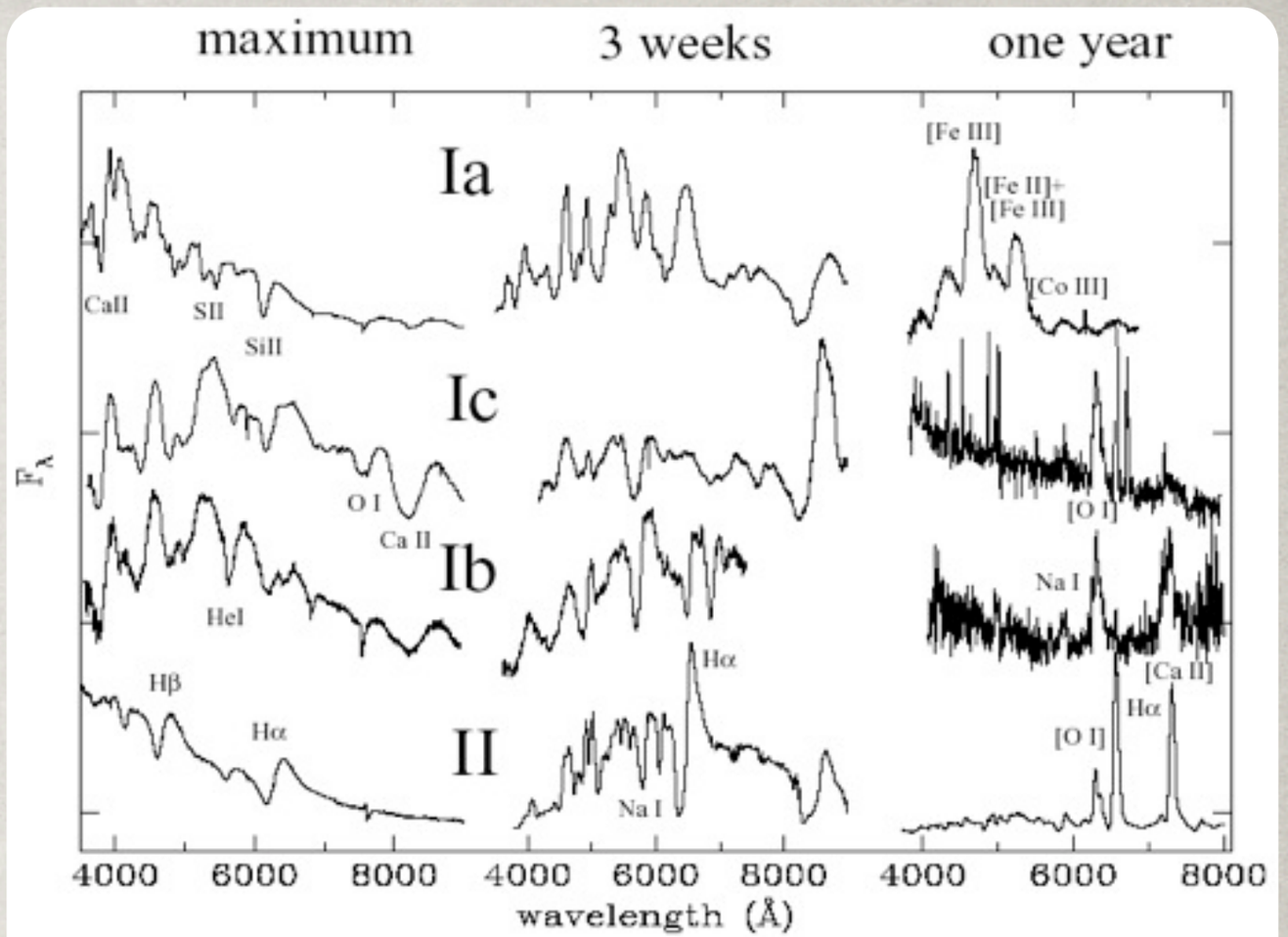

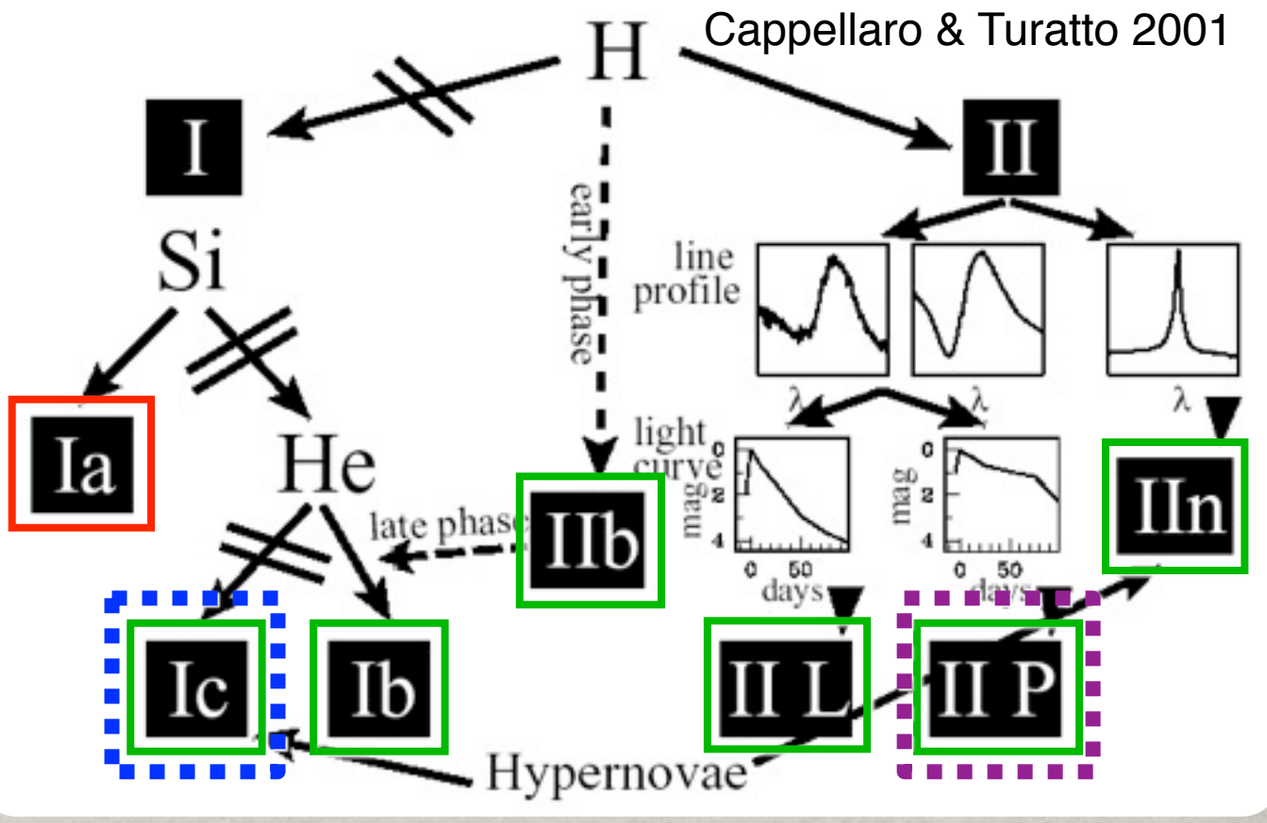

6 from 1, 1 from another

The core collapse mechanism results in supernovae with quite varied spectra and light curves.

Differences are due to variations in the stellar envelope that surrounds the central engine.

In contrast, the Type Ia SN are remarkable similar, suggesting a mechanism with little variation.

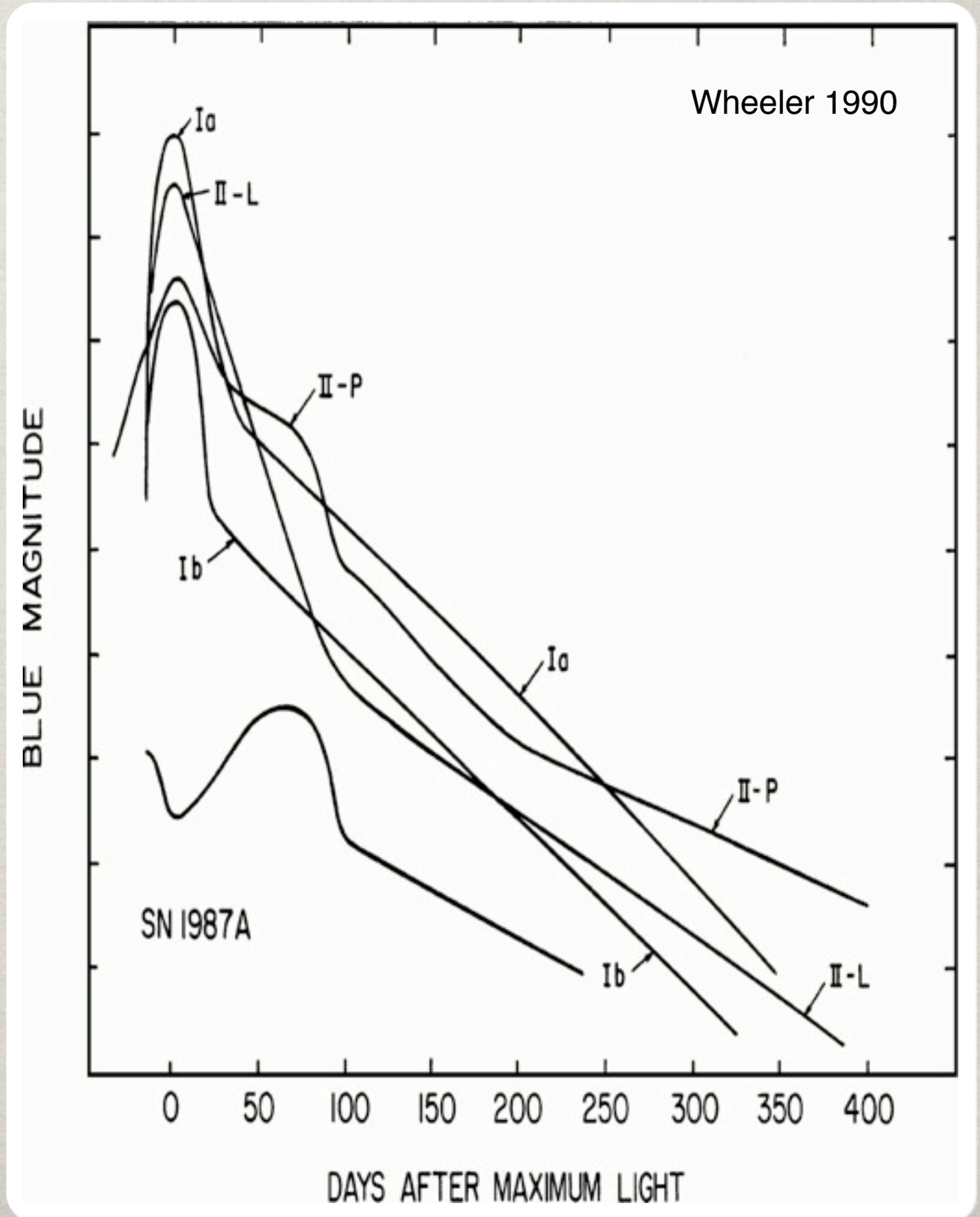

Archived Progenitors

Archives of digital photometry, especially from Hubble Space Telescope, are providing pre-explosion identification of progenitor stars.

These allow determination of mass from theoretical models, which may introduce a systematic error.

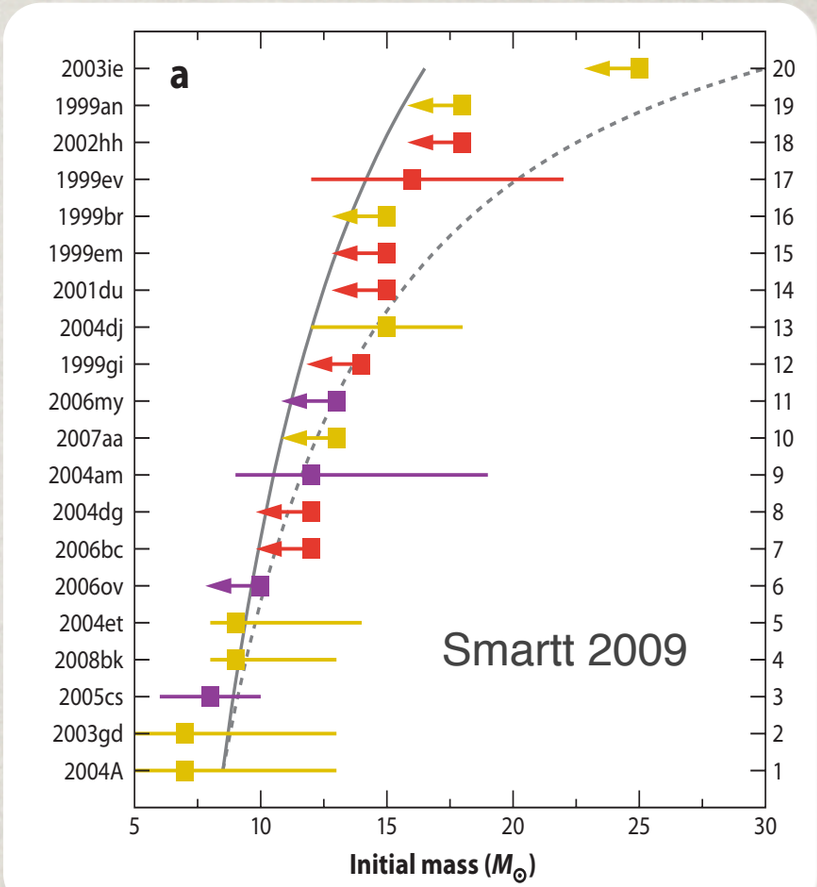

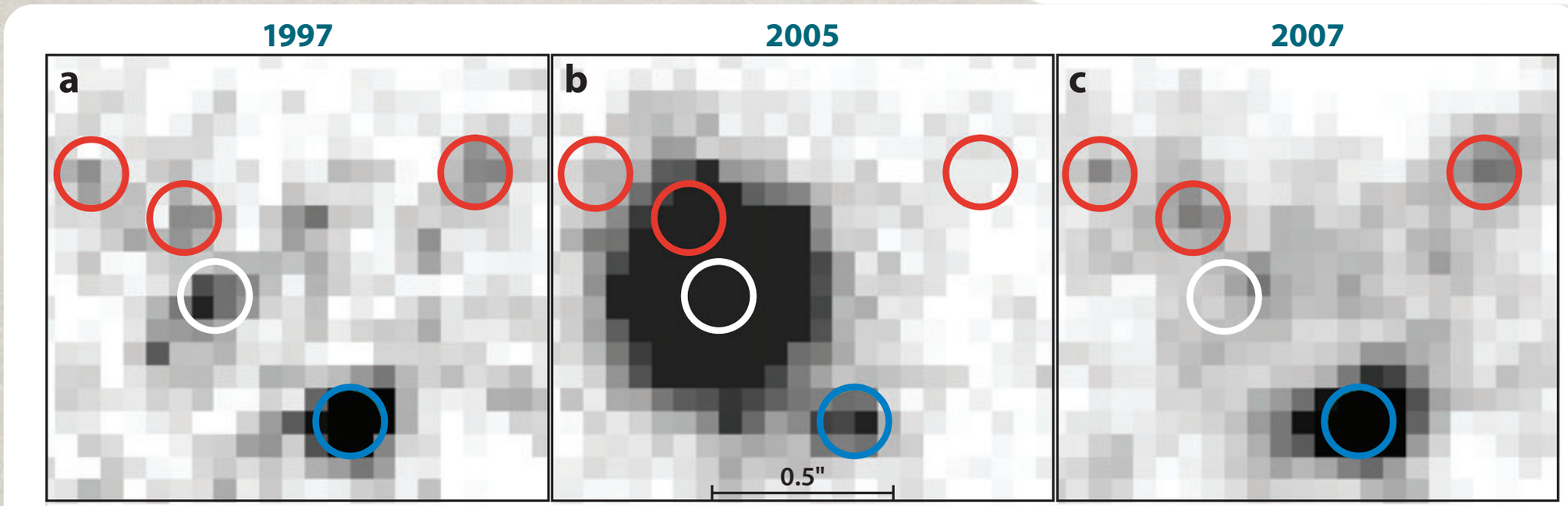

Wind Interactions

Supernovae begin interacting with their environment almost immediately, starting with their own stellar wind.

In the case of SN1987A, the first interaction was a light echo illuminating a hourglass shaped wind.

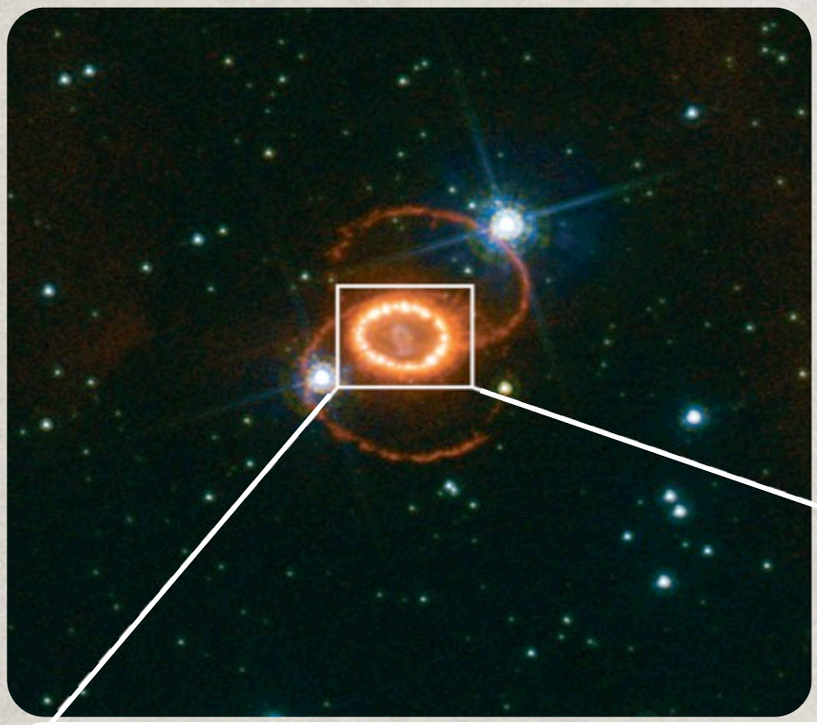

The UV flash of the supernova ionized gas in the waist of the hourglass and along both funnels.

The supernova shock then struck the central ring, which was ejected 20,000 years earlier.

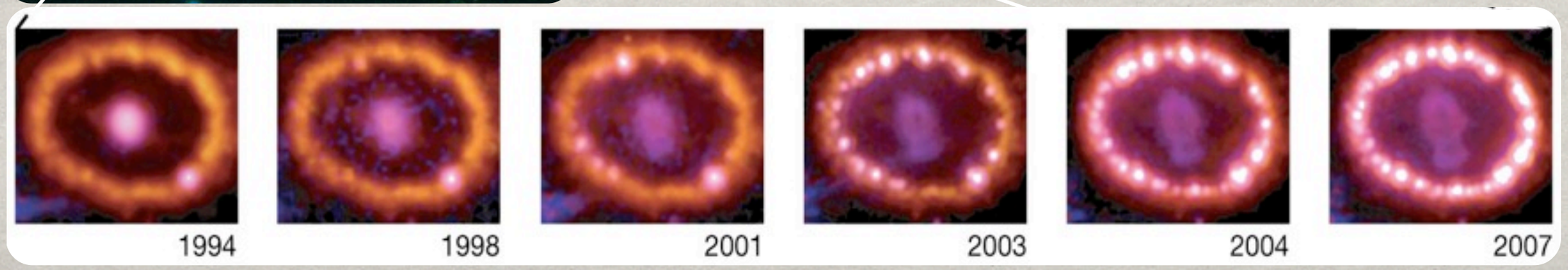

320 Year Old Supernova

Cassiopeia A

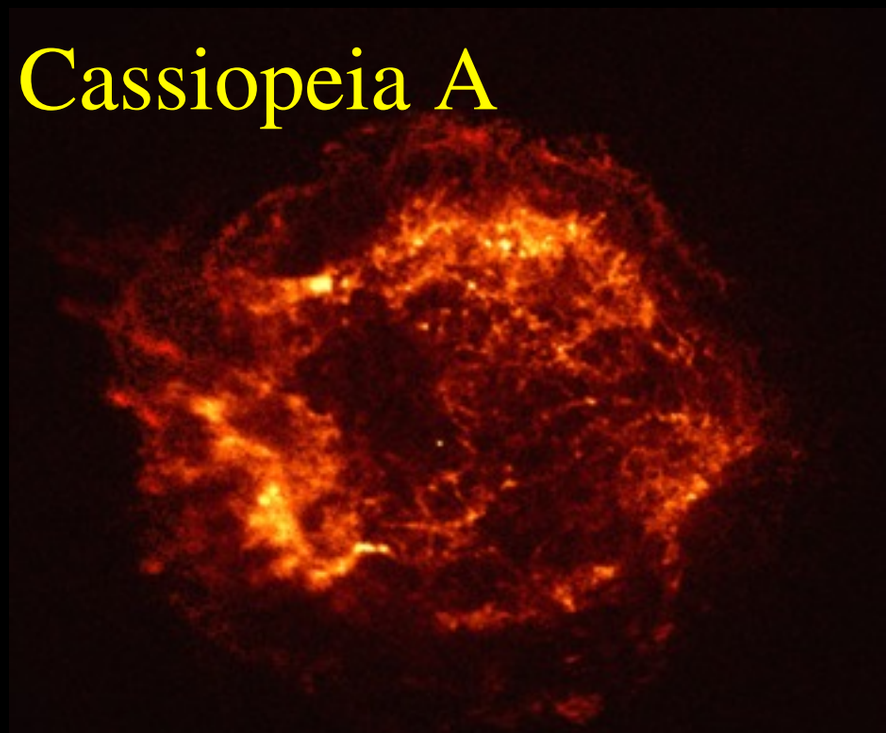

X-ray (NASA/CXC/SAO)

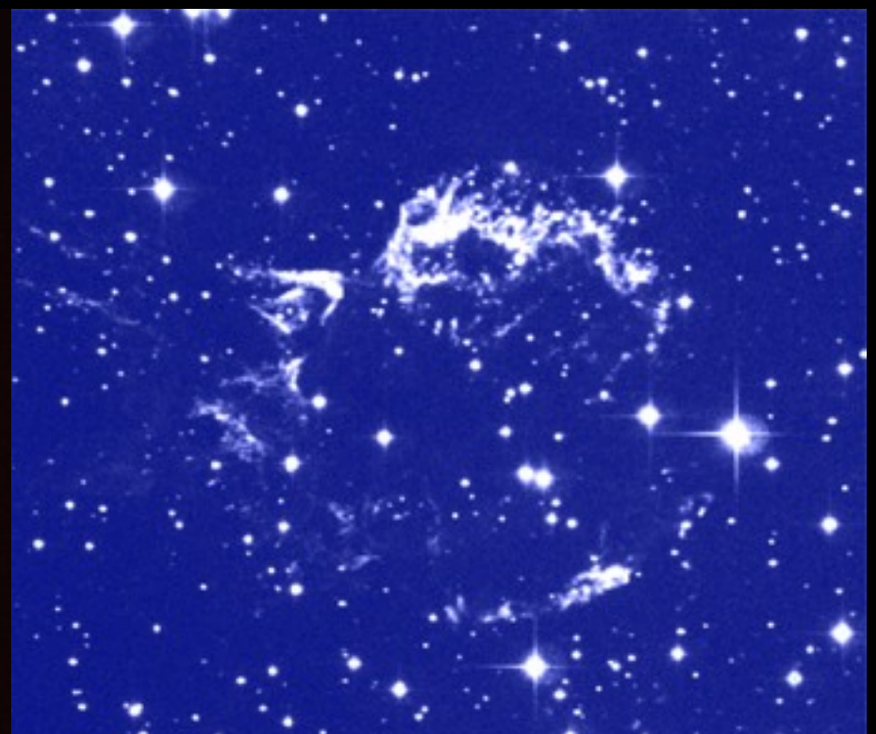

Optical (MDM Obs.)

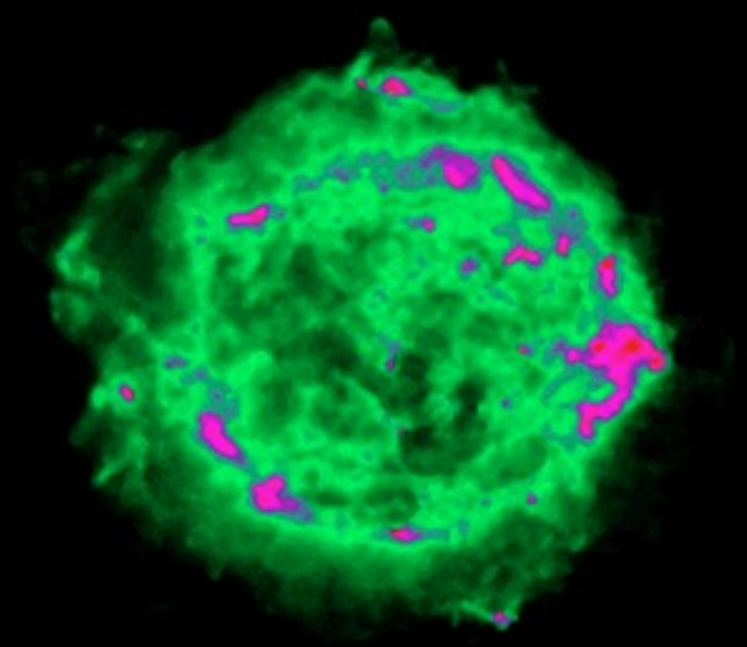

Radio (VLA)

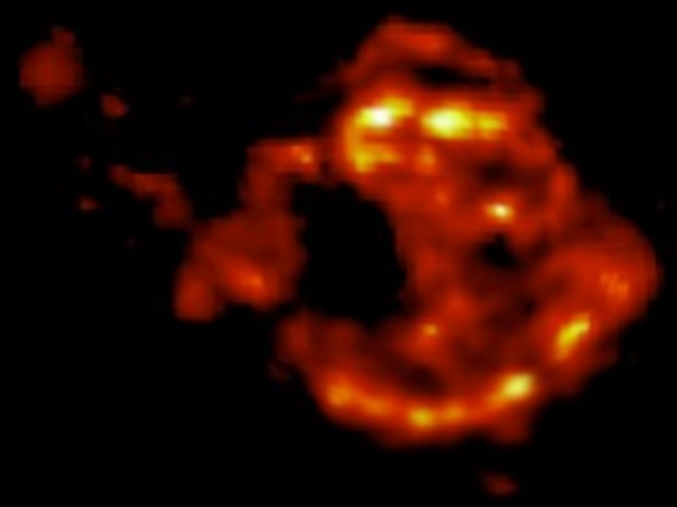

Infrared (ISO)

Supernova deposits 10^{44} J of Kinetic Energy into the ISM, providing a major source of heat to interstellar gas.

Central Source

Even with complex morphology of supernova remnants it is generally possible to reconstruct their origin.

Positive and negative photographs of the Crab Nebula 14 years apart show the the gaseous filaments moving away from the site of the explosion.

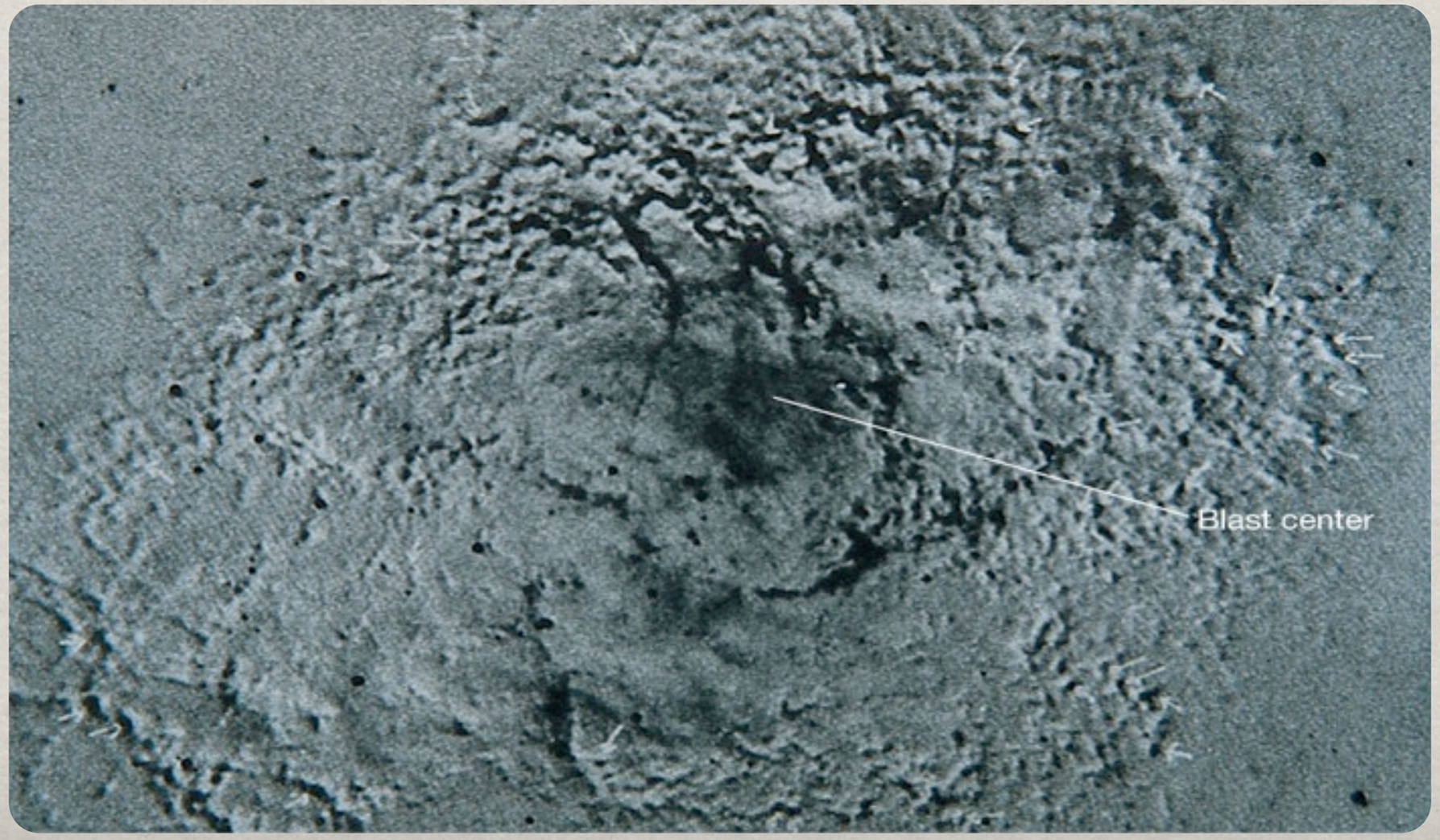

Old Supernovae

Supernova remnants sweep up the interstellar medium as they spread, which gradually slows the ejecta. Thus old remnants lose their spherical shape as they encounter irregularities in the interstellar medium, including other supernova remnants.

Vela SNR is 8° on the sky, the Vela pulsar sits at the center of the Vela SNR.

Gum SNR is 40° on the sky.

Remnant Phases

Supernova remnants go through 3 stages of shock propagation as they age.

1) Free Expansion Phase: Relatively cold ejecta initially free expands into cold ISM.

As it sweeps up and shocks ISM matter, a reverse shock forms, heating the ejecta.

2) Sedov-Taylor Phase: Shock expands adiabatically, driven by pressure.

3) Snowplow Phase: Once the temperature in shocked ISM drops below 10^6 K, a cooling layer develops behind the shock, robbing pressure support. Shock is now driven by momentum.

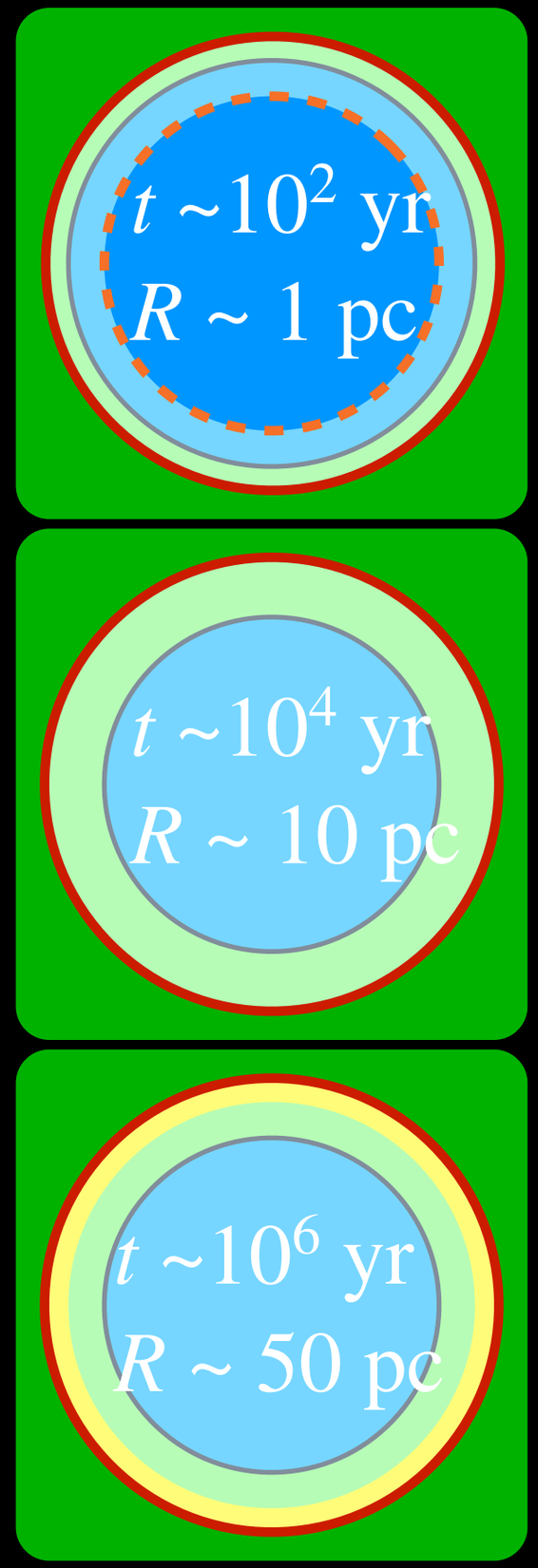

Local Bubble

Our Sun lies near the center of a 100 pc diameter bubble of hot gas. This *local bubble* encompasses most of the nearby stars.

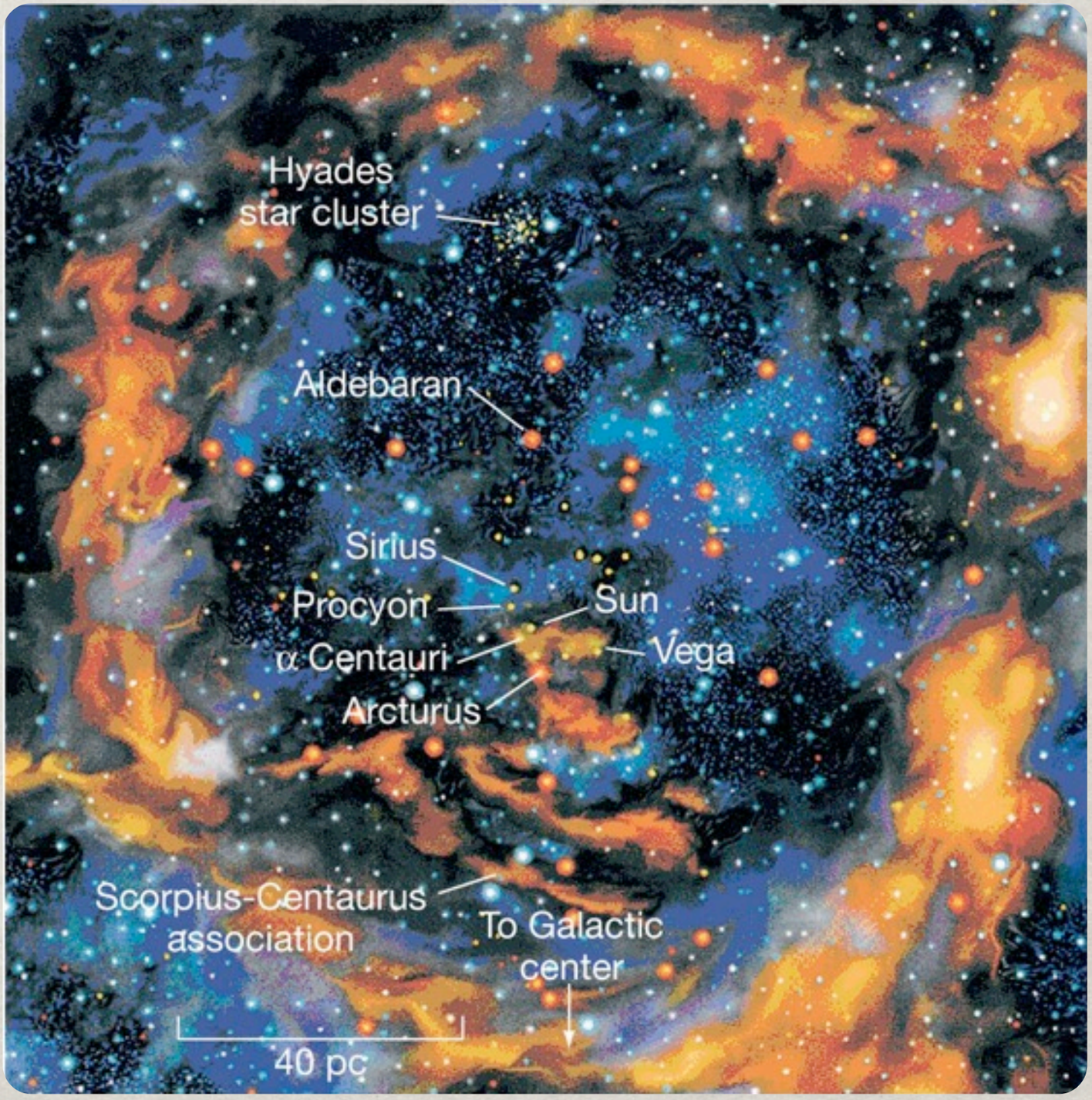

Coronal gas is believed to be heated by successive supernovae.

Such coronal gas ($n < 10^4$ m^{-3}, $T \sim 10^6$ K) is quite common, taking up more than half of the volume of the interstellar medium, but relatively little mass.

PLERION

Many supernova remnants caused by core-collapse supernovae combine the shell caused by the blast wave with a pulsar wind nebulae.

The Crab nebula is an example where the shell remnant is missing leaving only the PW nebula or *plerion*.

Pulsar Winds

The blast wave carries 10^{44} J into the supernova remnant. This is augmented over the course of thousands of years by 10^{43} J of pulsar magnetic dipole radiation and pulsar winds.

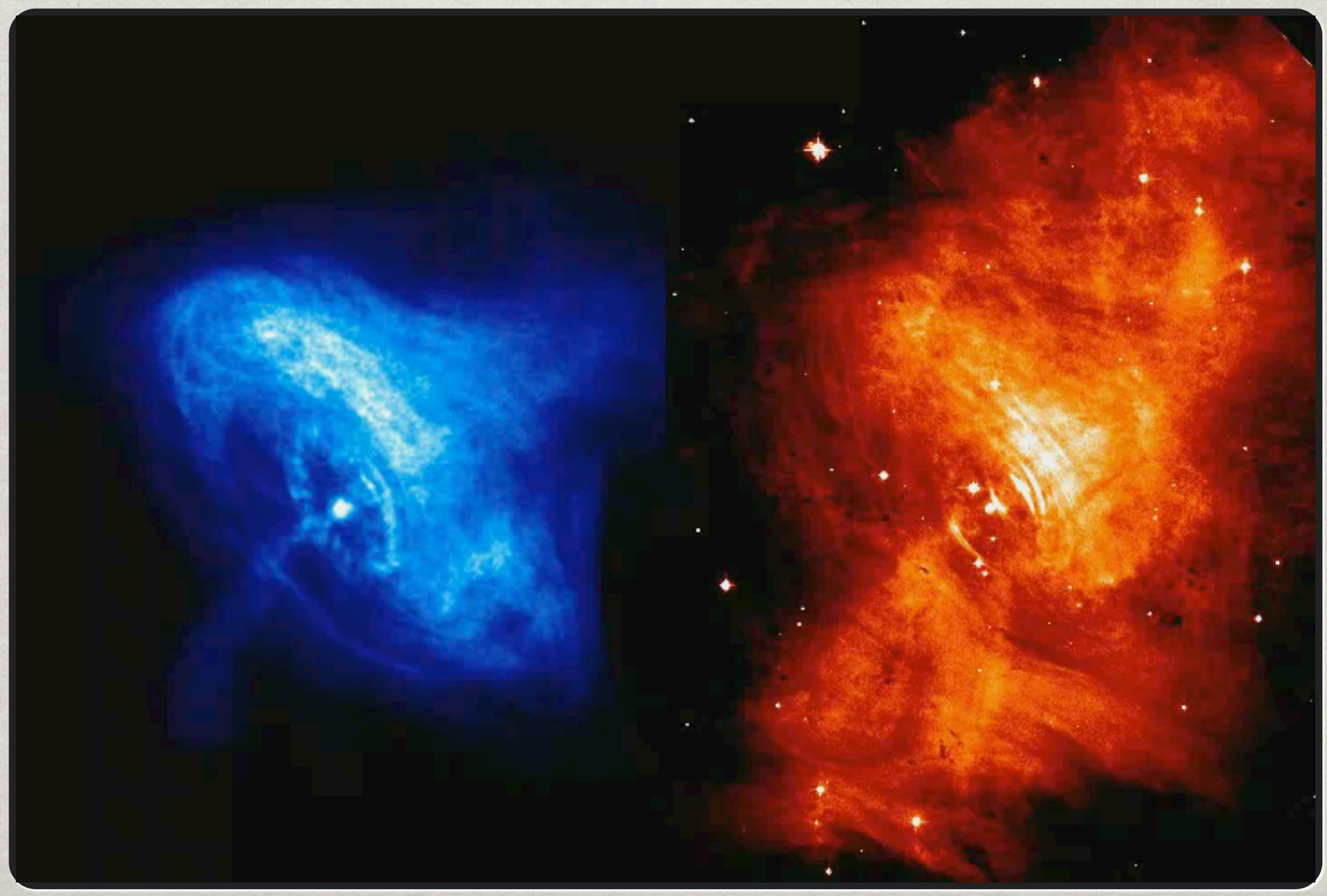

Invisible Supernova

As bright as supernova are, you might think they can be seen whenever they occur nearby, but this is untrue.

As young stars, O & B stars occur predominantly in the Galactic Disk. In the disk, the UV and optical light that carries much of their light is heavily extinguished by interstellar dust, making some supernova invisible.

The young supernova remnant G1.9+0.3A lies in the direction of the Galactic Center, in the Sagittarius. From X-ray and radio observations, we know its angular expansion rate and size, we can calculate an age of 140 years, but no SN was seen.

Rich in Heavy Elements

Hughes, Rakowski, Burrows & Slane 2000

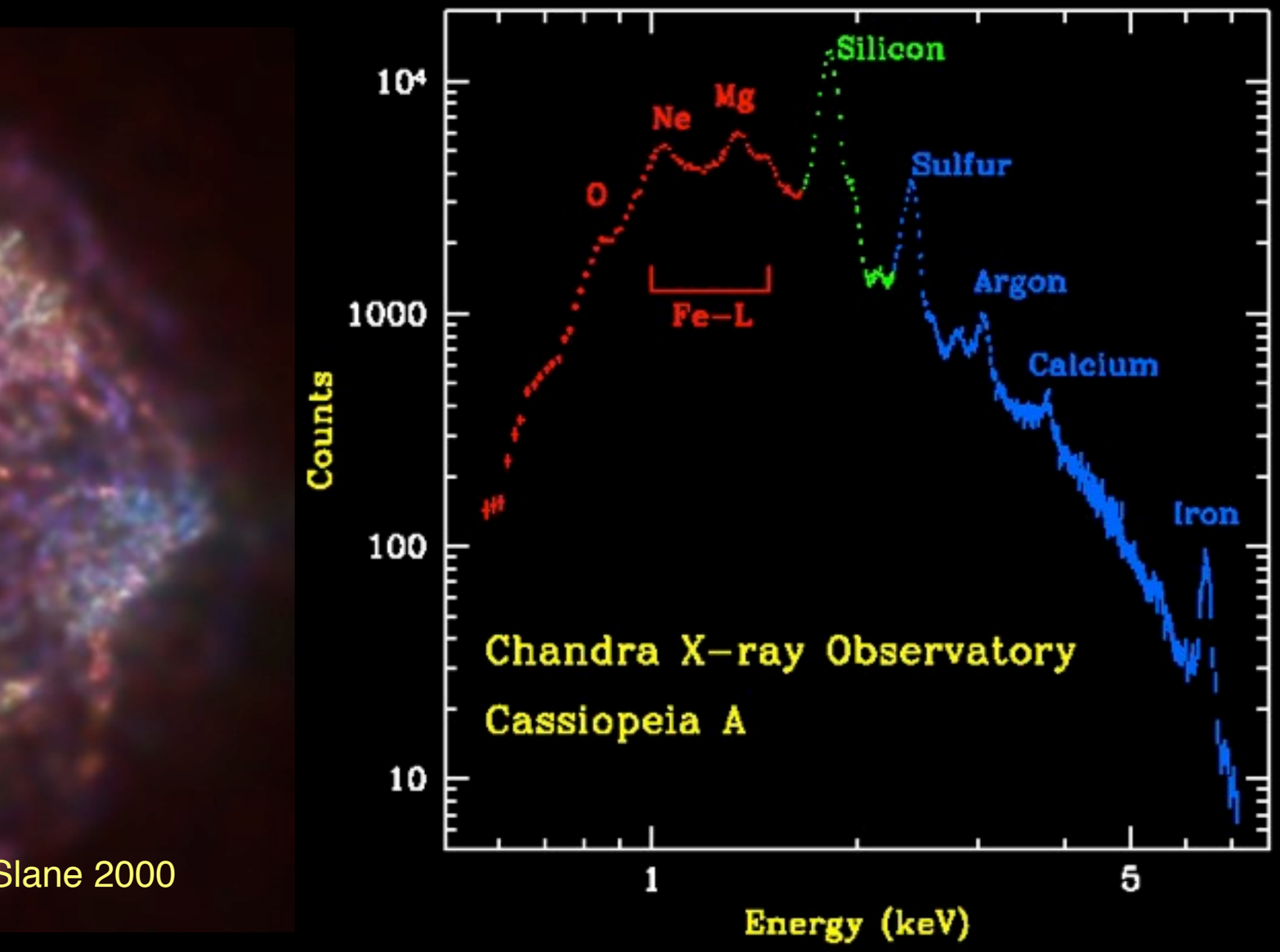

Supernovae from Massive Stars produce most of the elements from Oxygen through Silicon and Calcium and half of the Iron/Cobalt/Nickel.

They may also be responsible for the r-process.

Photons of all sorts!

Chandra (NASA)

X-rays

Integral (ESA)

γ-rays

HST (NASA)

visible

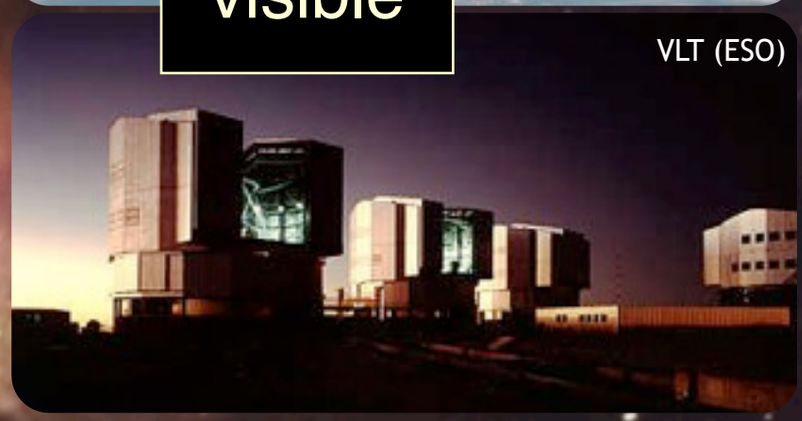

VLT (ESO)

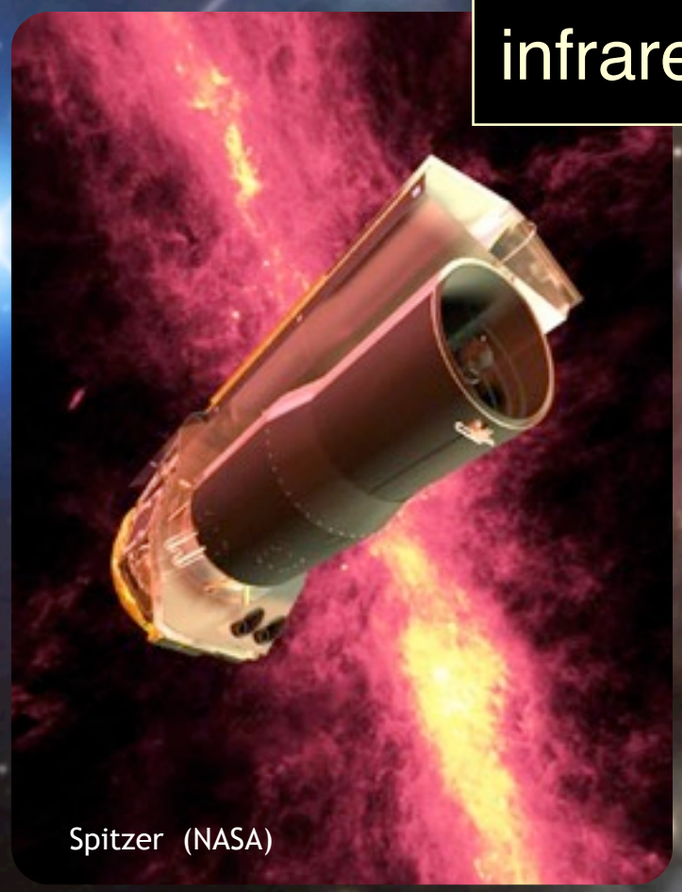

infrared

Spitzer (NASA)

Planck (ESA)

radio

VLA (NRAO)

Golden Age of Observation

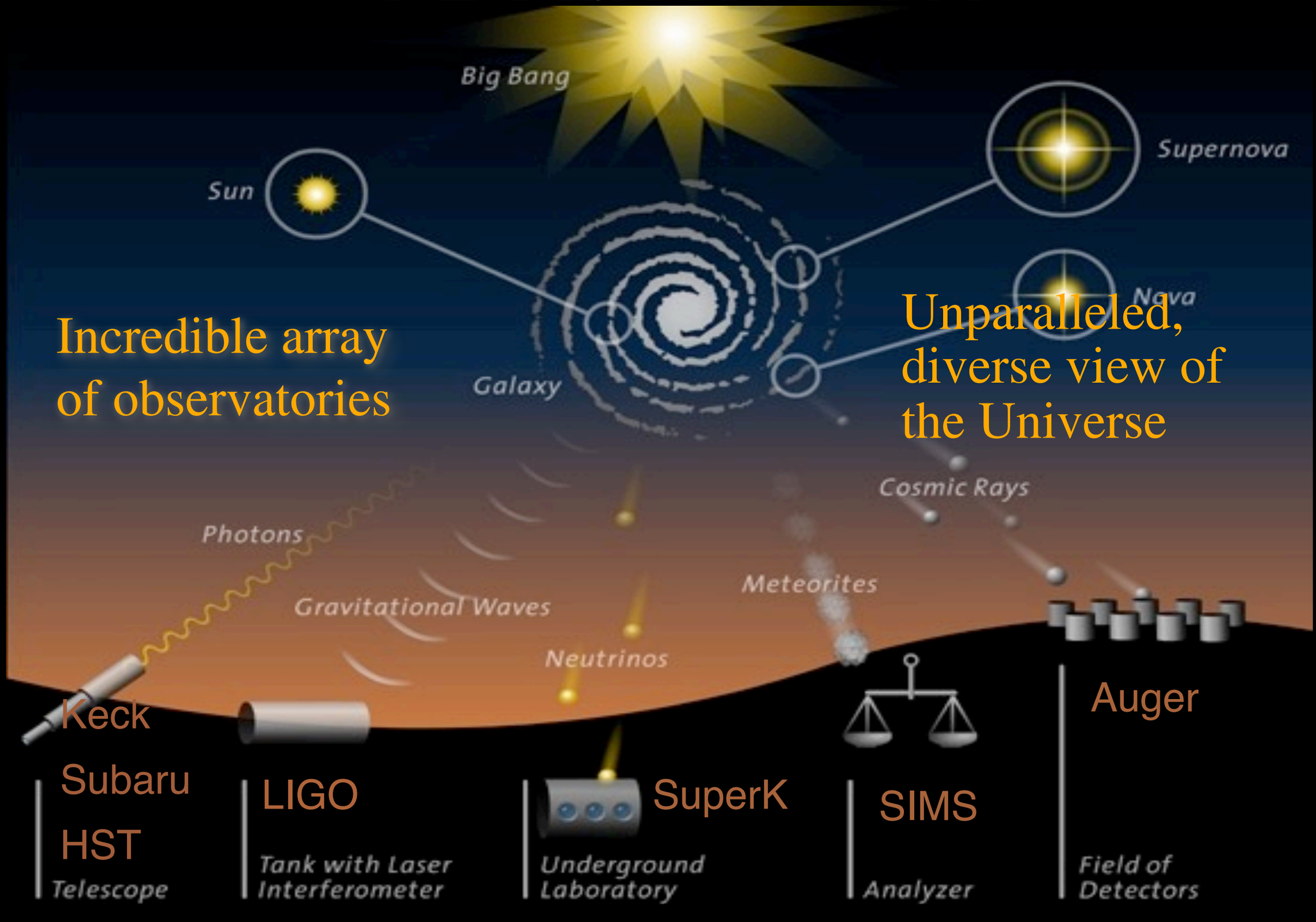

Incredible array of observatories

Unparalleled, diverse view of the Universe

Observing Neutrinos

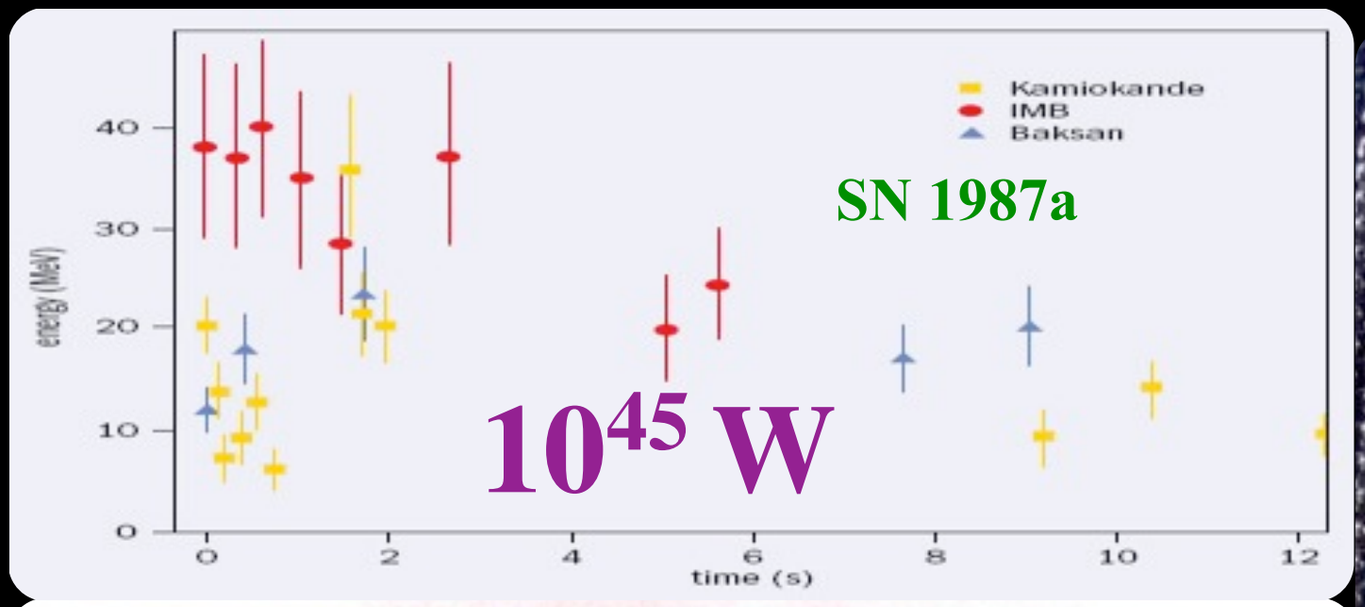

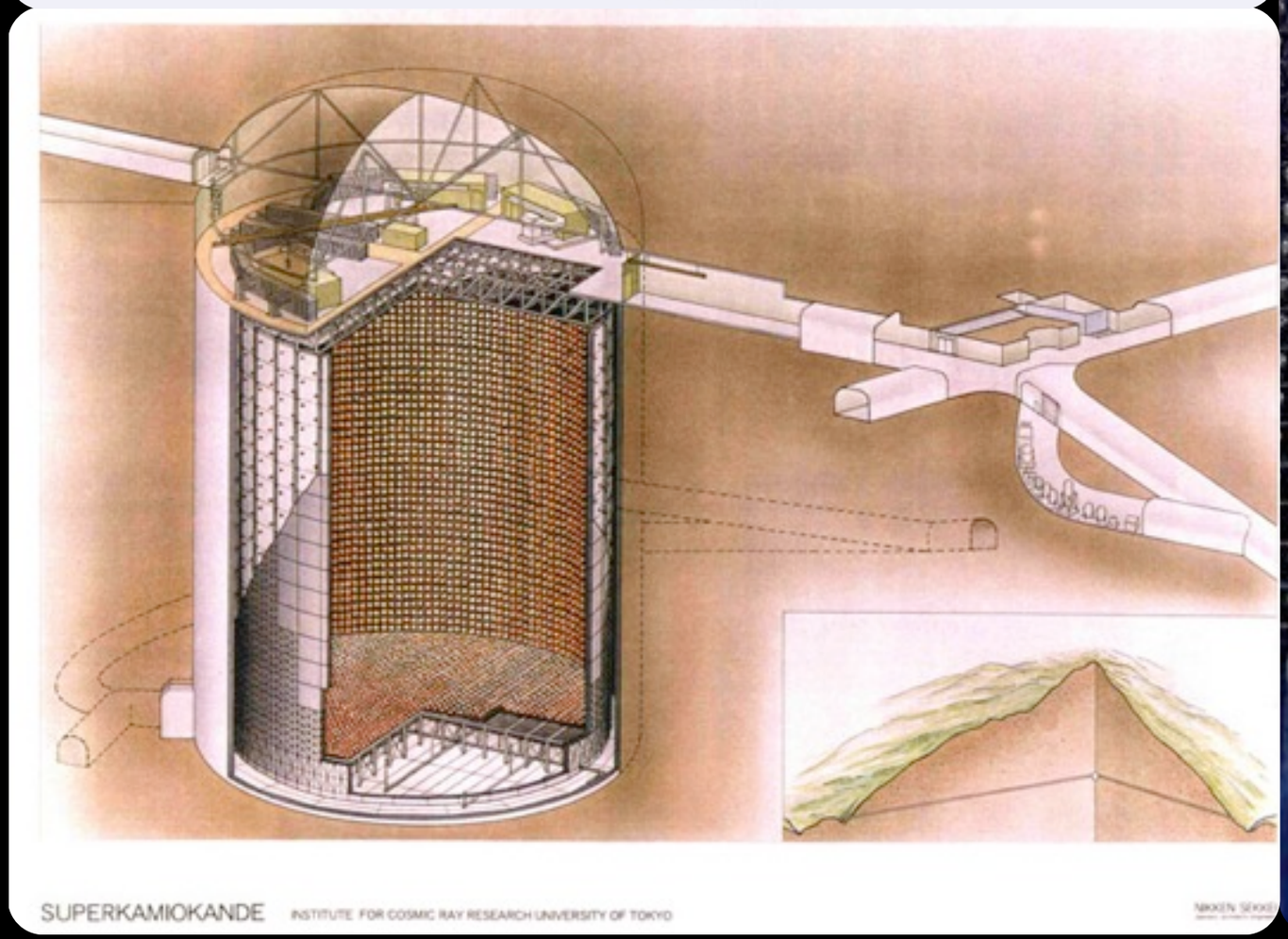

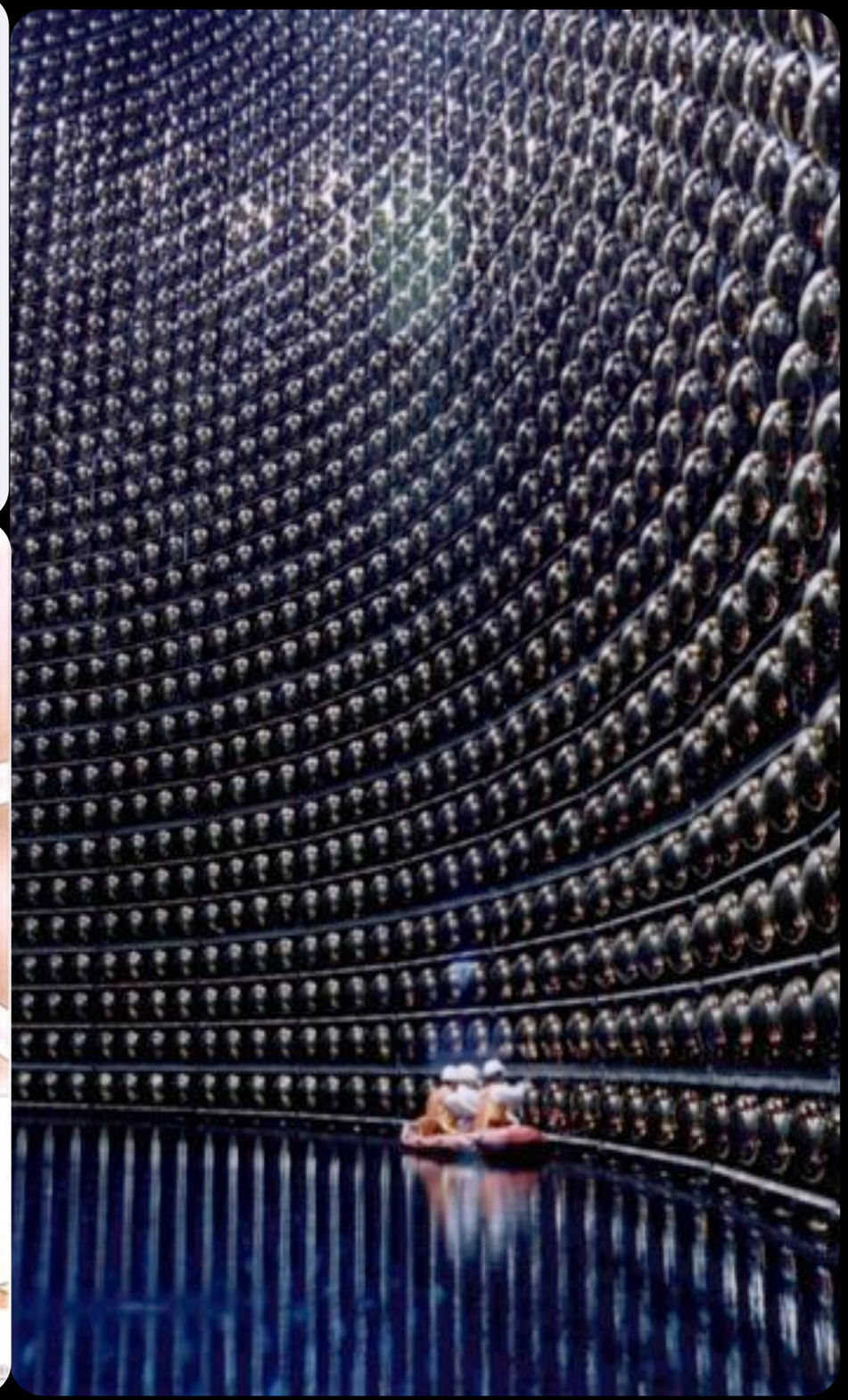

Observing Gravity

The Laser Interferometer Gravitational-Wave Observatory (LIGO) has detectors in Livingston LA and Hanford WA.

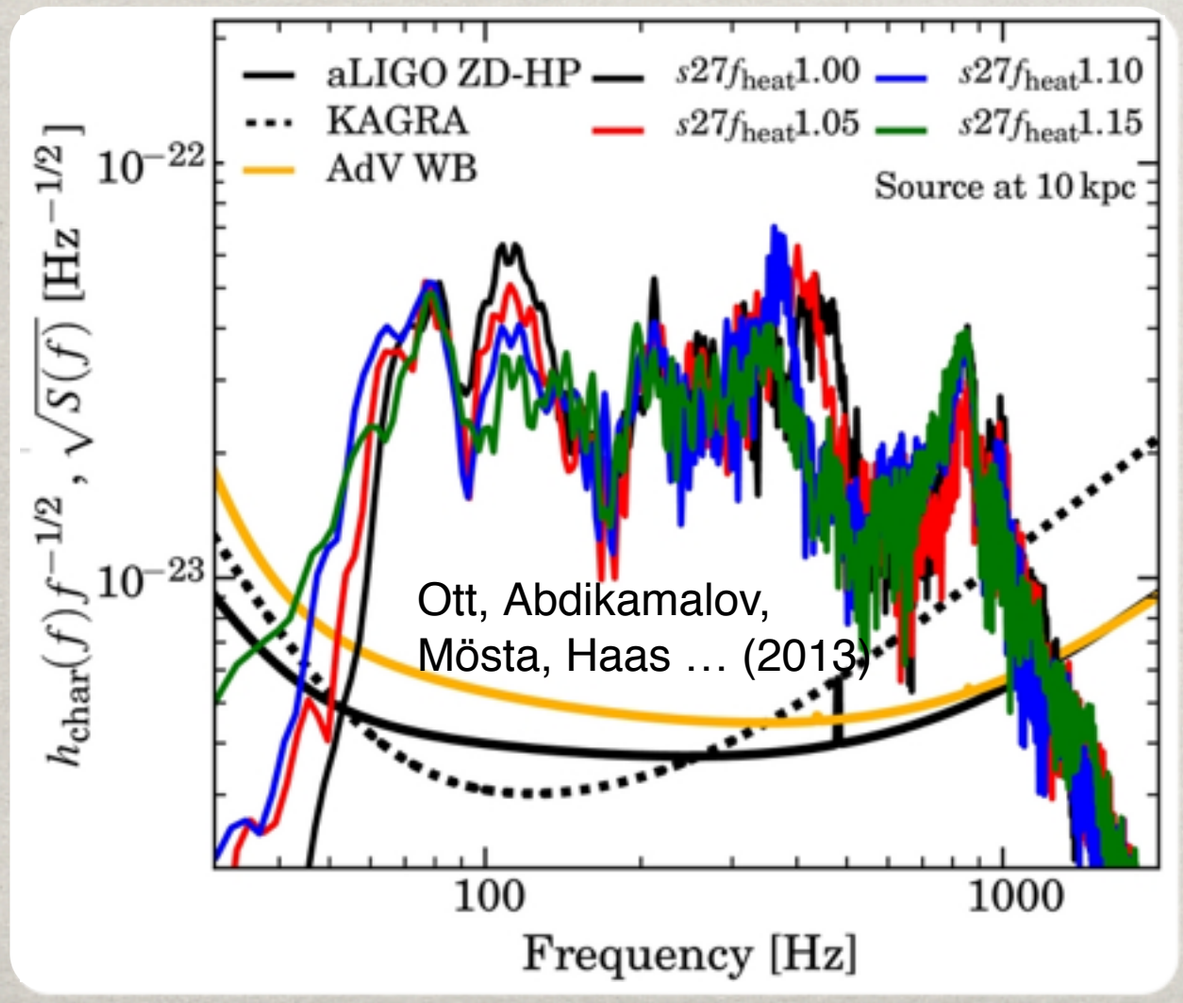

In the event of a galactic CCSN, they hope to detect gravitational waves from the motions of matter deep within the supernova.

Stellar Stages

When H is exhausted in core, hydrogen burning ignites in shell around the core.

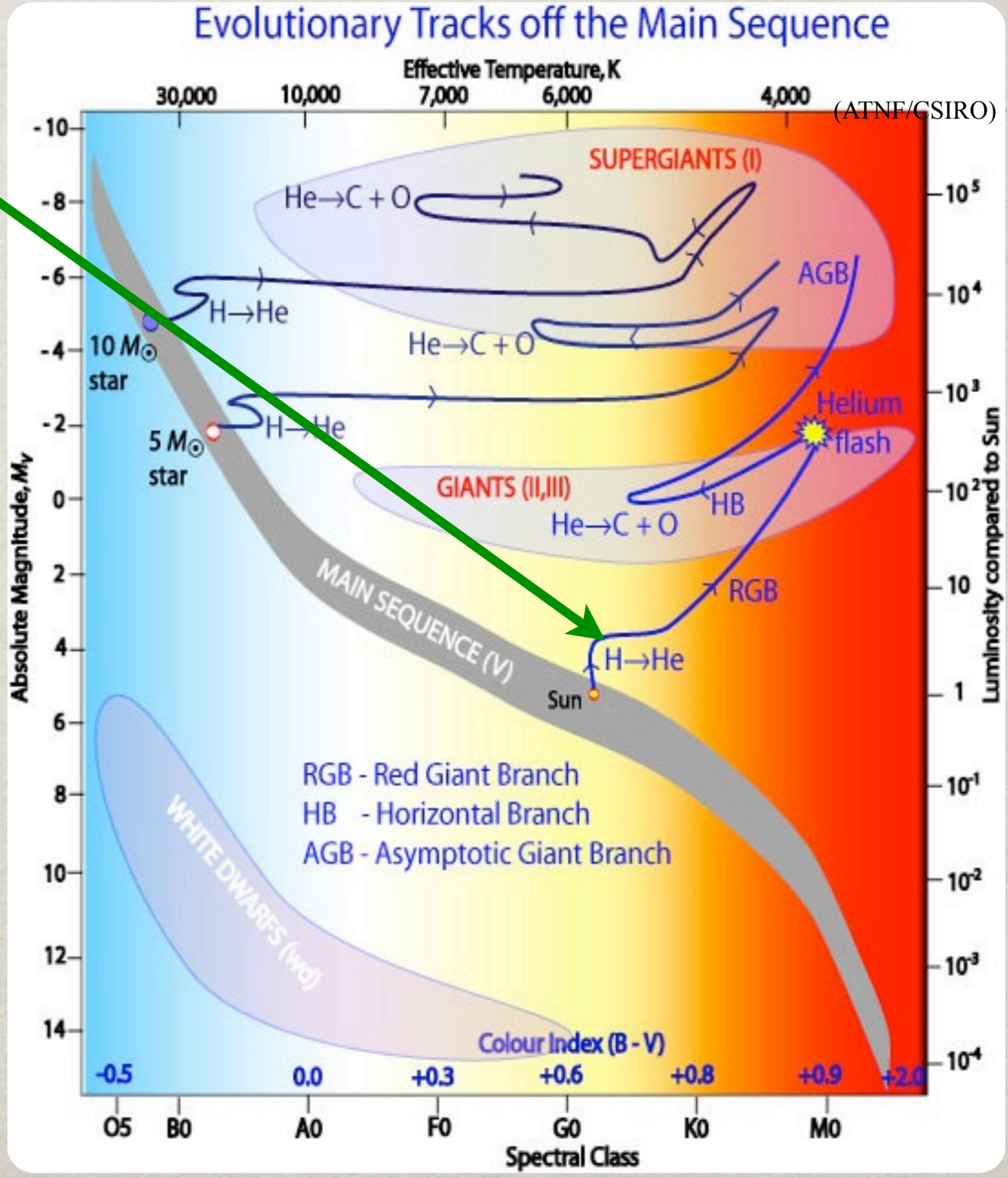

Stellar Stages

When H is exhausted in core, hydrogen burning ignites in shell around the core.

Once hot enough, He burning begins in the core, until He is exhausted.

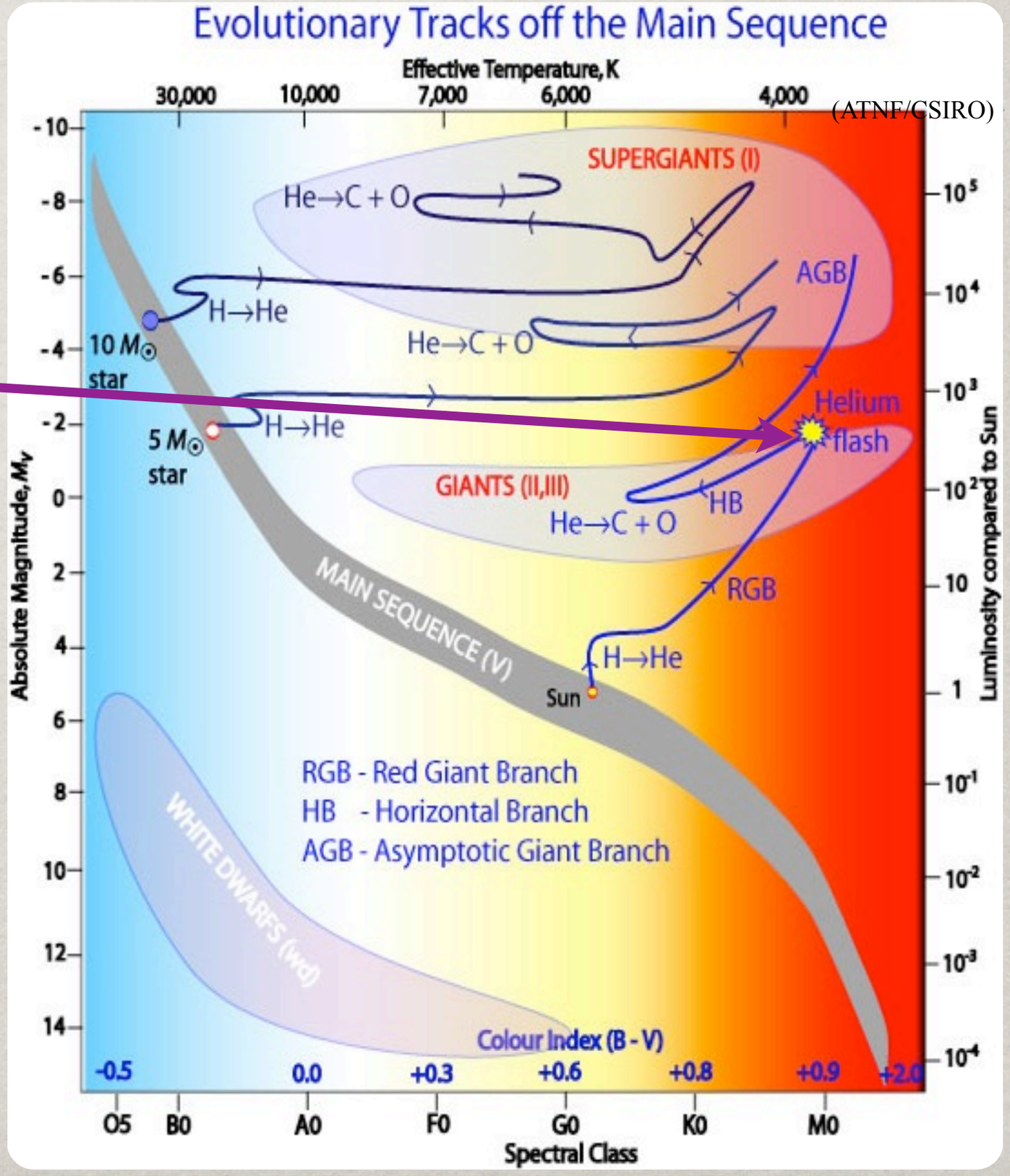

Stellar Stages

When H is exhausted in core, hydrogen burning ignites in shell around the core.

Once hot enough, He burning begins in the core, until He is exhausted.

Another round of contraction leads to H and He burning shells around a C+O core producing a Asymotic Giant Branch (AGB) Star for solar-like stars or a Supergiant for massive stars.

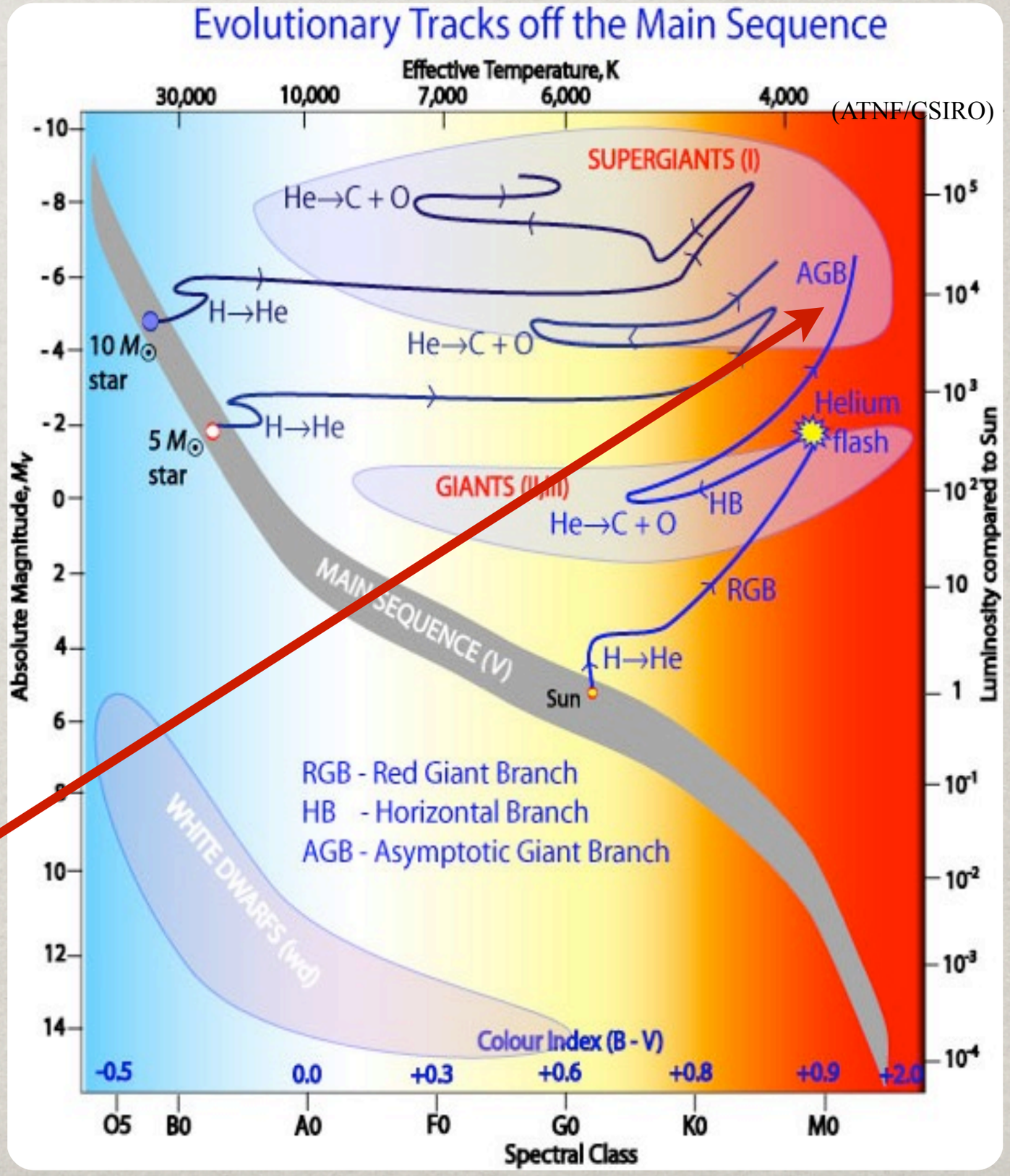

Russell-Vogt Theorem

The final fate of a single star depends on many facets, the most important is its mass at birth.

Mass loss is also important. Very Massive stars can lose much of their envelope, leaving the He or C/O core visible.

Metallicity, the abundance of non-H and He is also important.

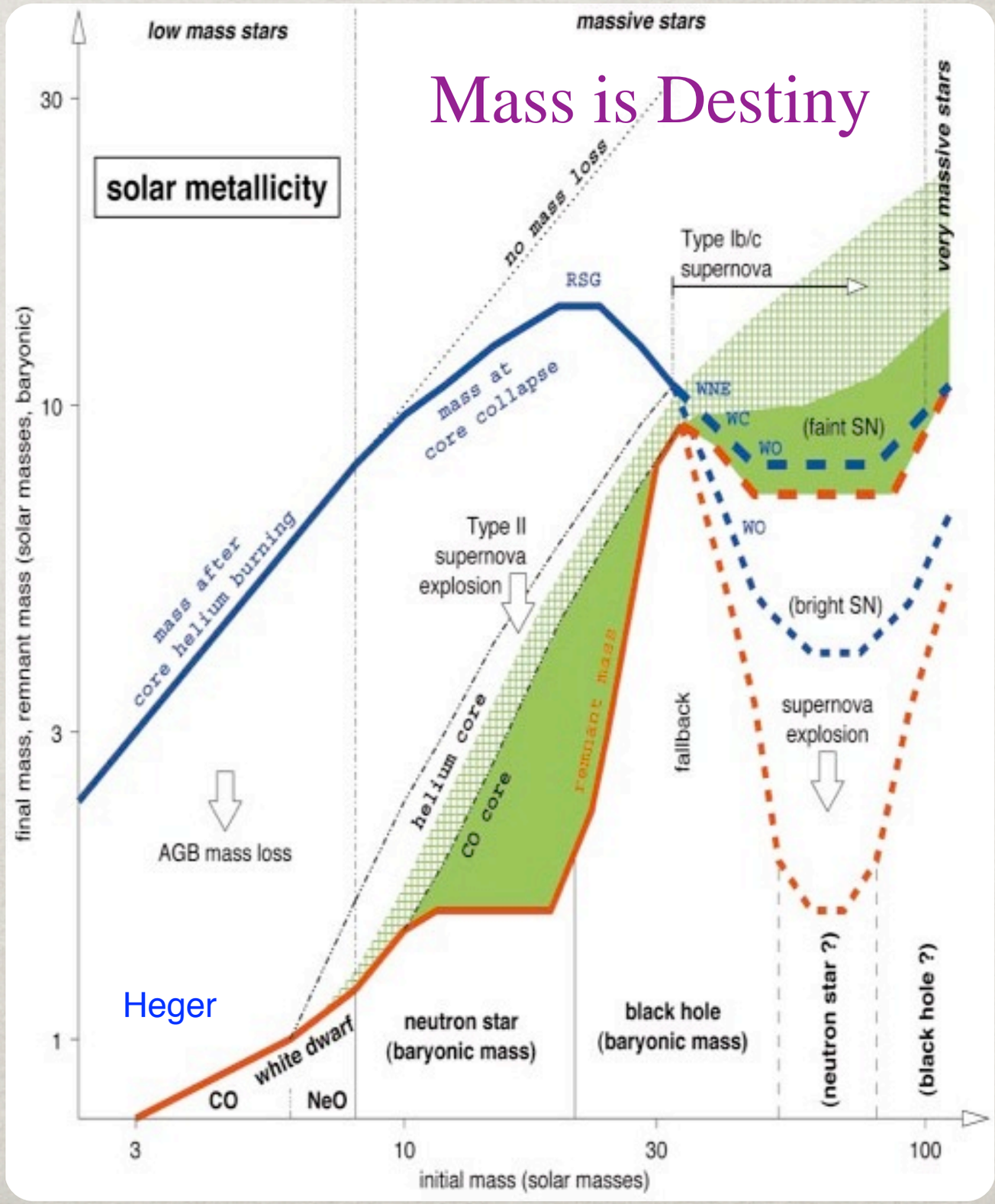

Inside a Massive Star

Stars that ignite Carbon burning meet a very different fate.

They progress through Carbon, Neon, Oxygen and Silicon burning, leaving a core of Iron surrounded by concentric layers of lighter elements.

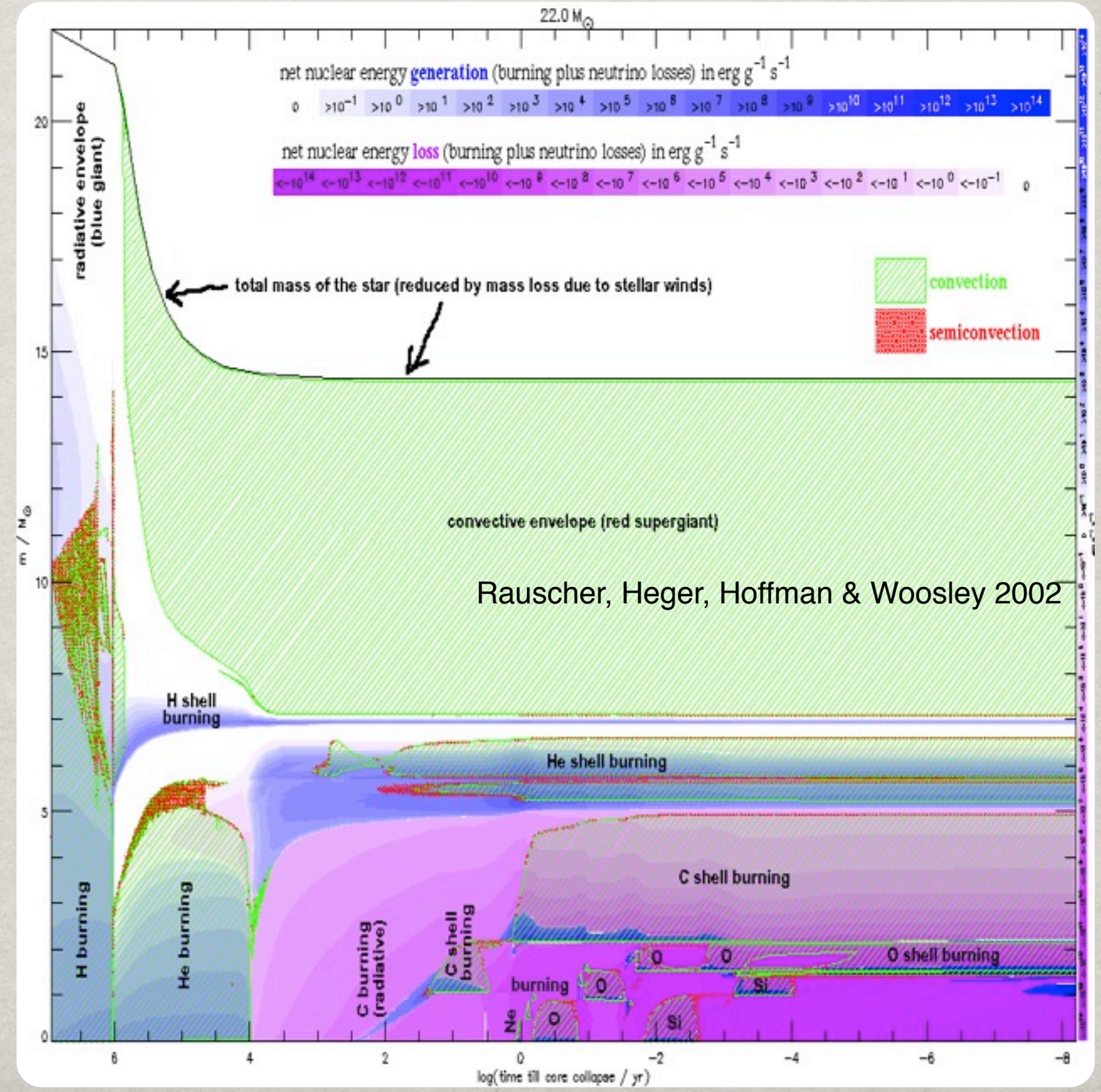

Rauscher, Heger, Hoffman & Woosley 2002

STELLAR BURNING STAGES

Process	Fuel	Ash	Temperature	Duration
H Burning	H	He	30 MK	10^{14} s
He Burning	He	C	200 MK	10^{13} s
C Burning	C	O, Ne, Mg	800 MK	10^{9} s
Ne Burning	Ne	O, Mg	1.5 GK	10^{7} s
O Burning	O	Mg-Si-S	2 GK	10^{7} s
Si Burning	Si	Fe-Co-Ni	3 GK	10^{5} s
Collapse		up to Th?	> 3 GK	0.3 s

Nuclear reactions drive the evolution of stars with the ash of each stage forming the fuel for the next stage.

Live Fast, Die Young!

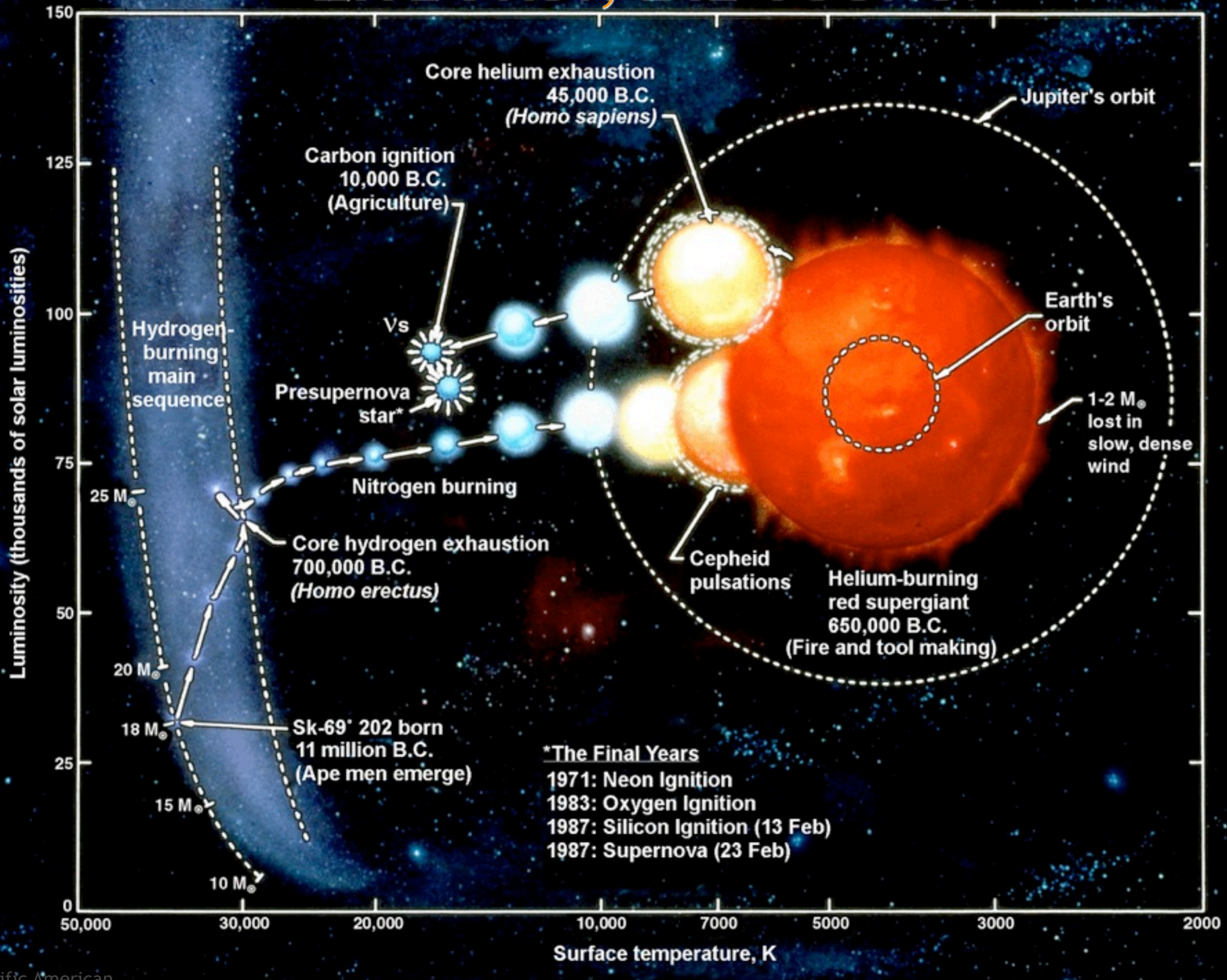

End of a Massive Star

By the time the helium shell burning ignites, the core is effectively decoupled from the envelope.

The star's remaining life is less than the Kelvin-Helmholtz timescale, $\tau \sim U/L \sim GM^2/RL \sim 10^4$ years.

The visible luminosity is largely provided by the helium shell.

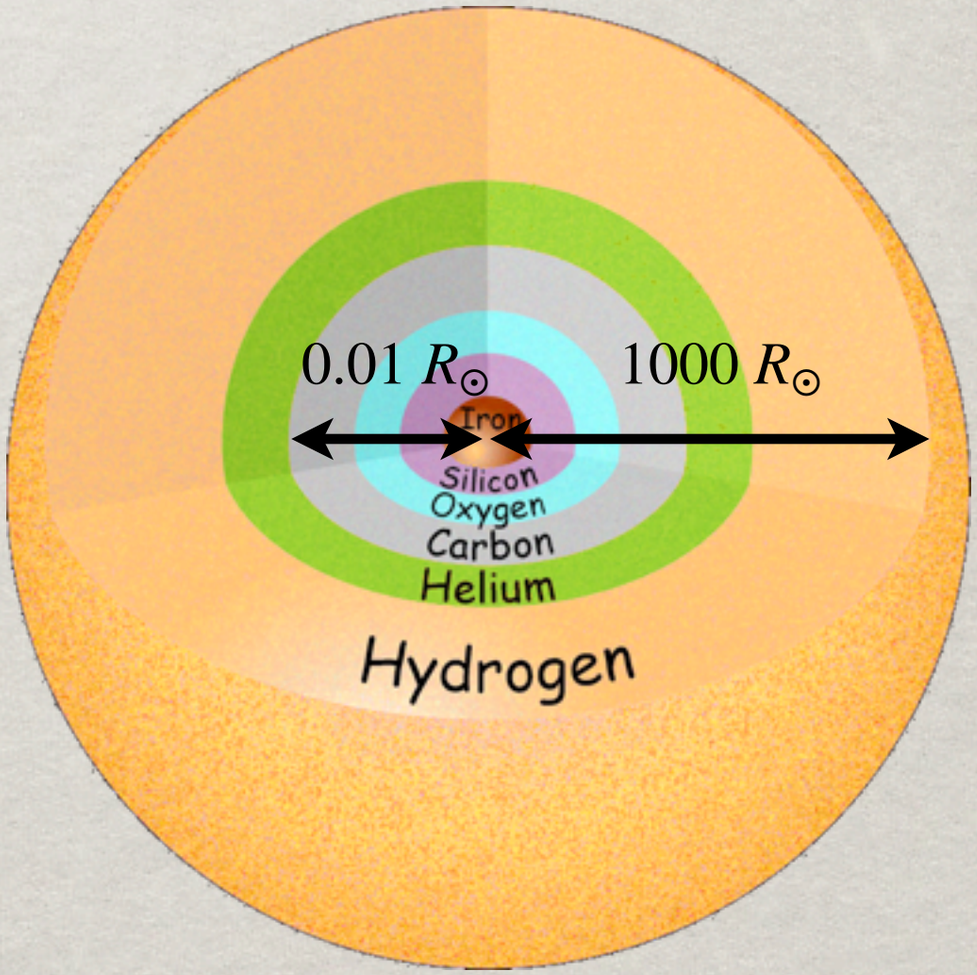

In the core, $T_c > 500$ MK lead to neutrino-pair production, allowing the luminosity of the core to escape primarily as neutrinos.

Successive burning stages proceed rapidly to form an iron core with lighter element shells.

Why Stop at Iron?

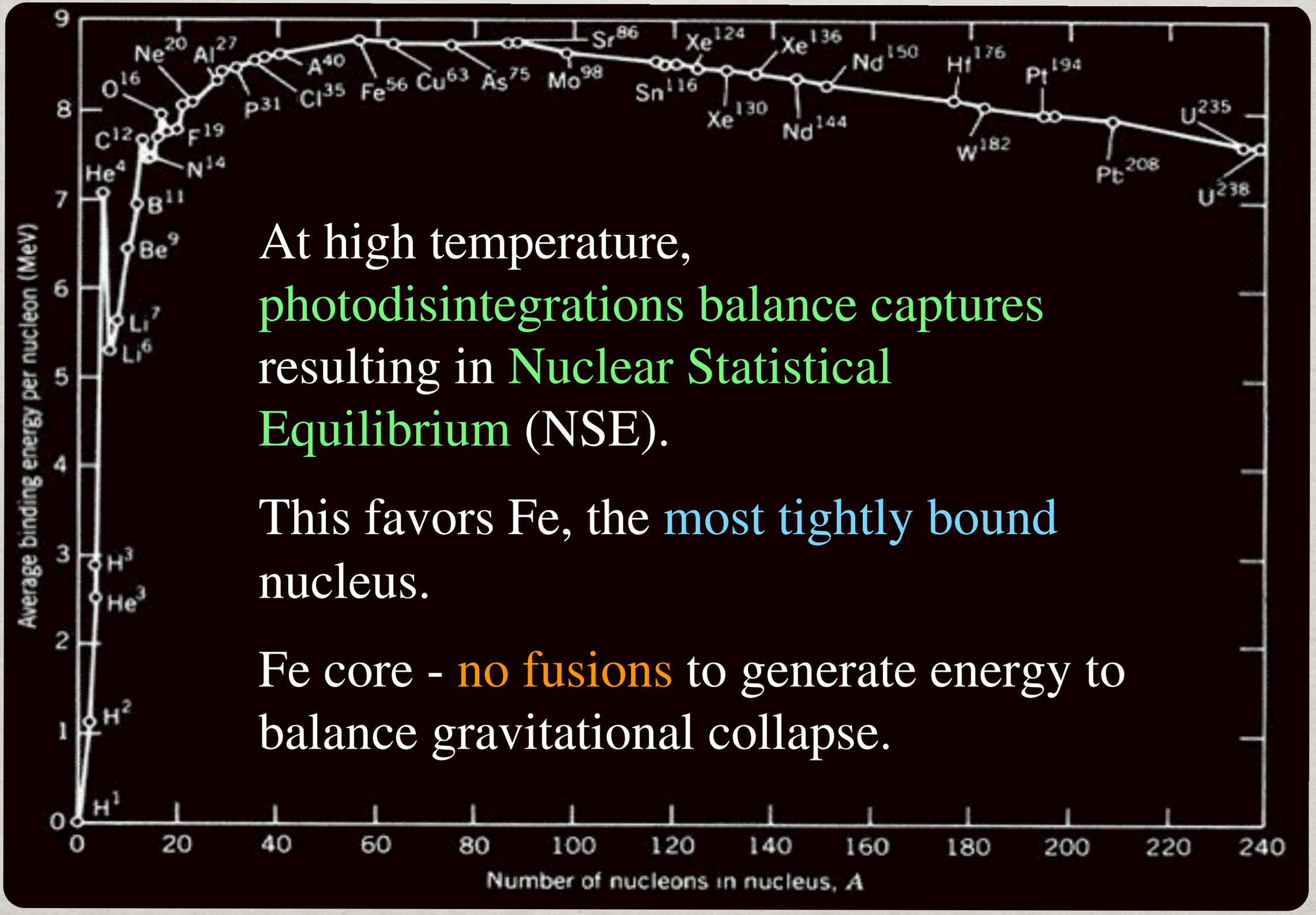

At high temperature, photodisintegrations balance captures resulting in Nuclear Statistical Equilibrium (NSE).

This favors Fe, the most tightly bound nucleus.

Fe core - no fusions to generate energy to balance gravitational collapse.

Weak reactions on Iron Peak Nuclei

In the iron core of a massive star the electron chemical potential becomes large, enhancing electron capture.

Iron core mass and leptonization depend on e^- capture and β decay rates for A~65.

Modern Shell Model calculations reduce the ec rate, altering stellar models.

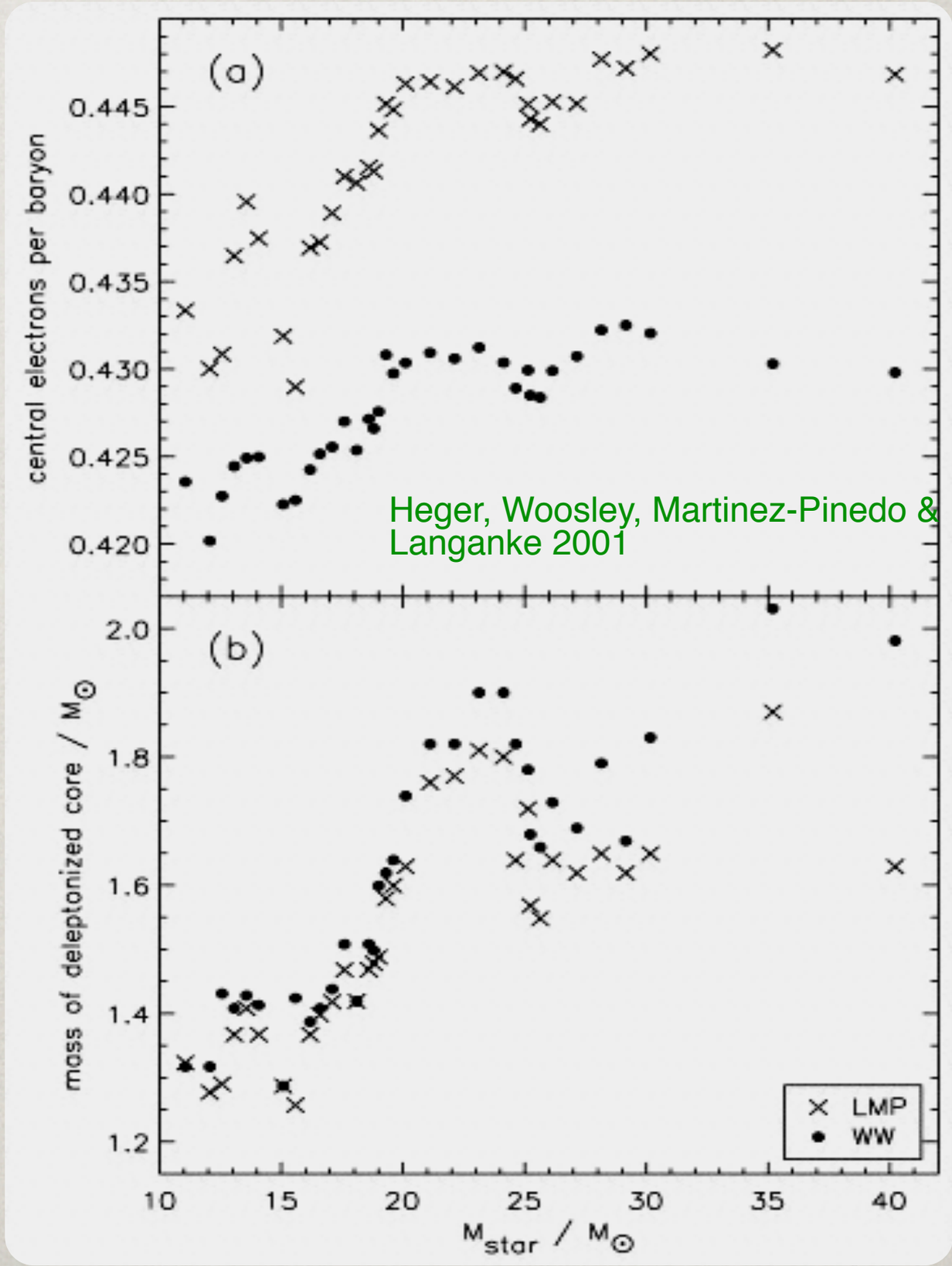

Future of Stellar Models

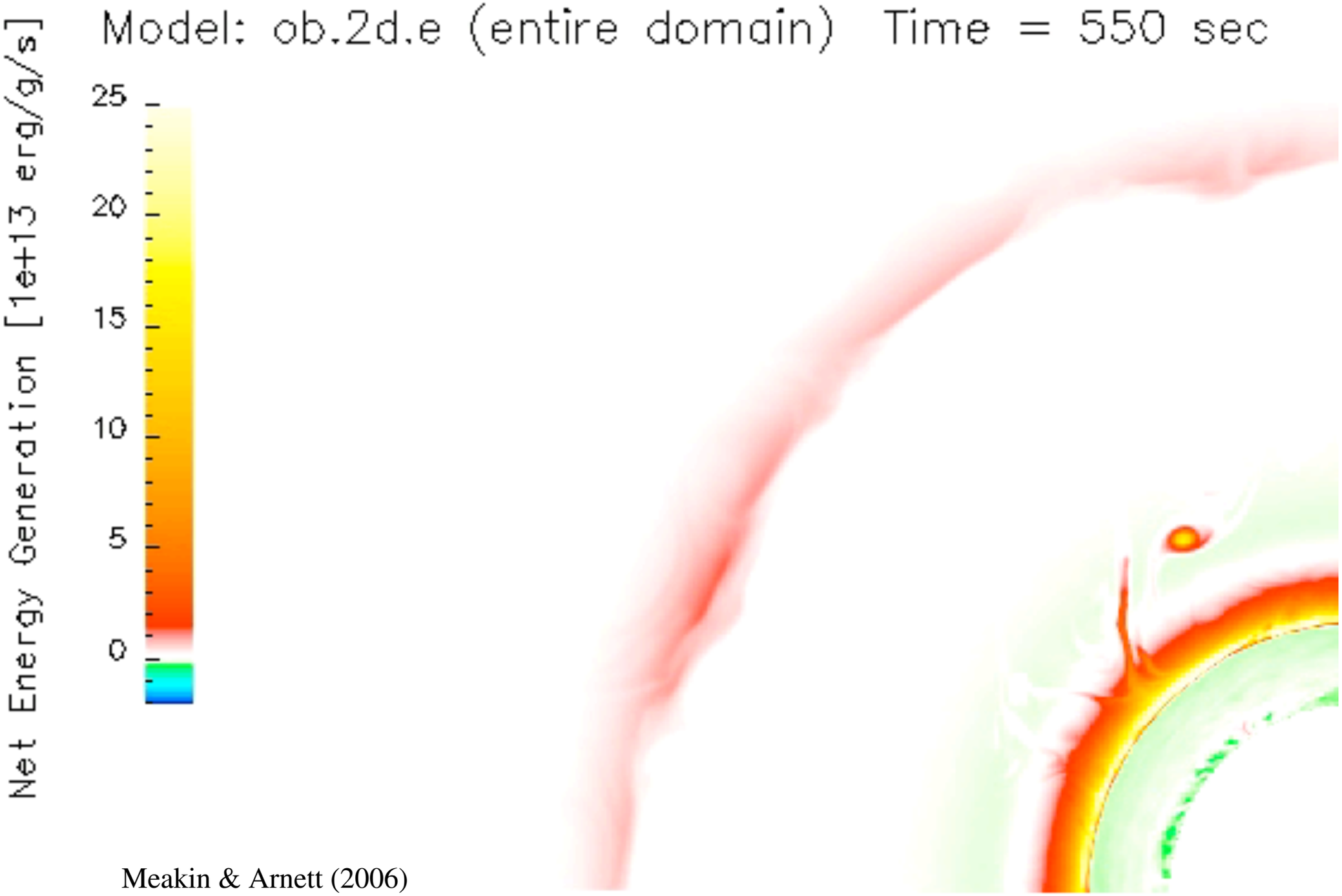

Meakin & Arnett (2006)

Stellar Evolution models are only beginning to transition to 3D.

Core-Collapse Supernova

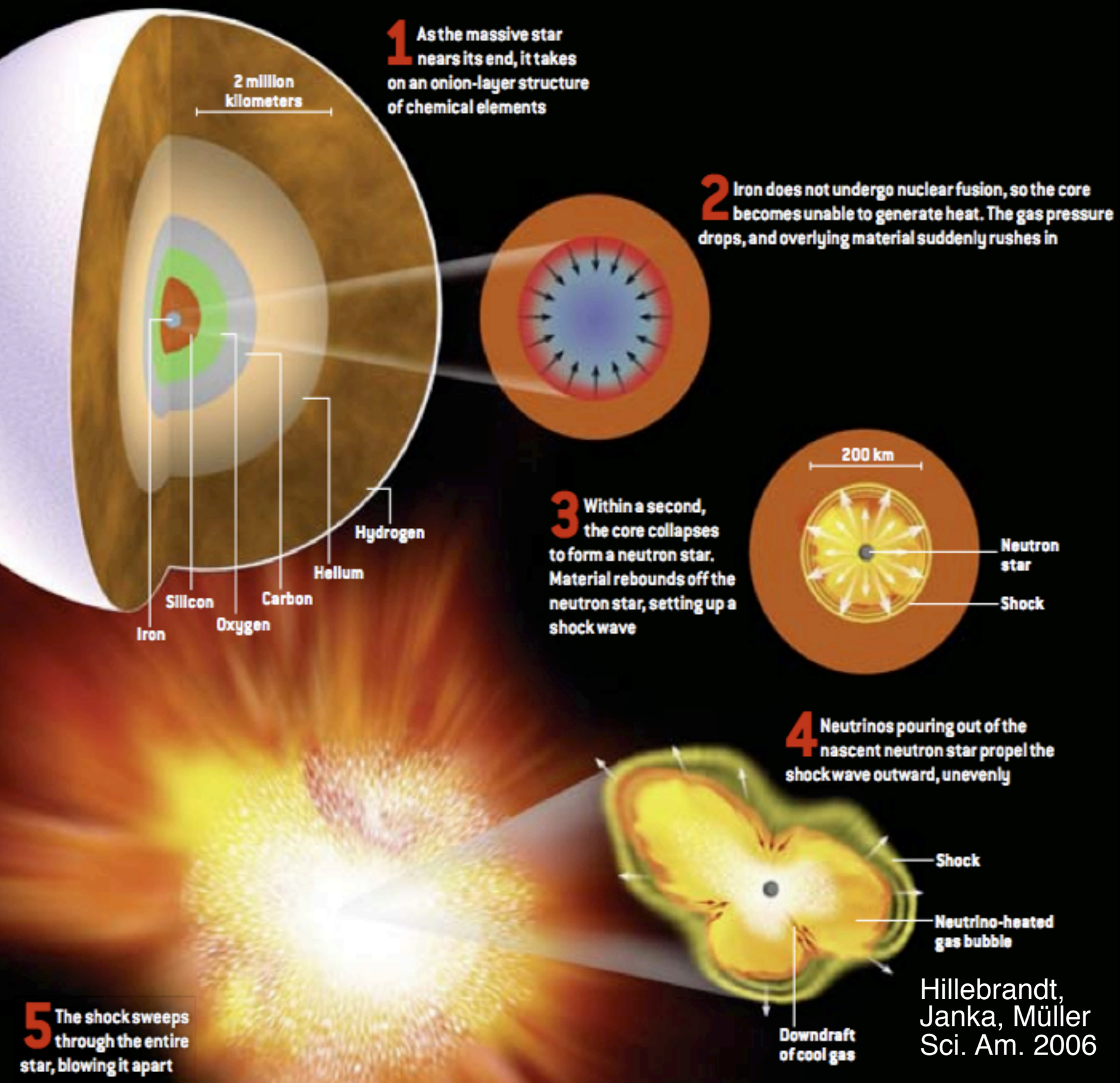

Hillebrandt, Janka, Müller Sci. Am. 2006

A Core-Collapse Supernova is the inevitable death knell of a massive star (~10+ $M_\odot$).

Once central iron core grows too massive to be supported by electron degeneracy pressure, collapse ensues, accelerated by electron capture.

Spherical Failure

The need for aspherical effects comes from the failure of spherically symmetric models.

Even with fully modern physics and spectral Boltzmann neutrino transport, 1D models fail to explode because heating in a stratified star is inefficient.

The exception is models which boost the luminosity by some means, for example, Wilson's models which invoke PNS convection.

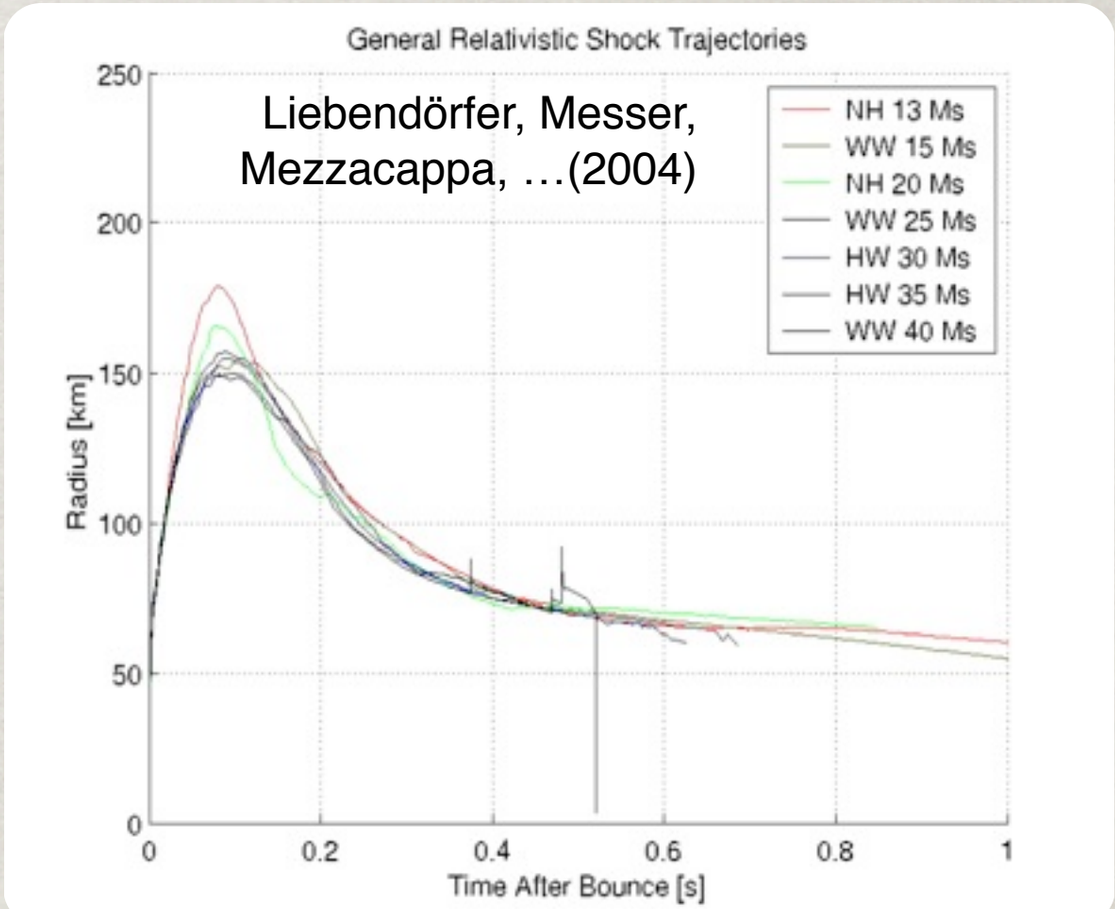

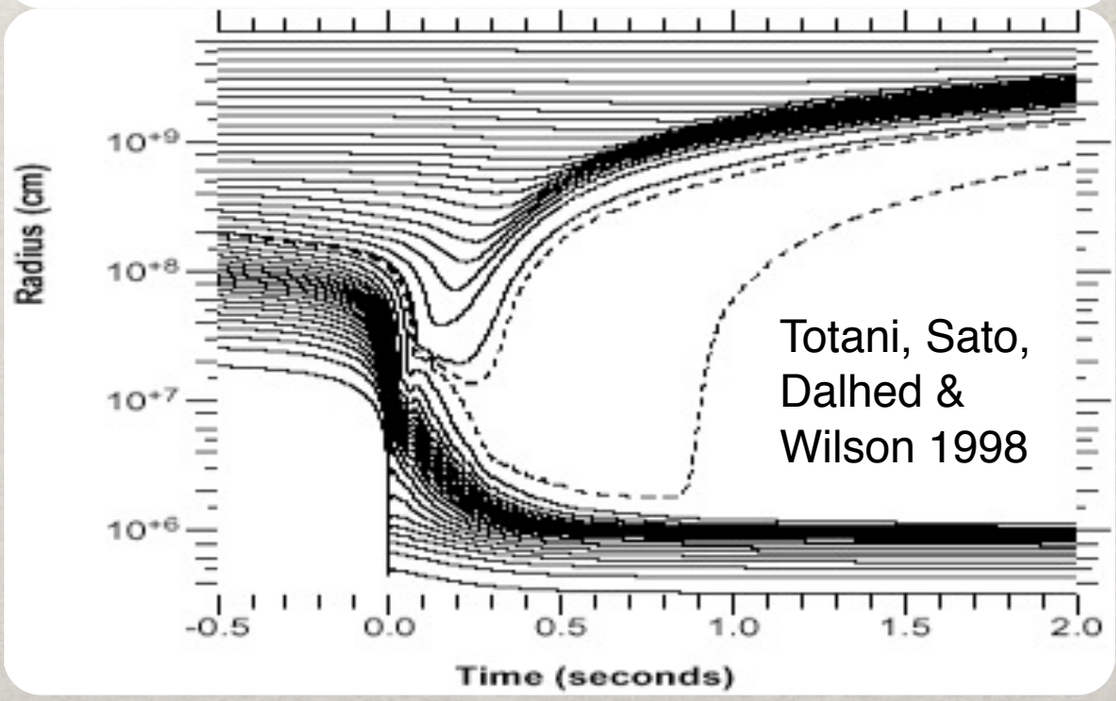

CHIMERA

CHIMERA has 3 “heads”

* Spectral Neutrino Transport (MGFLD-TRANS, Bruenn) in Ray-by-Ray Approximation
* Shock-capturing Hydrodynamics (VH1, Blondin)
* Nuclear Kinetics (XNet, Hix & Thielemann)

Plus Realistic Equations of State, Newtonian Gravity with Spherical GR Corrections.

Models use a variety of approximations

Self-consistent models use full physics to the center.

Leakage models simplify the transport.

Parameterized models replace the core with a specified neutrino luminosity.

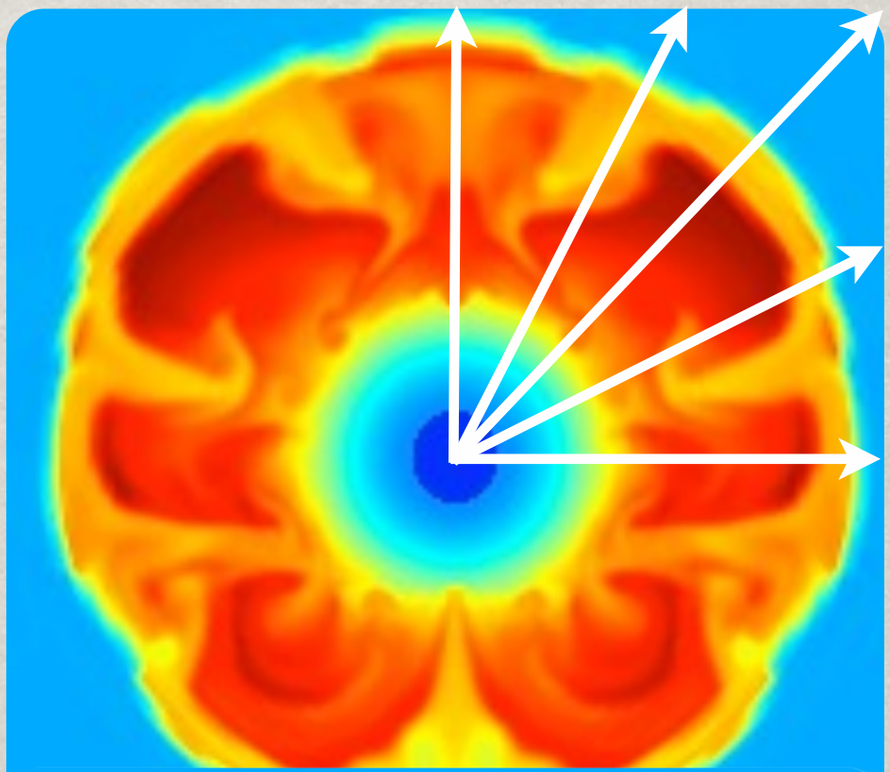

The Early Phase

For the first ~100 ms after bounce, the supernova shock is essentially spherical, with 1D models identical to 2D models.

Once the Standing Accretion Shock Instability (SASI) and neutrino-driven convection begin, the shock deforms and gradually progresses outward in radius.

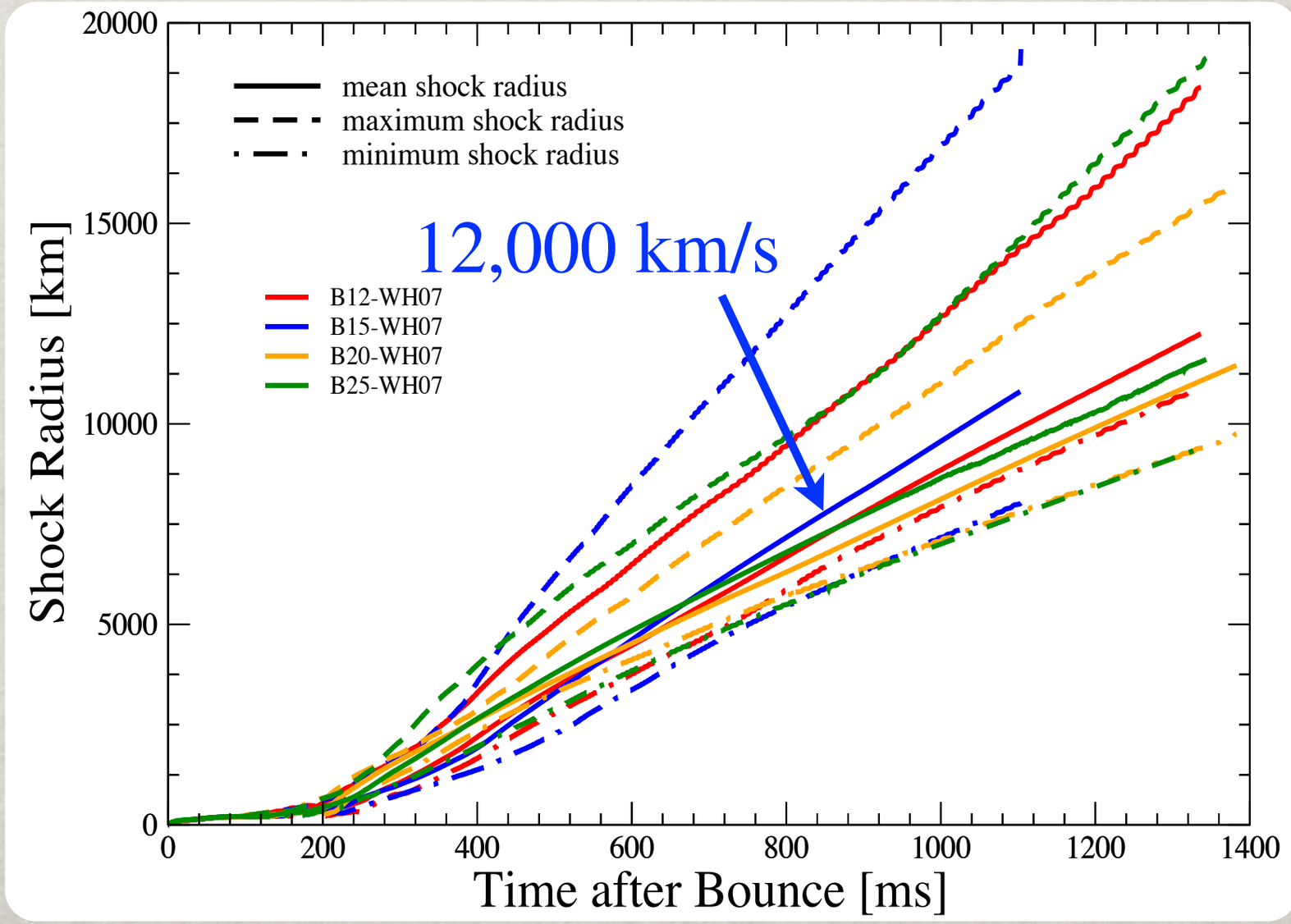

The Early Phase

For the first ~100 ms after bounce, the supernova shock is essentially spherical, with 1D models identical to 2D models.

Once the Standing Accretion Shock Instability (SASI) and neutrino-driven convection begin, the shock deforms and gradually progresses outward in radius.

One notable feature is the considerable delay in launching an explosion, >150-200 ms slower compared to older models.

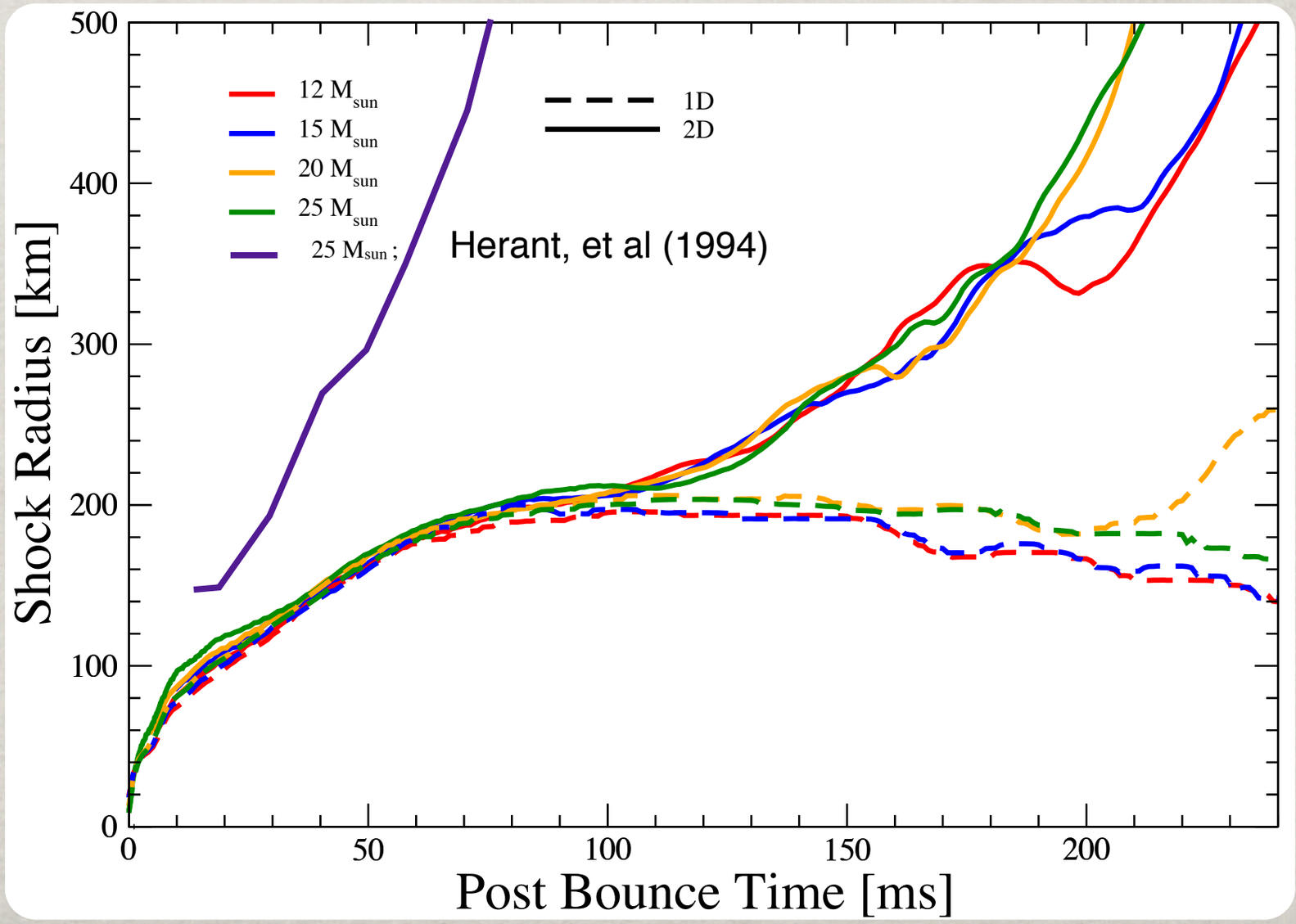

The Early Phase

For the first ~100 ms after bounce, the supernova shock is essentially spherical, with 1D models identical to 2D models.

Once the Standing Accretion Shock Instability (SASI) and neutrino-driven convection begin, the shock deforms and gradually progresses outward in radius.

One notable feature is the considerable delay in launching an explosion, >150-200 ms slower compared to older models.

Competitive models exhibit even longer delays.

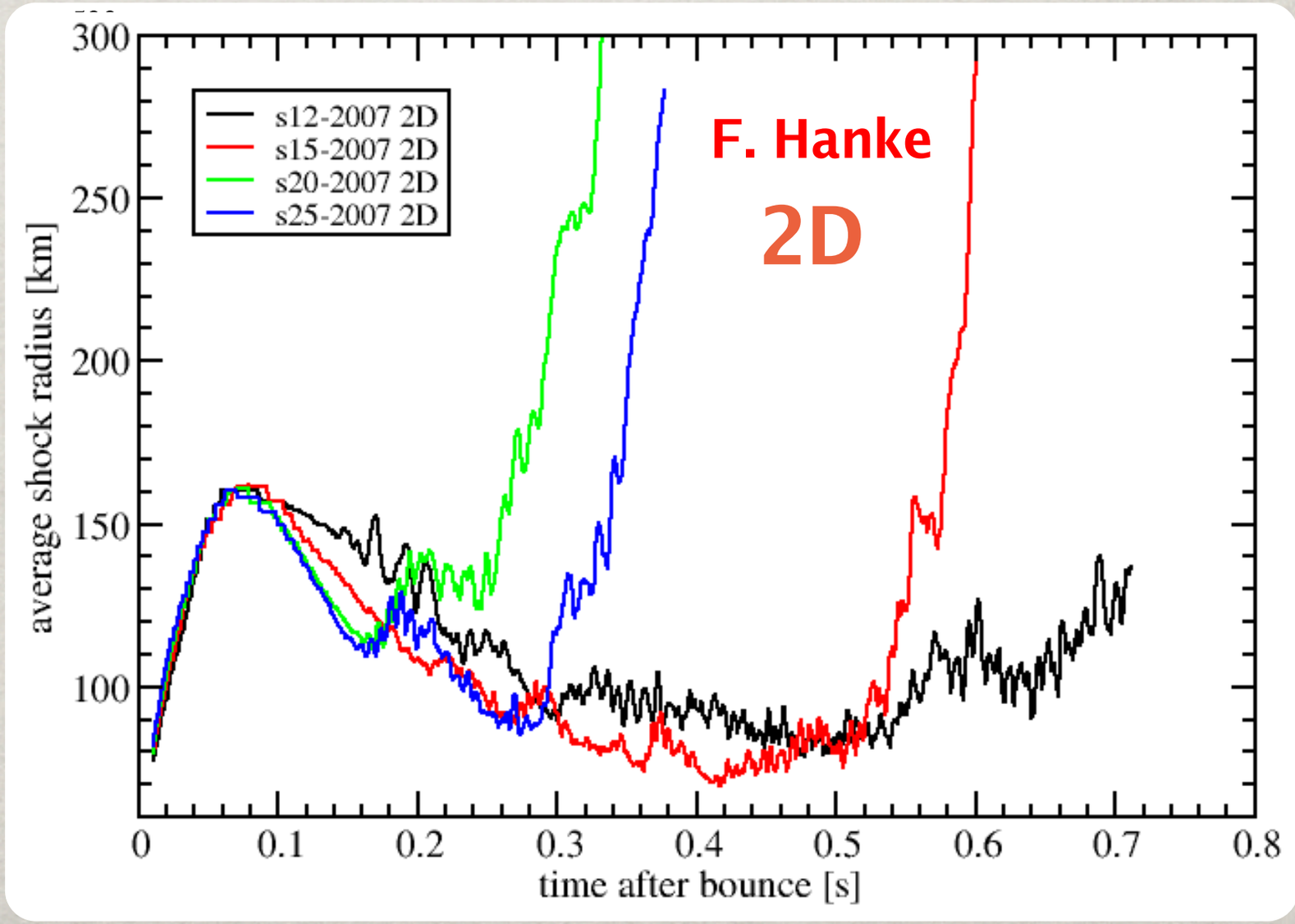

Supernova: the Movie

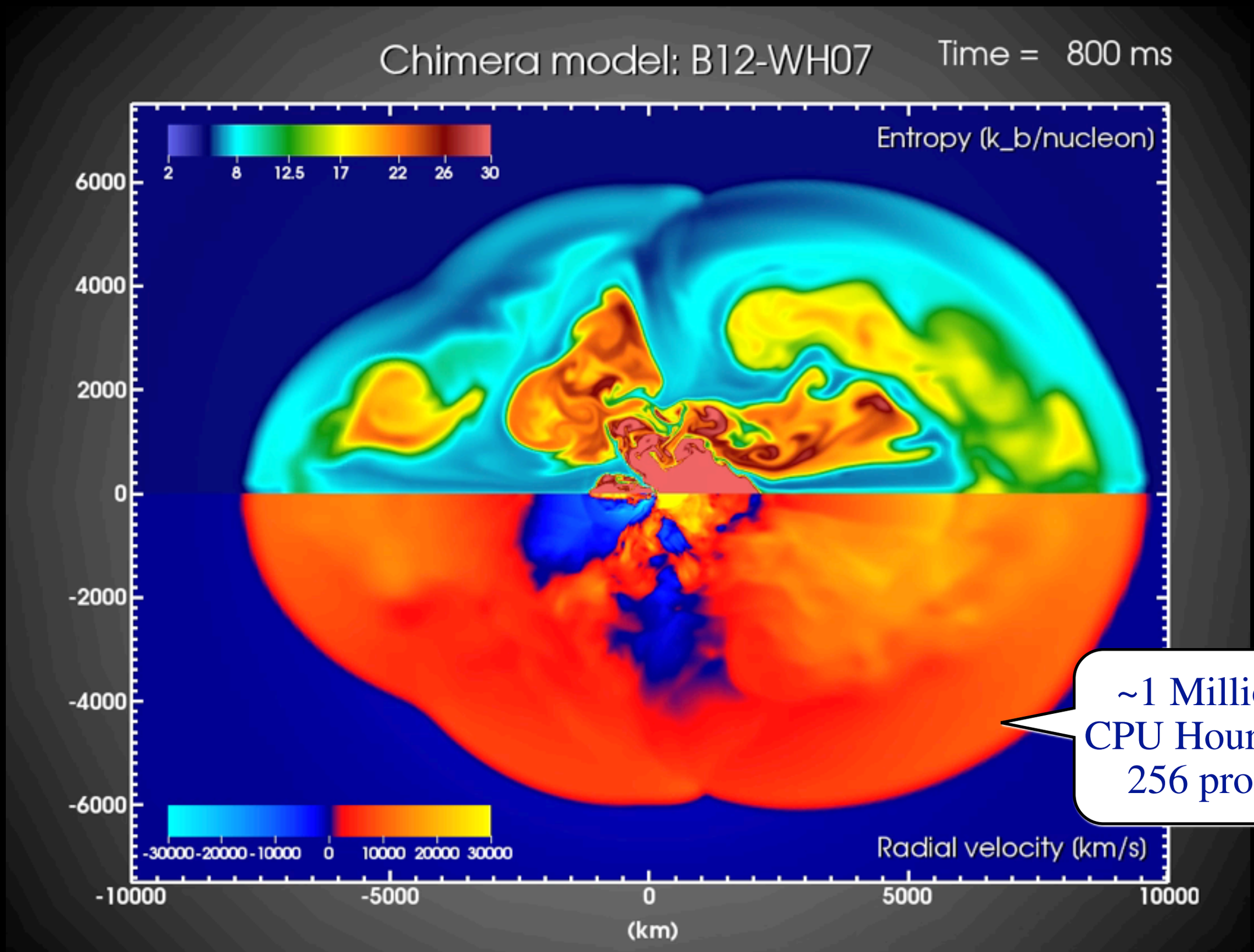

How to make an explosion

SASI & Convection gradually push the shock outward, increasing the size of the heating region until heating timescale ($\tau_{heating}$) is smaller than advection timescale ($\tau_{advection}$).

Much of the explosion energy comes from the neutrino heating region, below the ejecta, in the form of PdV work and advected internal energy.

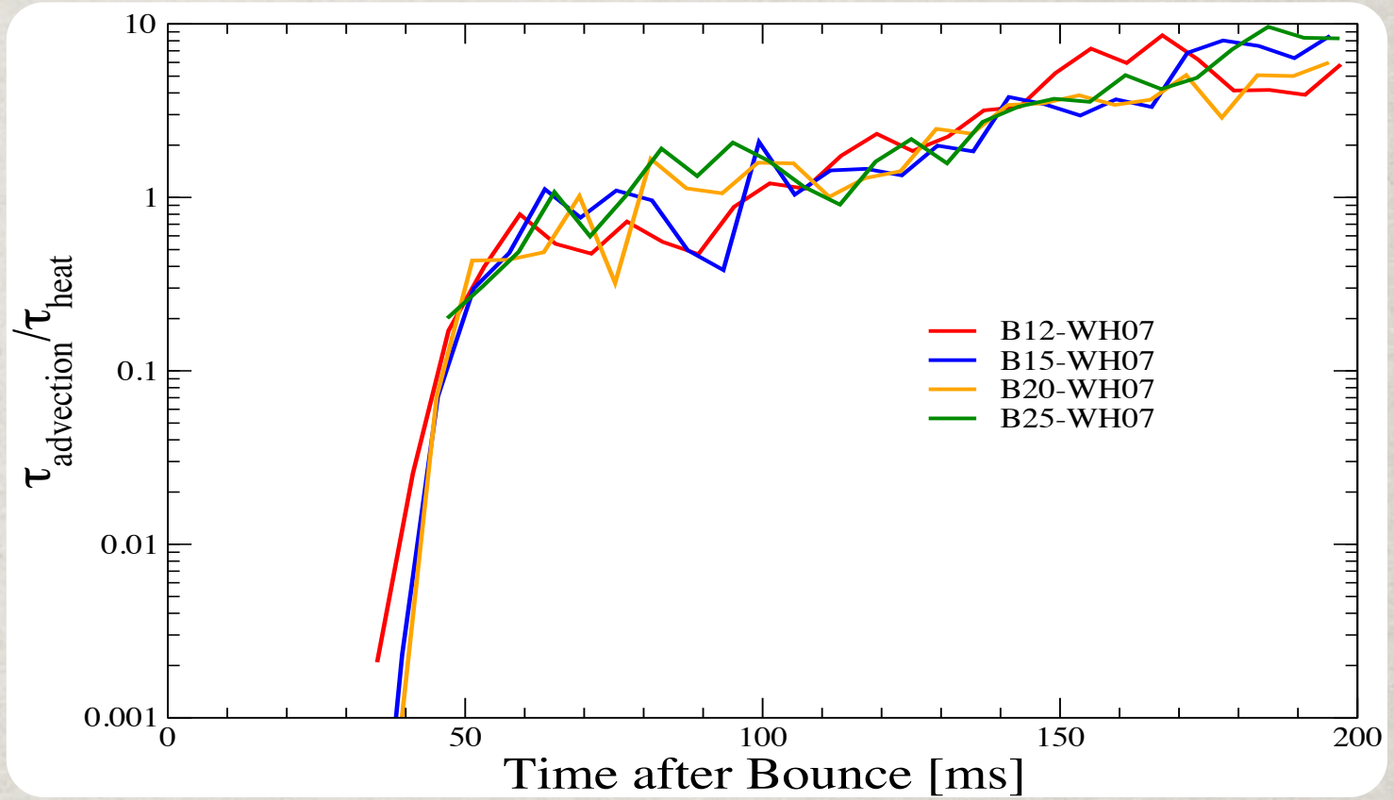

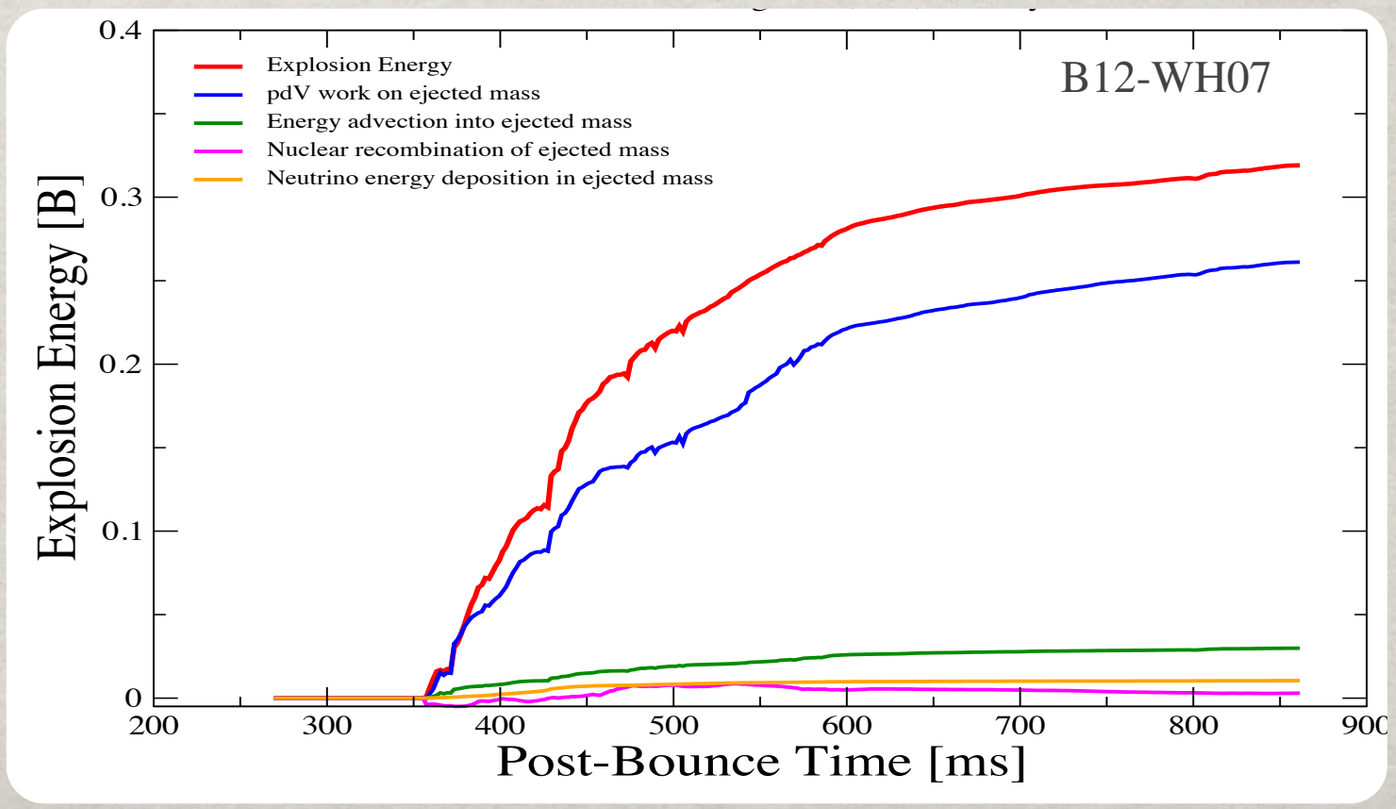

Neutrinos at Work

The initially spherical gain surface between the cooling and heating regions begins to distort ~70 ms after bounce.

Beginning ~120 ms, the heating region is marked by low entropy downflows, with the strongest heating at their base.

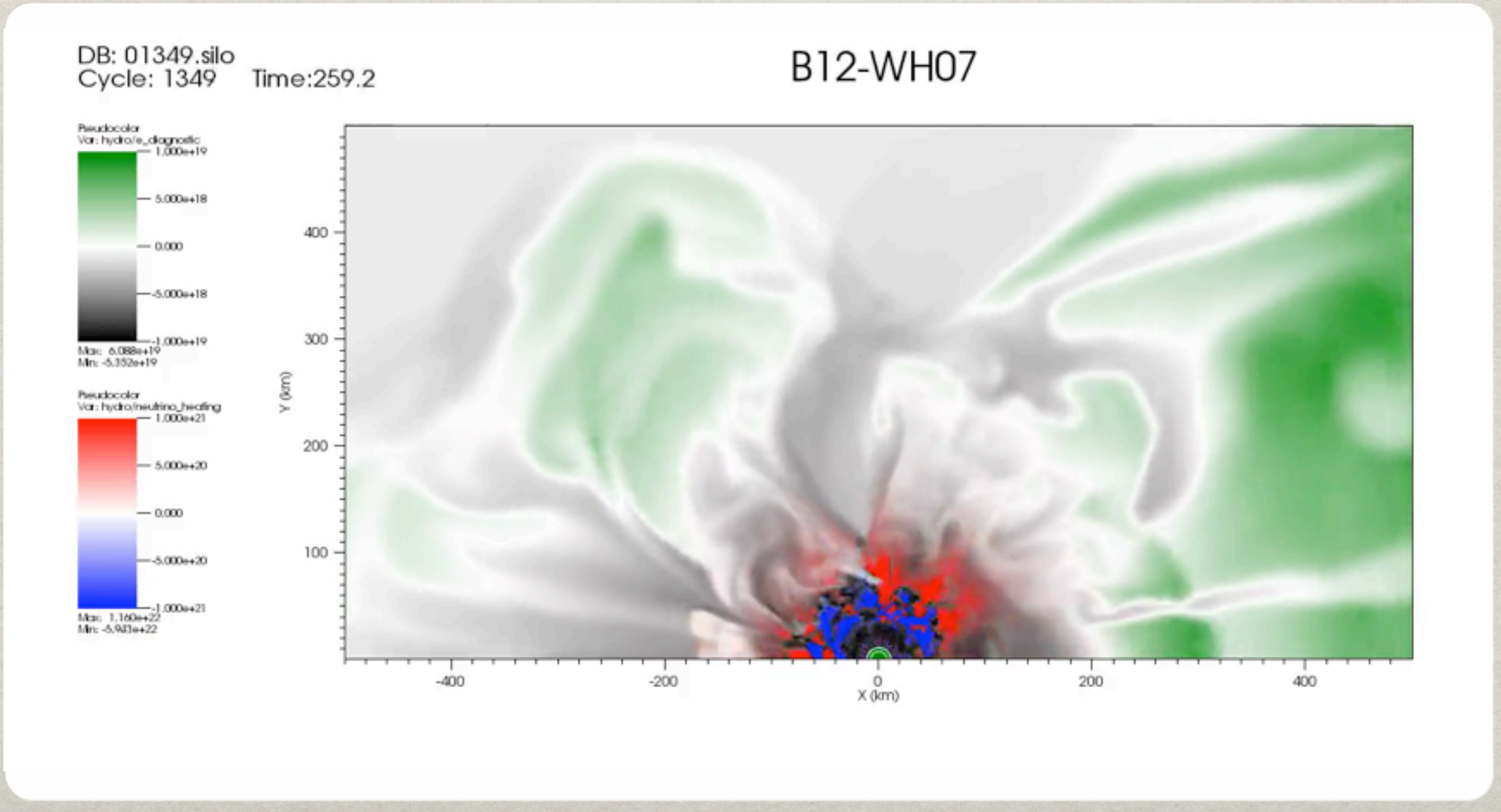

Shock Shape

The shape of the shock is determined by the interplay between convection and the SASI, with large individual plumes producing strongly prolate to mildly oblate shocks, depending on the plume's orientation.

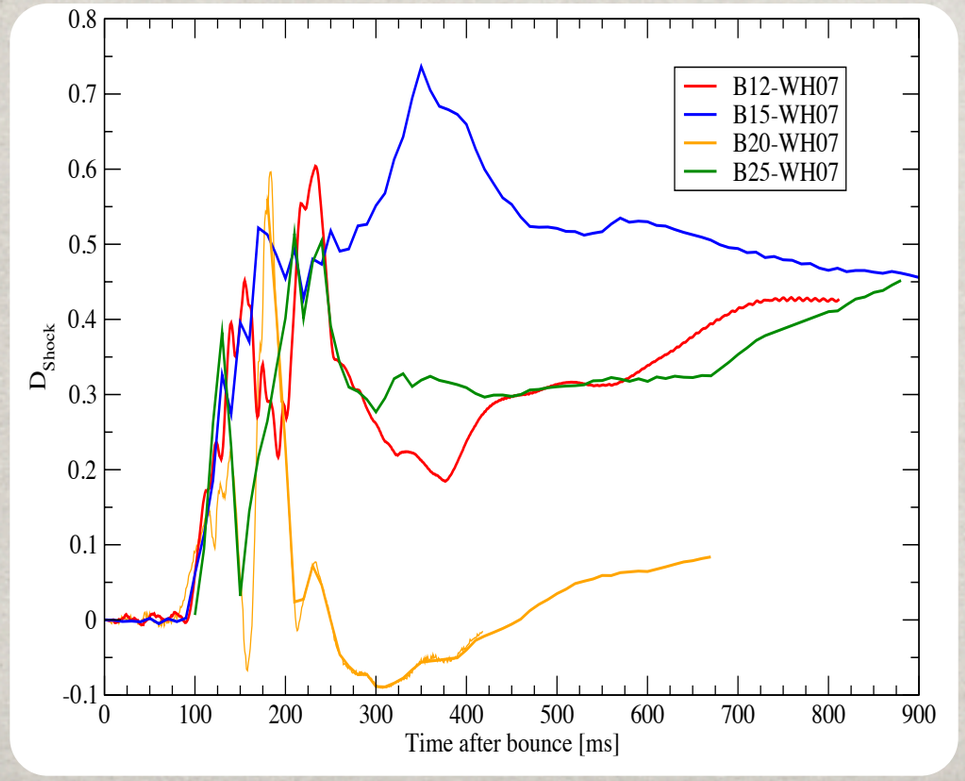

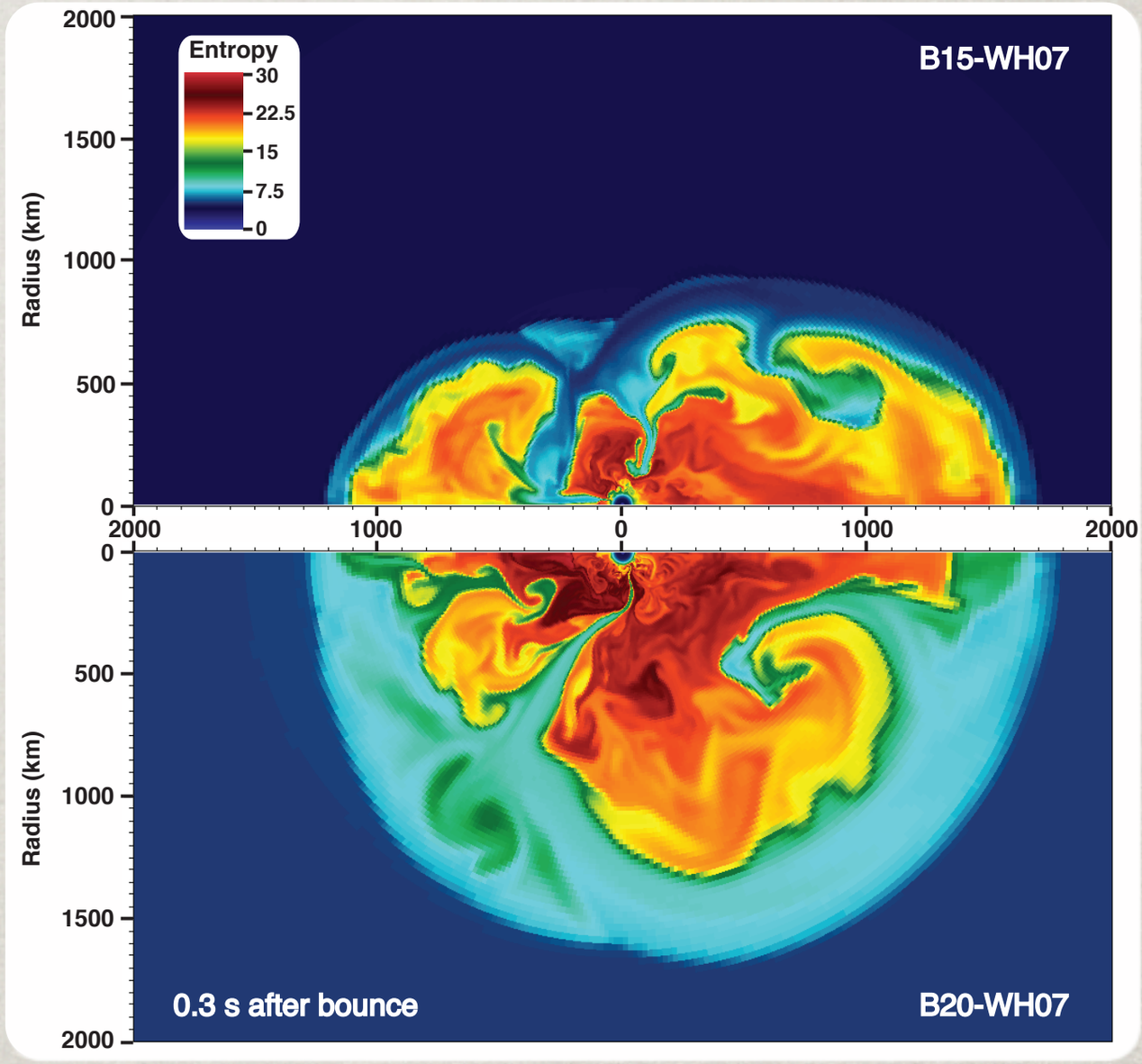

Shape has dynamic effects, for example, oblate B20-WH07 cuts off accretion through the shock 100 ms earlier than in prolate models.

Shock Shape

The shape of the shock is determined by the interplay between convection and the SASI, with large individual plumes producing strongly prolate to mildly oblate shocks, depending on the plume's orientation.

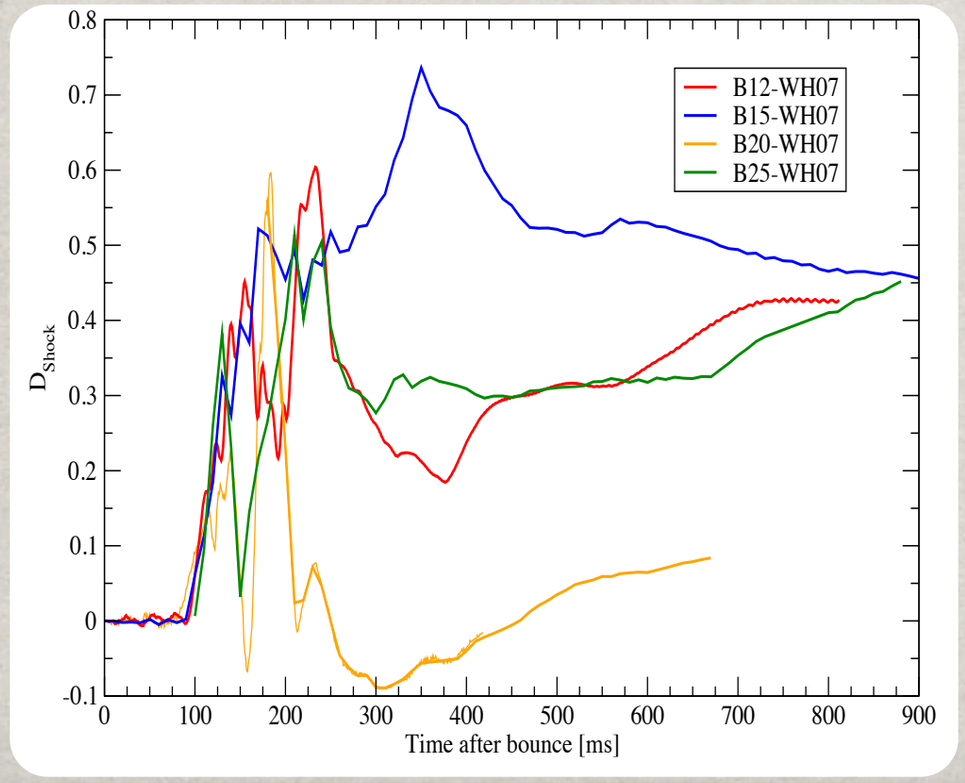

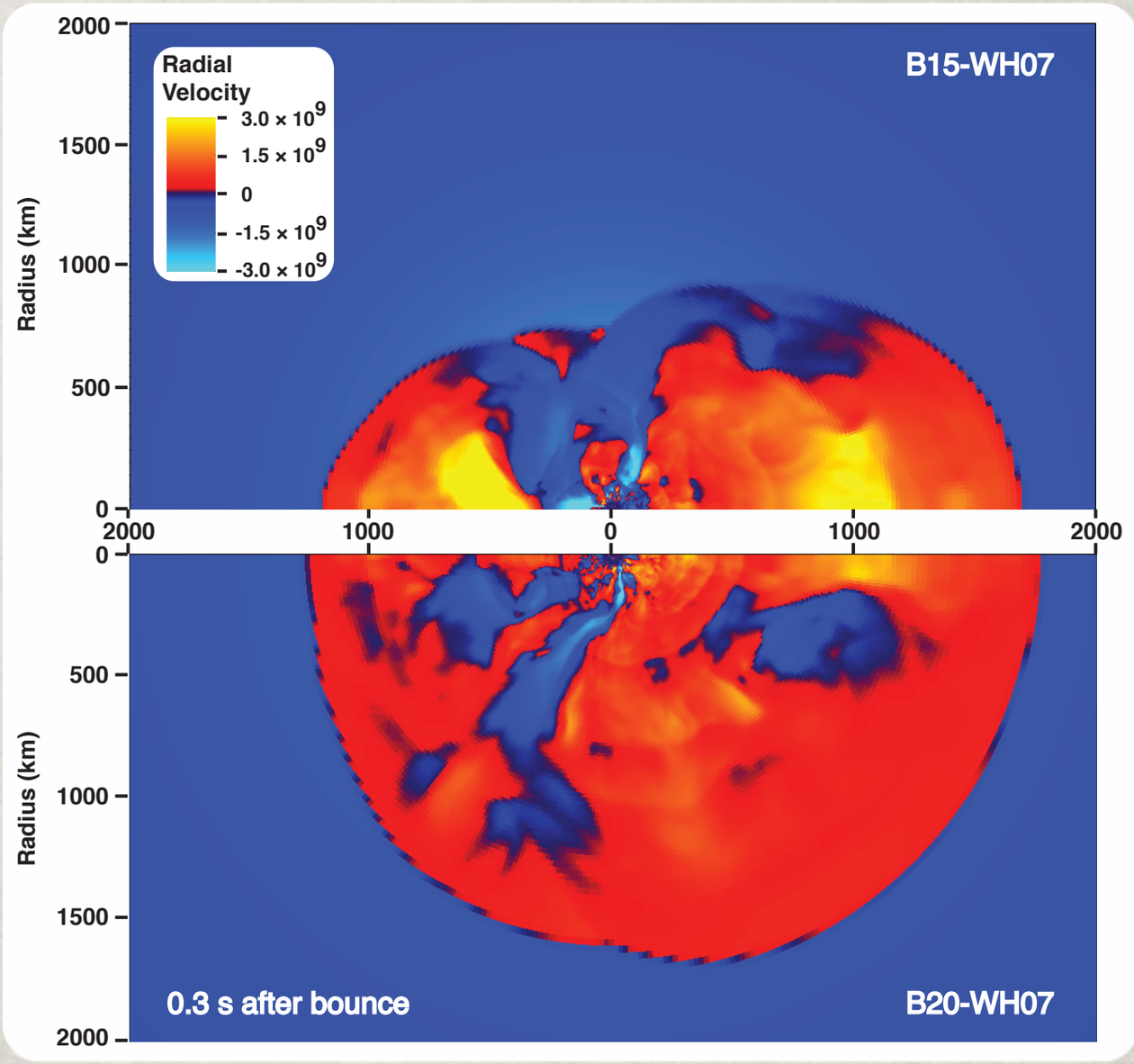

Shape has dynamic effects, for example, oblate B20-WH07 cuts off accretion through the shock 100 ms earlier than in prolate models.

Late time behavior

The accretion rates decline steadily as less dense layers accrete through the shock. The developing explosion, especially cutting off of the downflows, accelerates this.

However, the accretion rates level off at late times.

The heating rate likewise shows a marked decline once the explosion cuts off the downflows, but continues to show heating episodes to late times.

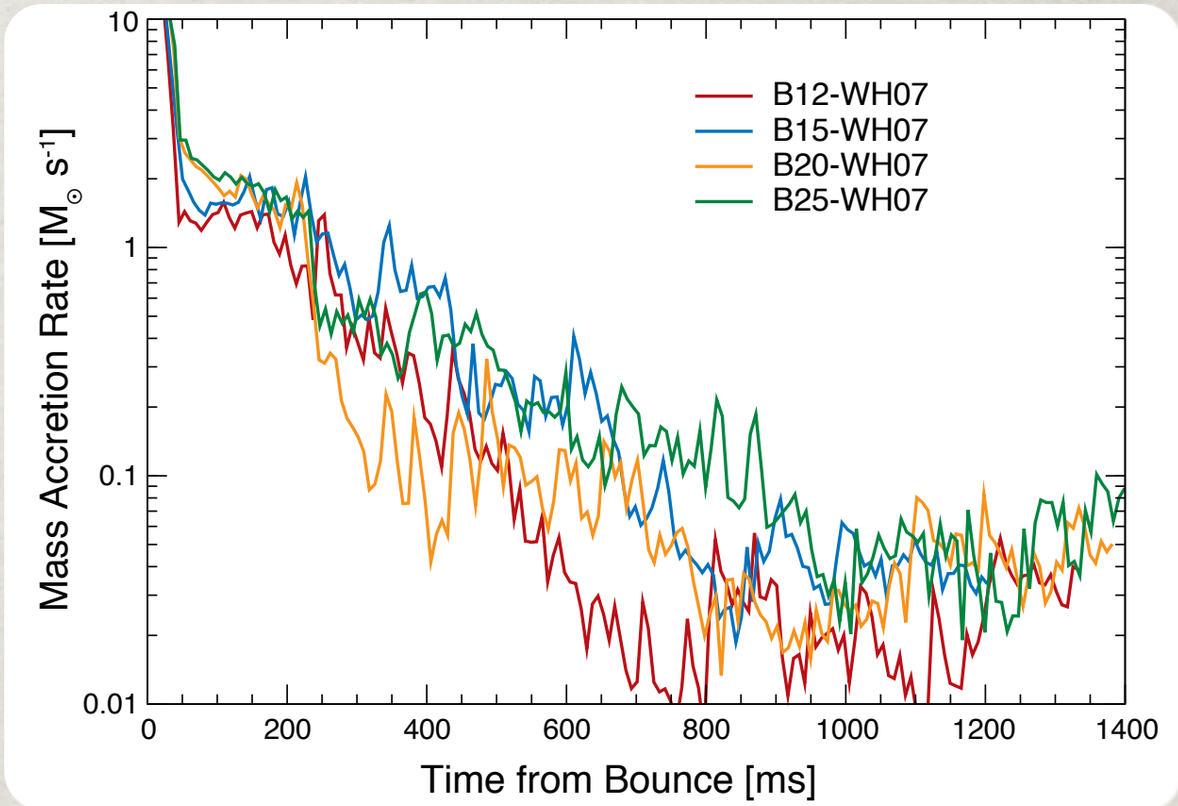

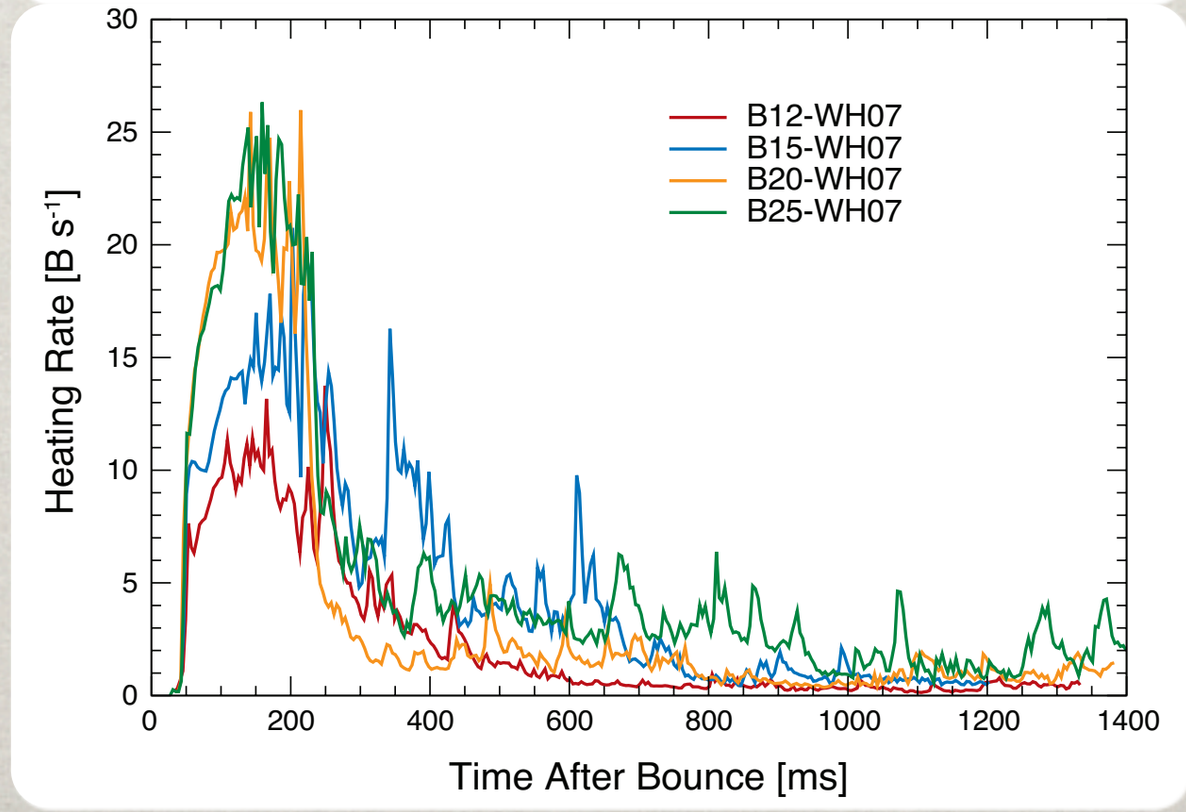

Explosion Energies

Beyond the most basic observable, an explosion, we can compare to the myriad of other potential observations, starting with the kinetic energy of the explosion.

Unfortunately, models are still in the stage where internal energy dominates, so we must estimate the explosion energy by assuming efficient conversion of $E_i \Rightarrow E_k$.

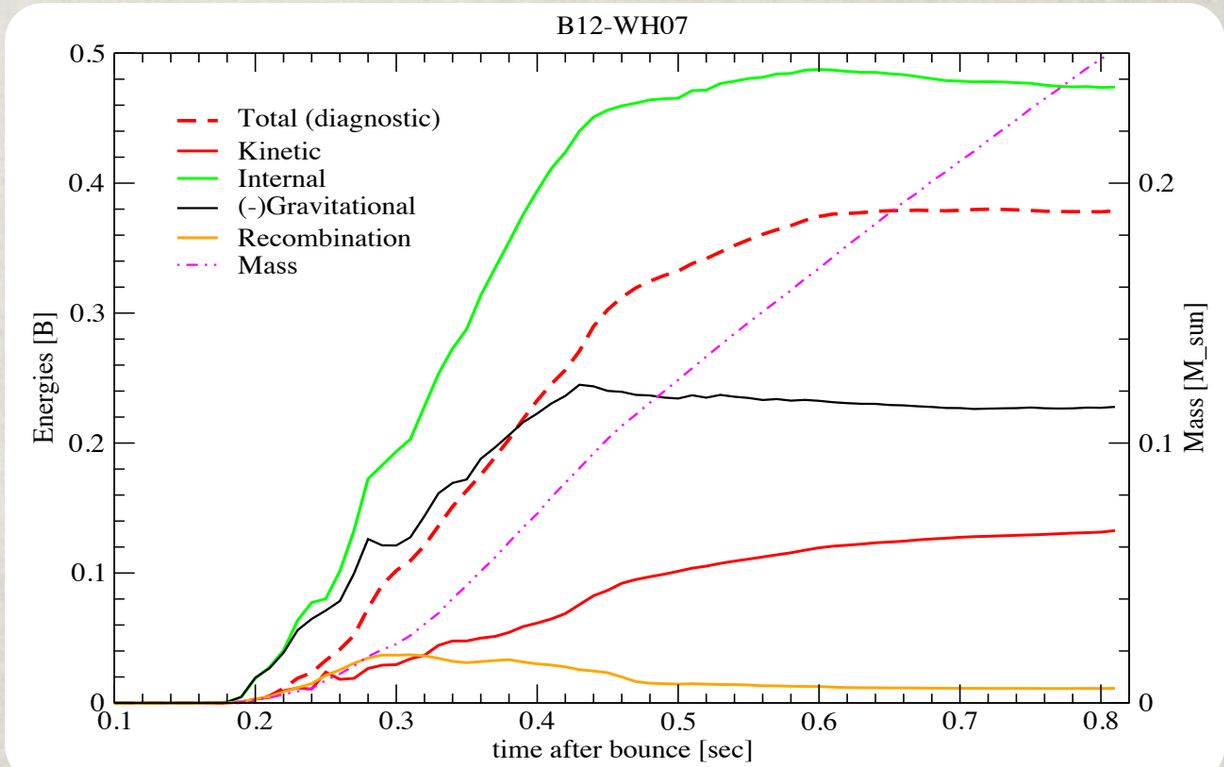

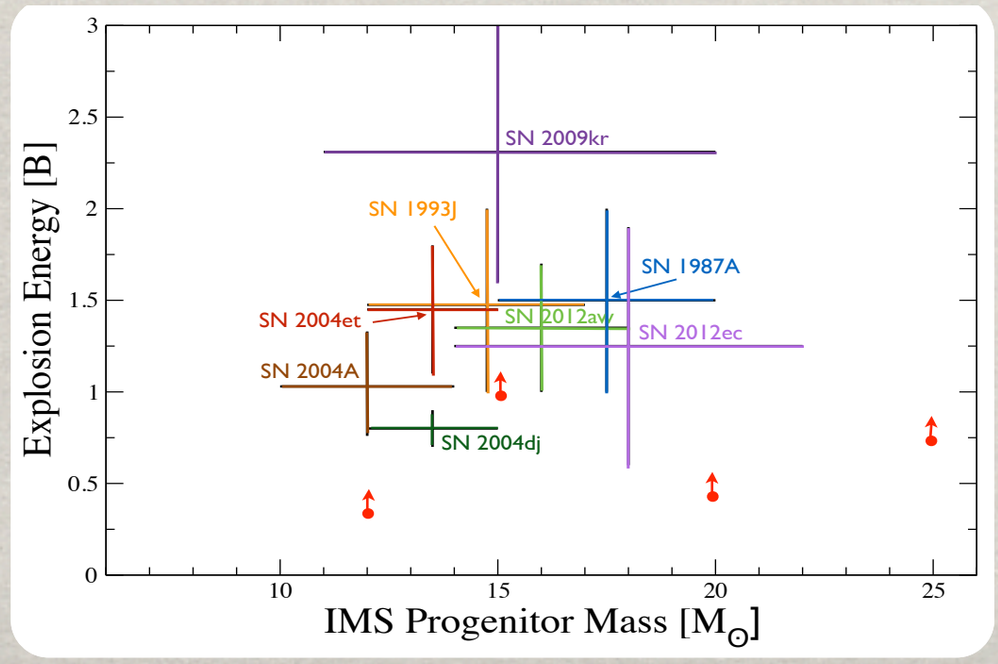

Explosion Energies

Beyond the most basic observable, an explosion, we can compare to the myriad of other potential observations, starting with the kinetic energy of the explosion.

Unfortunately, models are still in the stage where internal energy dominates, so we must estimate the explosion energy by assuming efficient conversion of $E_i \Rightarrow E_k$.

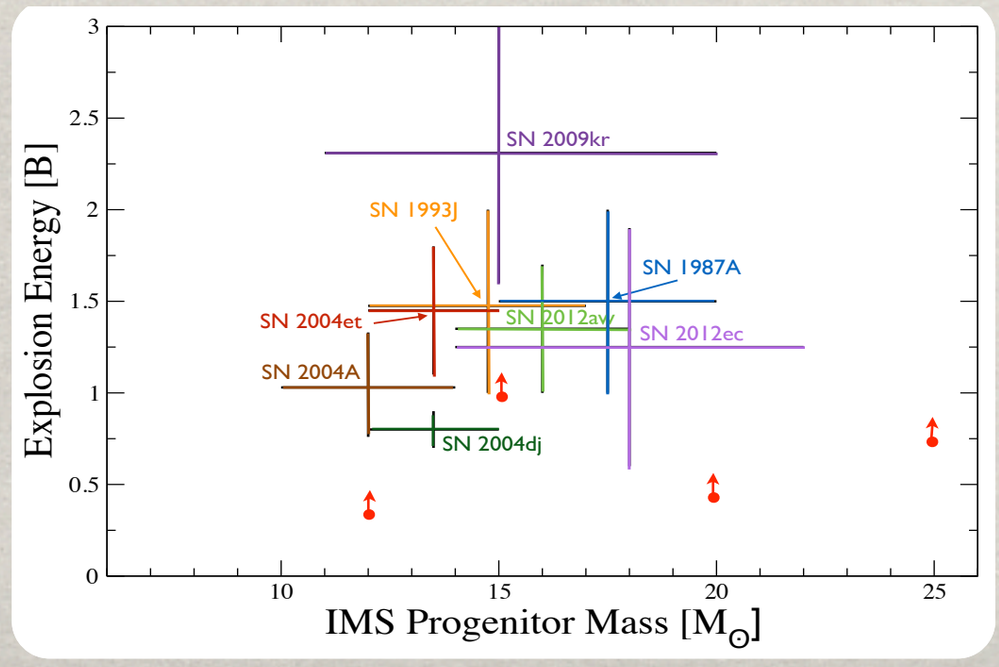

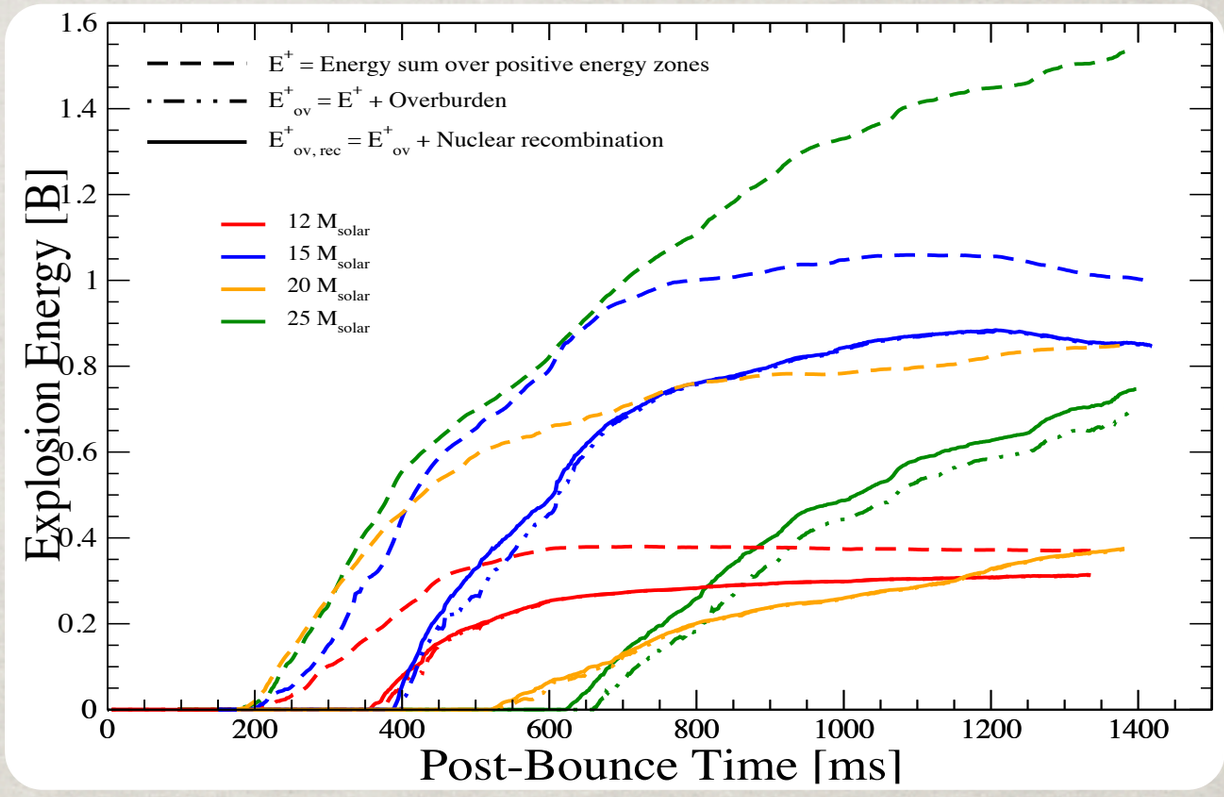

One can construct a "diagnostic" energy, $E^+ = E_i + E_g + E_k$, summed over zones where $E^+ > 0$. To this we add contributions from nuclear recombination and removing the envelope.

Neutrino Signals

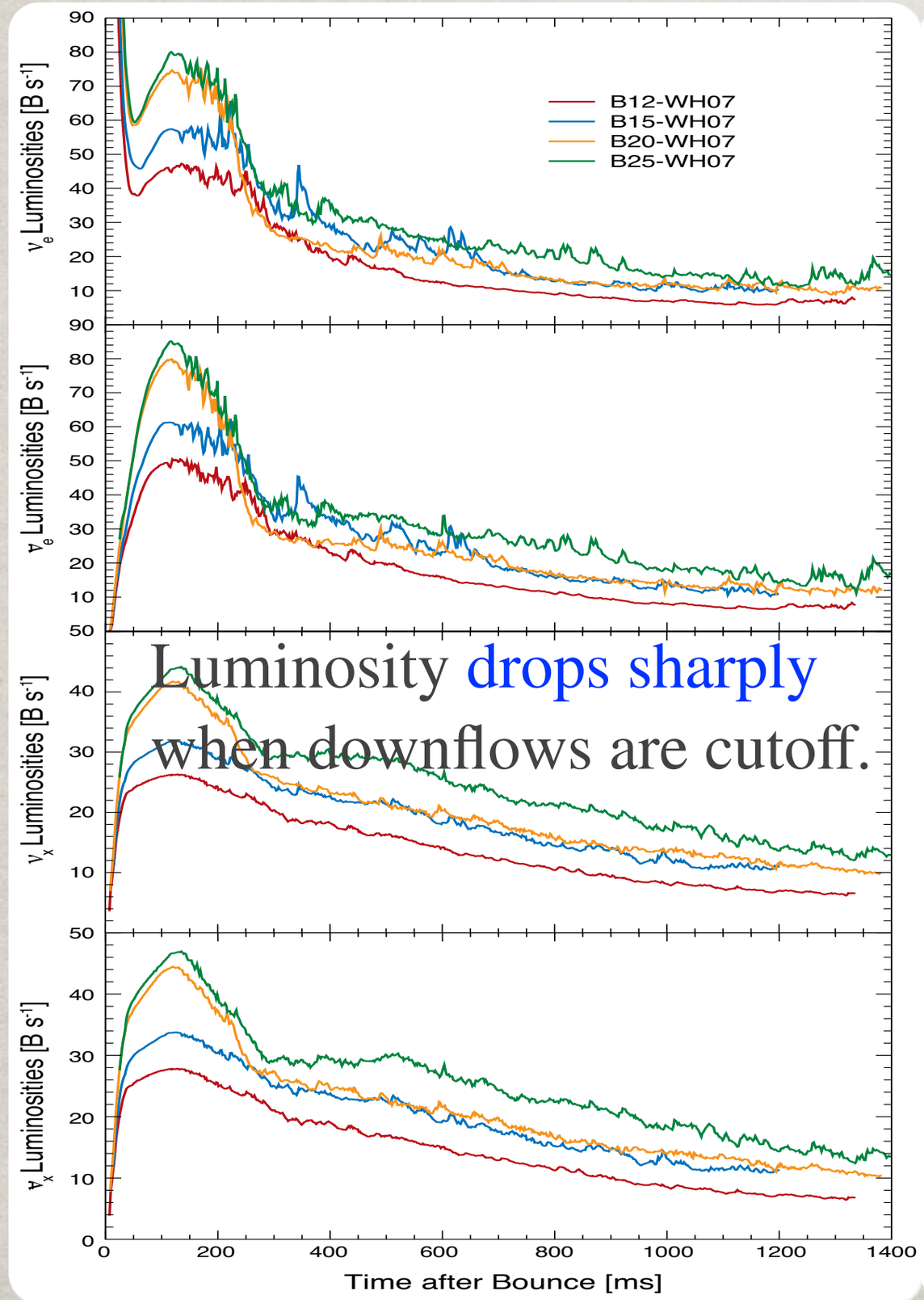

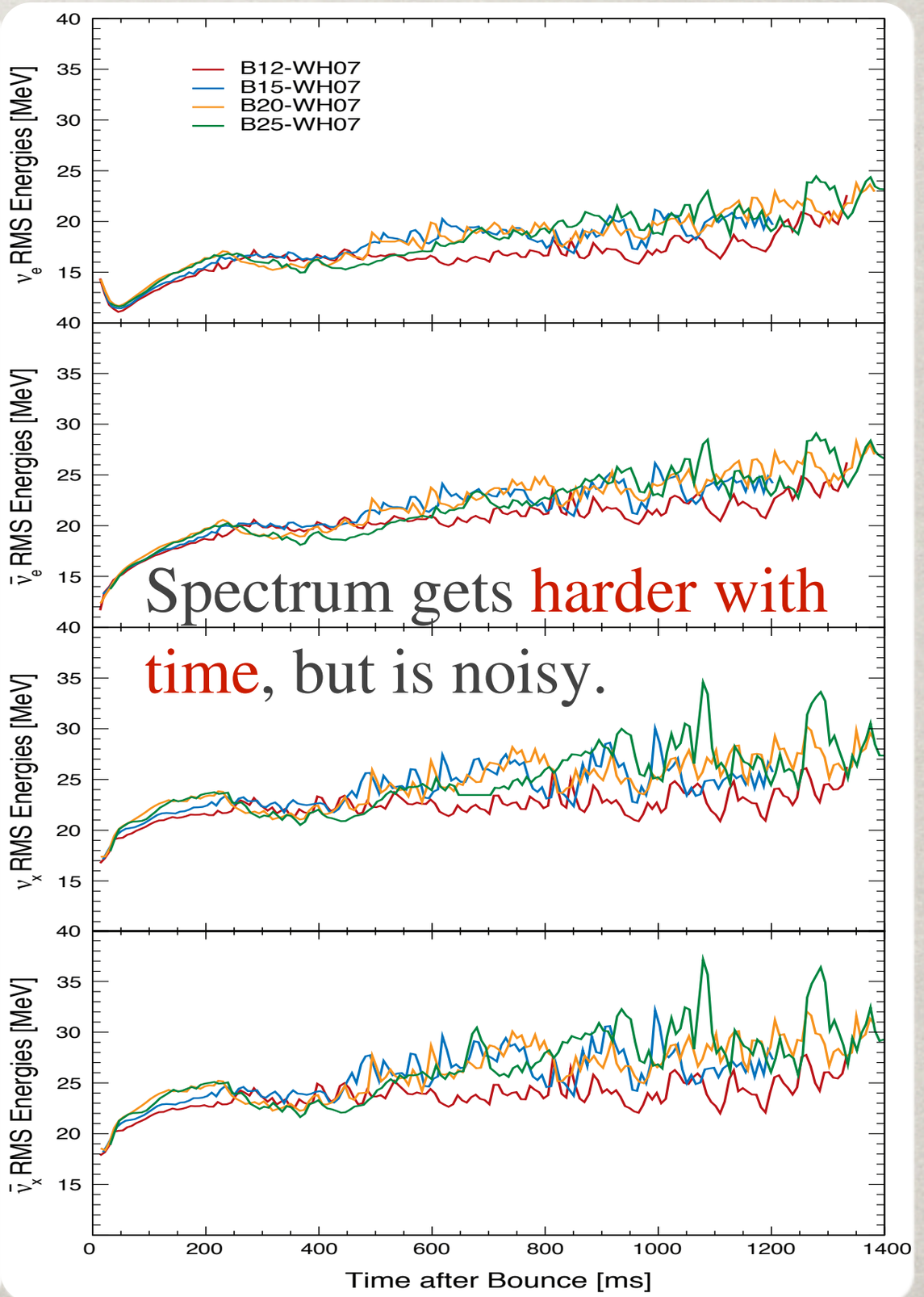

Gravitational Waves

GW signals (by Yakunin & Marronetti) are a qualitative match to predictions based from parameterized models by Murphy, Ott, & Burrows (2009)

However, in this self-consistent model time for the explosion to develop is significantly shorter.

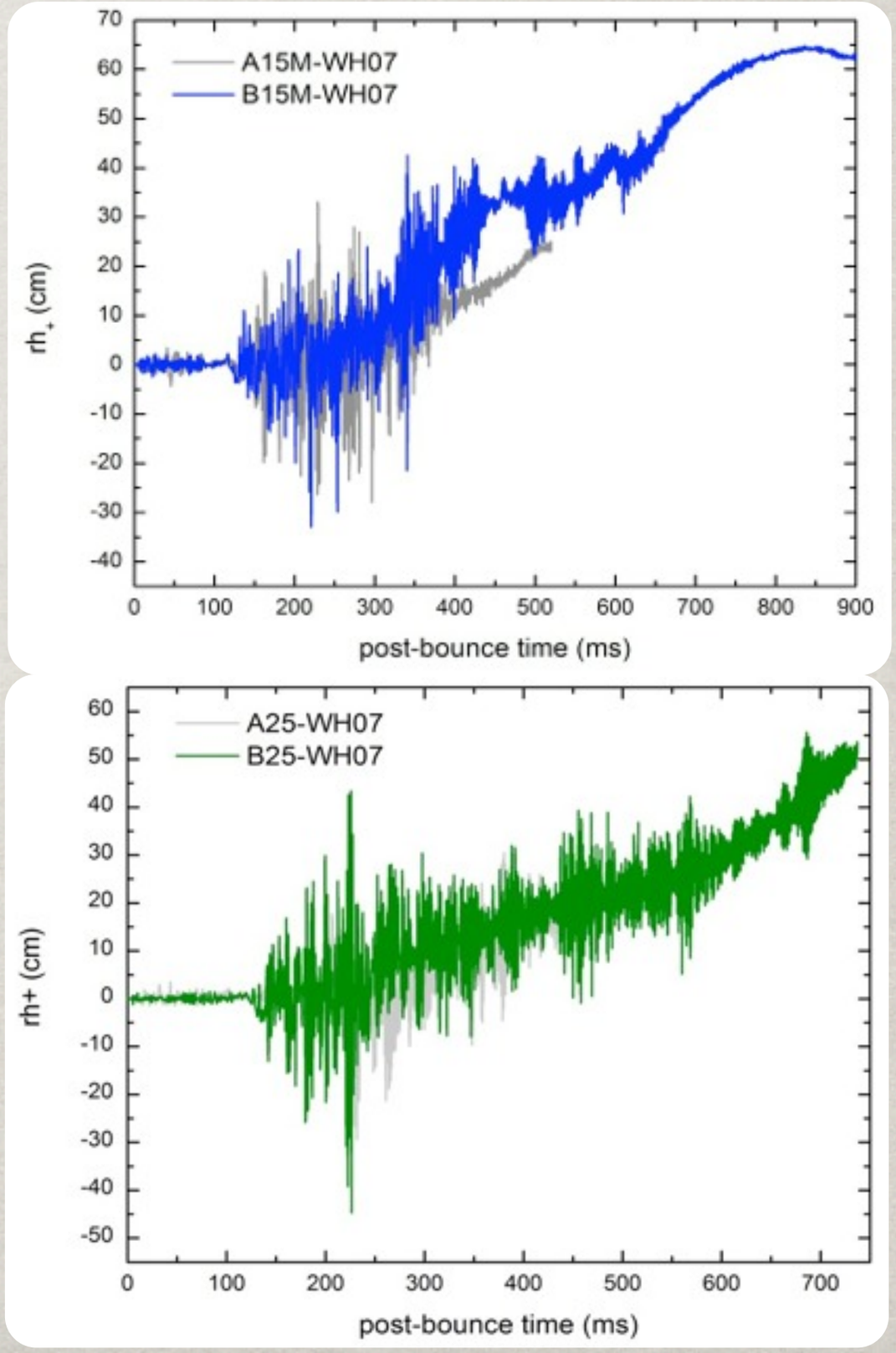

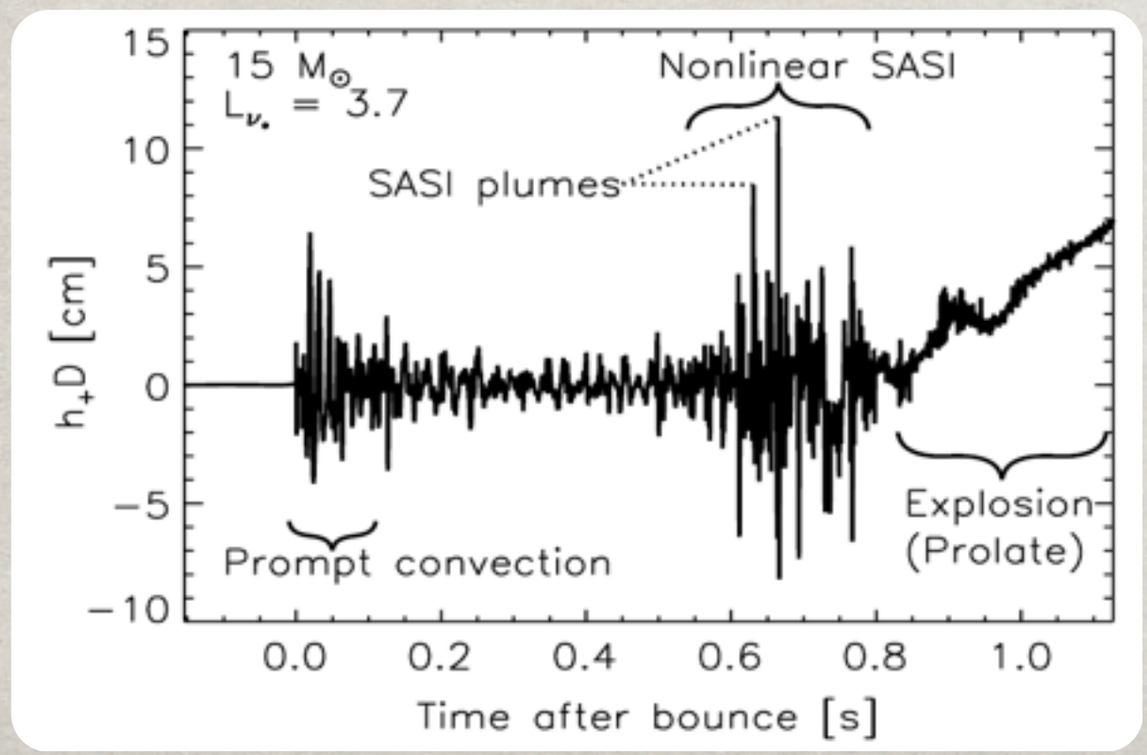

Anatomy of a GW Signal

Gravity Wave signal shows 3 separate phases

1) Prompt Convection & Early Shock Deceleration

2a) SASI-Induced Shock Excursions leads to lower-frequency envelope.

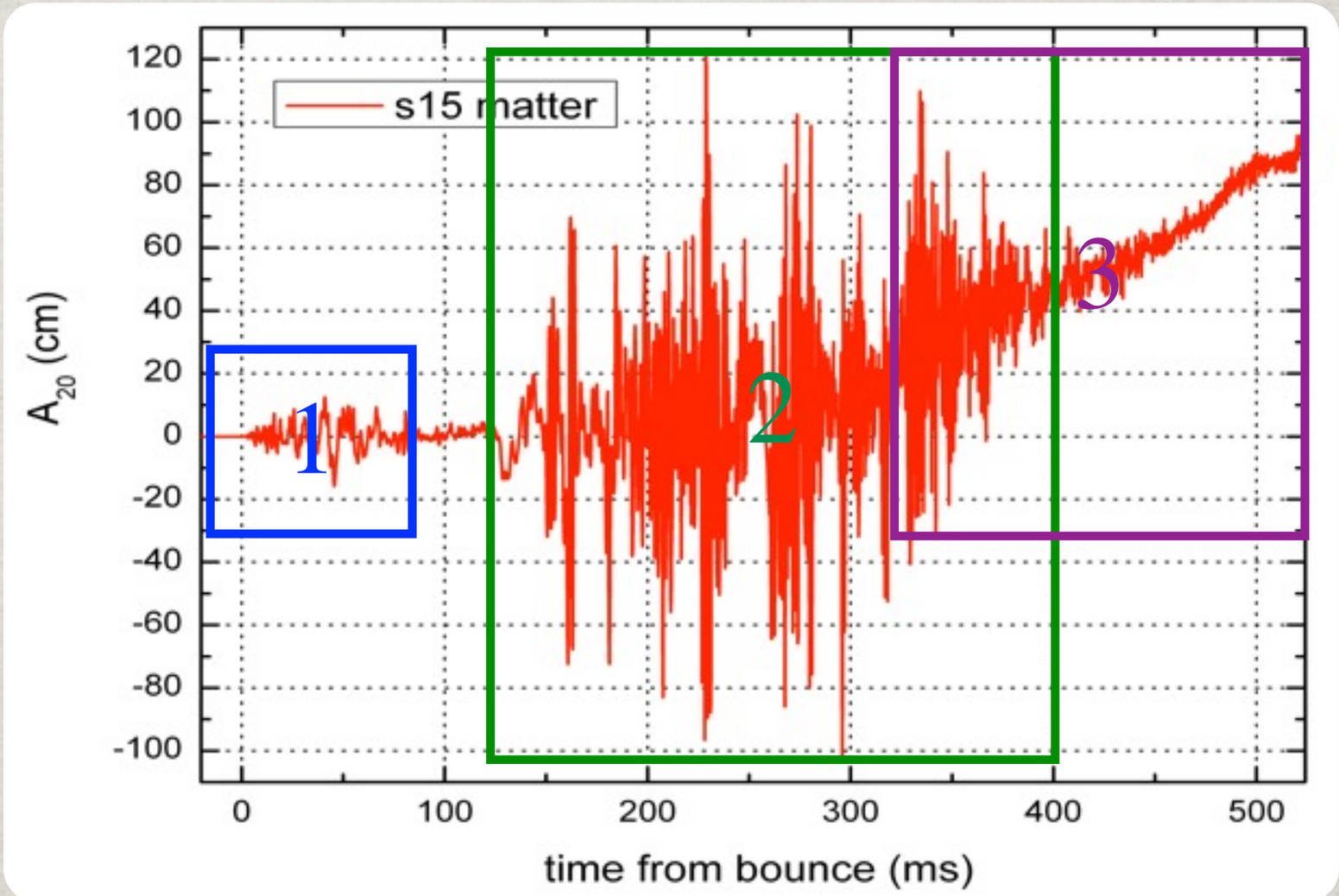

2b) Impingement of downflows on the PNS, resulting from neutrino-driven convection and SASI, lead to higher-frequency variations.

3) Prolate Explosion/Deceleration at Shock

3D SIMULATIONS

CHIMERA3D (2009)

Ran 150 ms on 11,552 processors (12M CPU-hours) with 304 adaptive radial zones, 2.4° in latitude & longitude.

3D model shows similar behavior to 2D at 150 ms after bounce.

To match 2D, resolution of 0.7° in latitude and longitude would be needed. This requires 131,072 processors.

CHIMERA3D (2011)

Ran 20 ms on 8096 processors with 512 adaptive radial zones, 2.8° in latitude and longitude, limited by Courant timestep of 38 nanosecond at the pole.

To run models to late times requires freezing the core or a different grid.

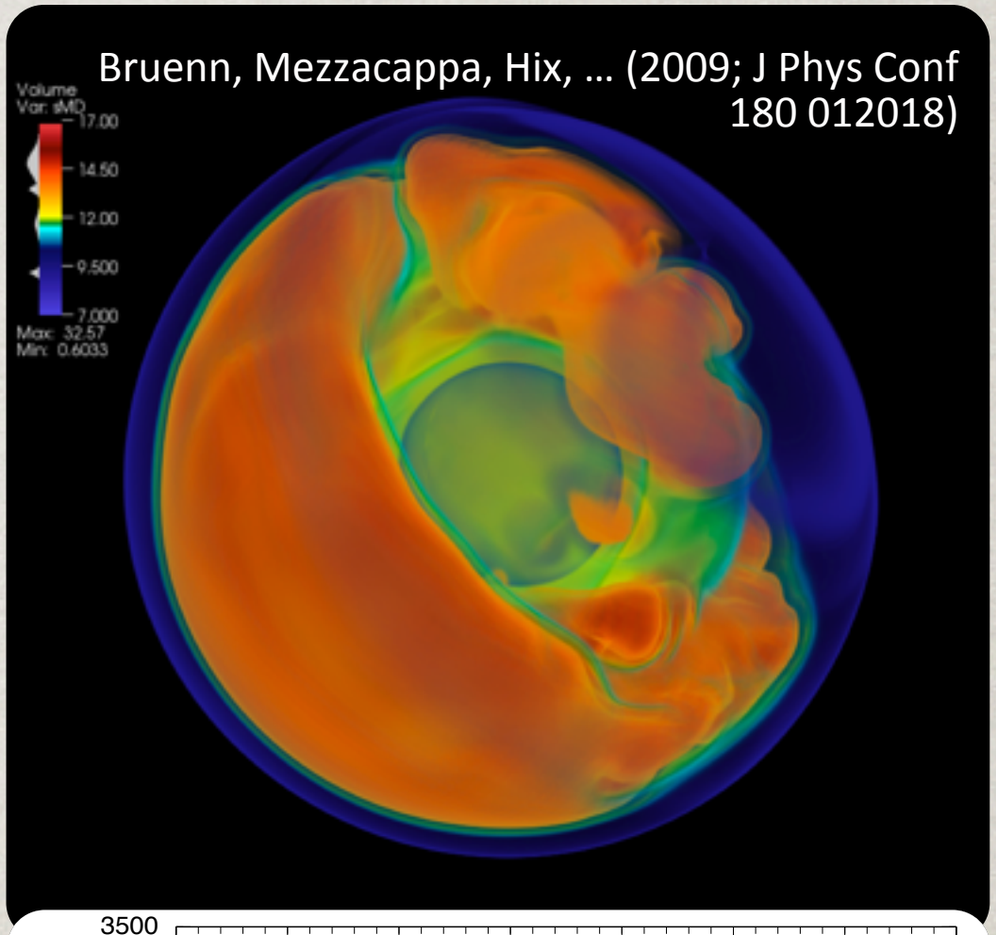

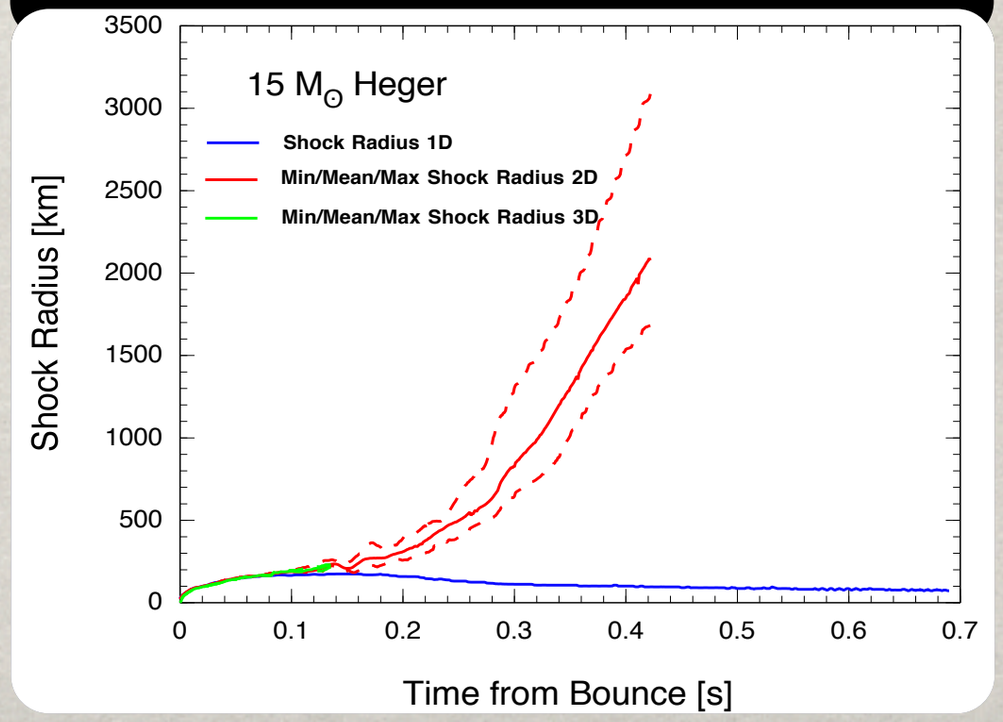

C15-WH07 3D

One solution is to use fewer zones in latitude & longitude.

However 2.8° is already ¼ of our 2D resolution.

For our 2013 model, we've adopted a grid which is uniform in cosine of latitude, with 180 zones of widths from ⅔° to 8°.

Consumed 70M core-hours in 2013 to run ~200 ms.

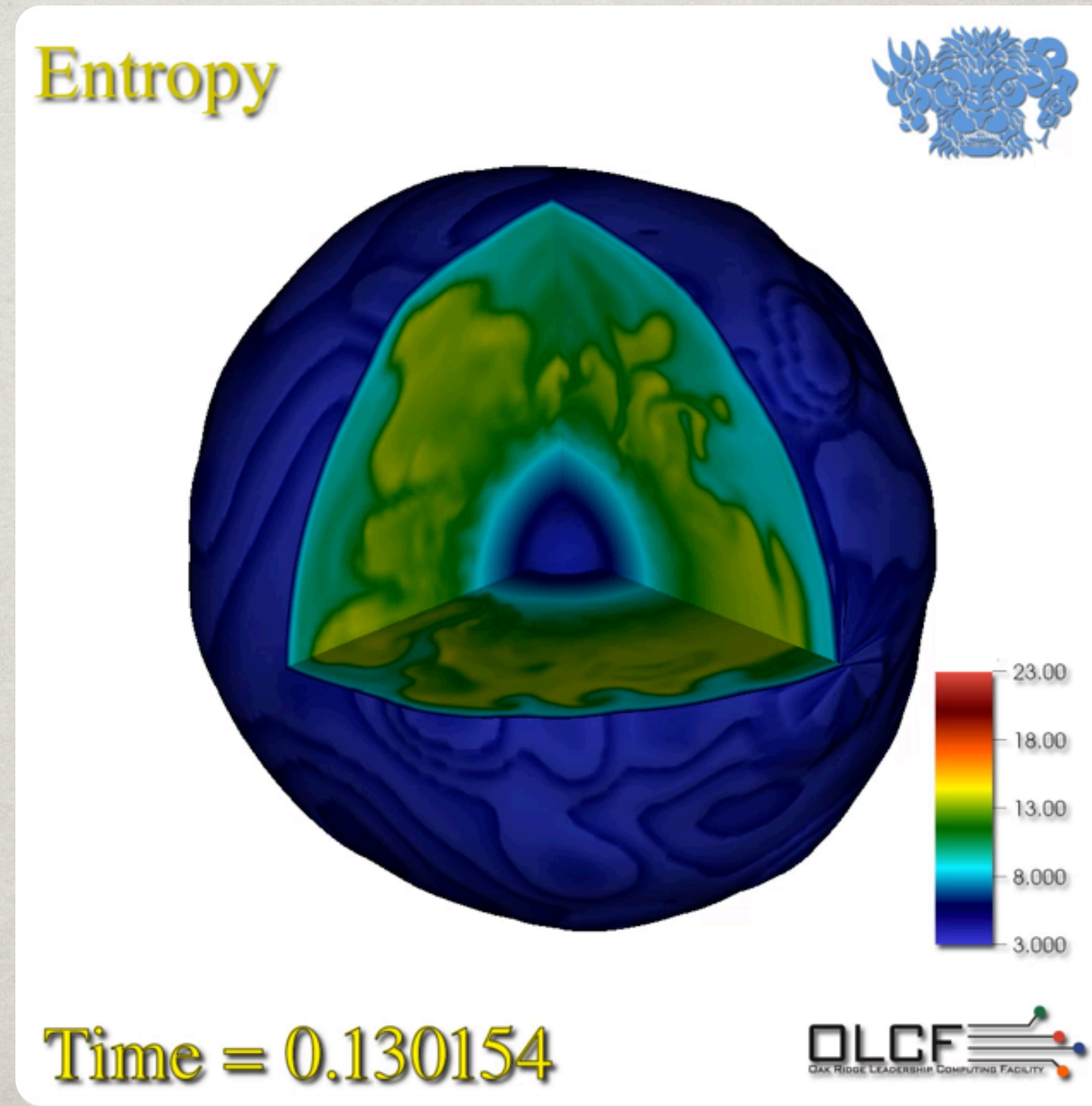

How does 3D compare?

The vital question is "How well do 2D models follow the behavior of 3D?"

Parameterized models produce mixed answers to this question. Some find 3D to be favorable, but most find 3D to impede the explosion.

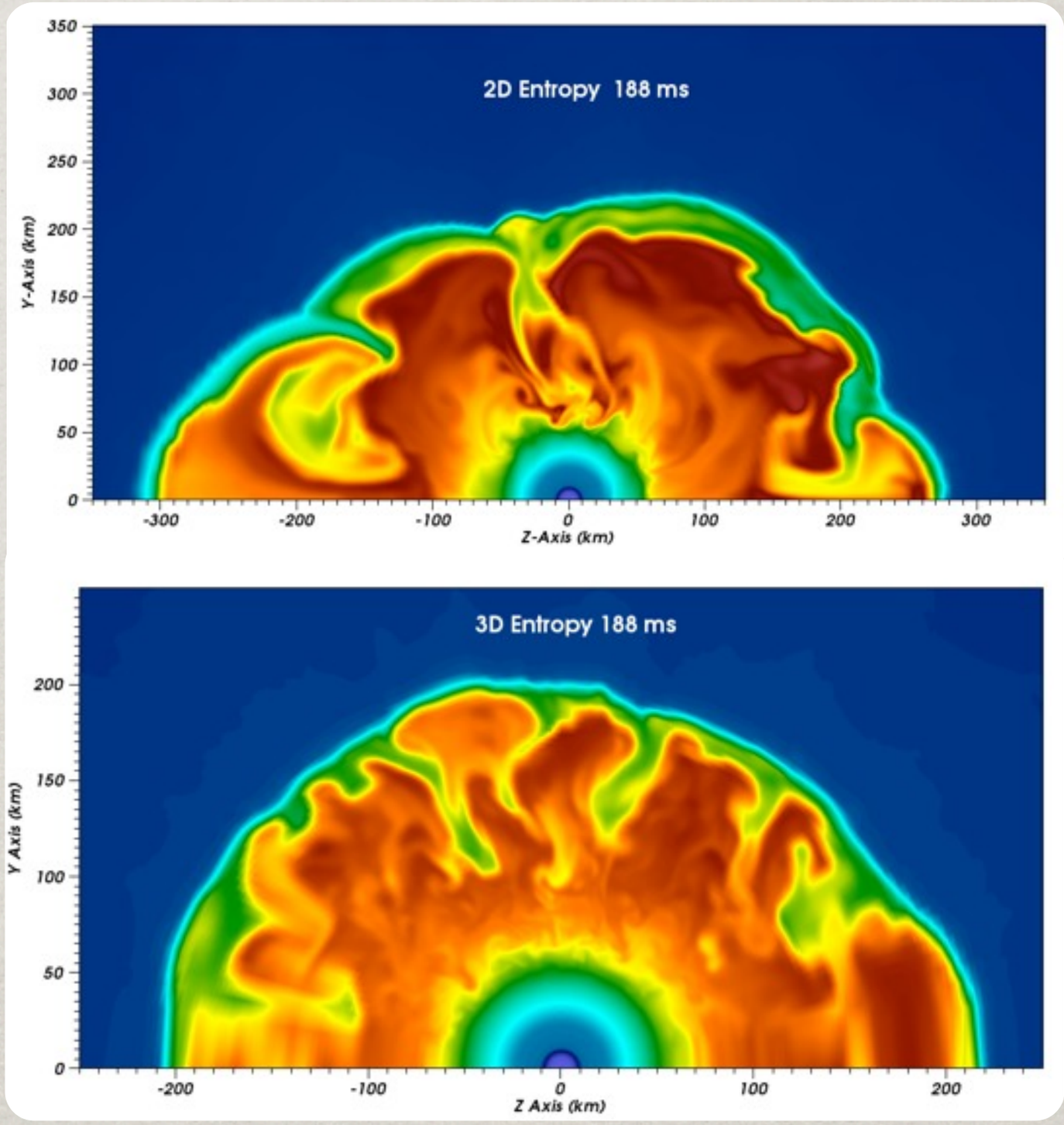

How does 3D compare?

The vital question is "How well do 2D models follow the behavior of 3D?"

Parameterized models produce mixed answers to this question. Some find 3D to be favorable, but most find 3D to impede the explosion.

Thus far, we find that 3D models stay quasi-spherical longer and exhibit longer delays the onset of explosion.

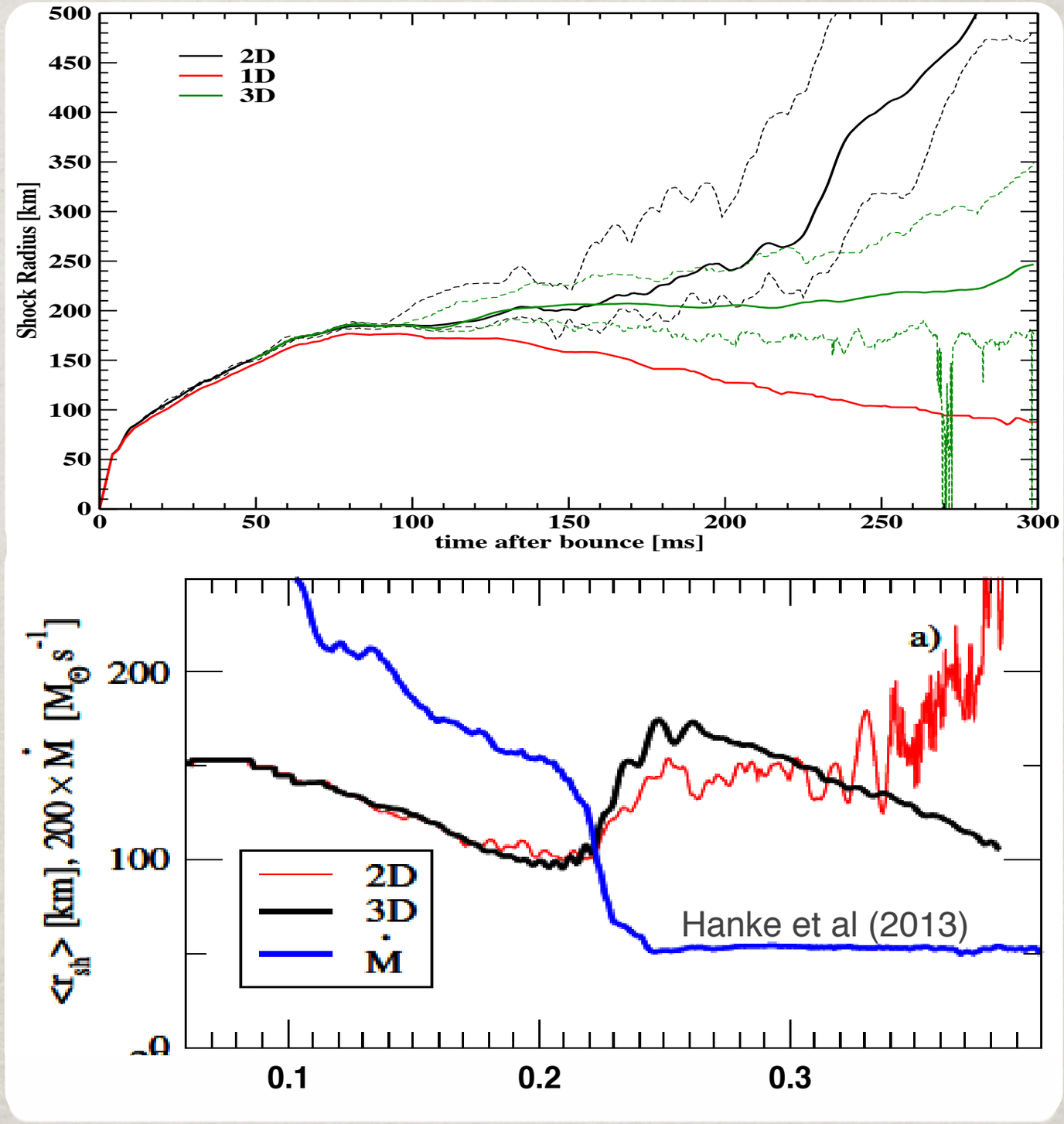

This agrees with self-consistent models from Hanke et al (2013).

Realistic?

Core-Collapse Supernovae combine an extraordinary range of physics: nuclear physics (electron and neutrino capture on nuclei; nuclear EoS; thermonuclear kinetics), magneto-hydrodynamics (MHD), radiation transport, General Relativity, etc. This requires multiphysics modeling.

A series of spherically symmetric studies uncover some of the physics (and level of numerical approximation) required to make a model realistic, at least in the early phases of CCSN.

These reveal the danger of ignoring GR, inelastic scattering and observer corrections.

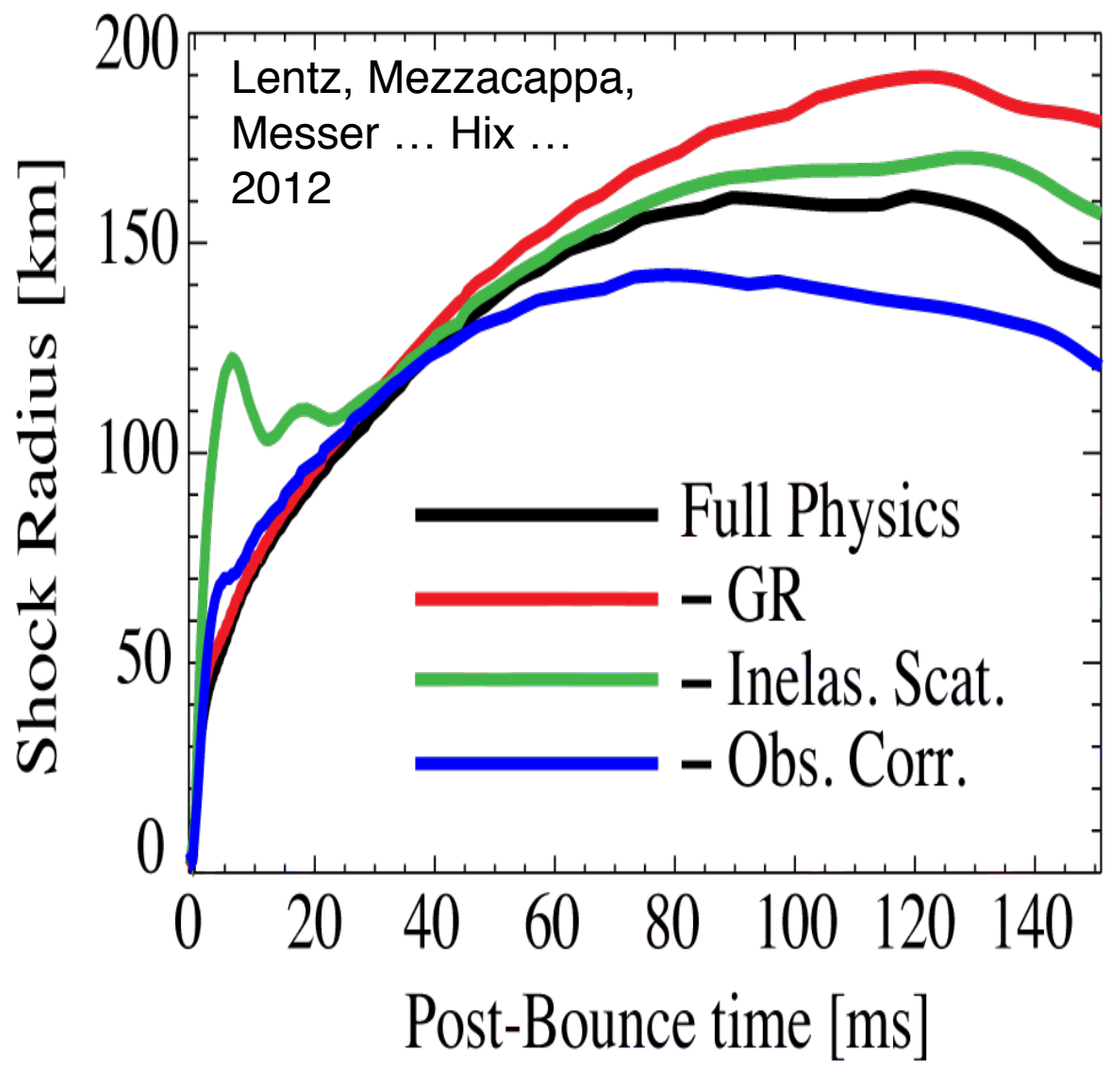

Nuclei in Core Collapse Supernovae

Much of the active phase of the neutrino reheating mechanism occurring in matter composed of shock-dissociated free nucleons.

Thus the occurrence of nuclei and the application of nuclear physics is limited. Exceptions include

- Weak interactions of pre-shock matter, during collapse and above the shock after bounce (neutrino-nucleus scattering and electron and neutrino captures on nuclei).
- Behavior of Nuclear Matter in the Proto-neutron Star (the nuclear Equation of State).
- Rebuilding of nuclei in cooling ejecta and shock heating of for overlying layers lead to nucleosynthesis; iron-peak and intermediate mass (Si-Ca) elements, νp & r processes.

Captures on Nuclei

Entropy of iron core is low (S/k ~1) so few free nucleons are present. Thus e^- and ν capture on heavy nuclei via $f_{7/2} \Leftrightarrow f_{5/2}$ GT transition should dominate. (Bethe,Brown, Applegate & Lattimer 1979)

During collapse, average mass of nuclei increases, quenching e^- capture (at N=40) in IPM.

Thermal unblocking and first forbidden were considered but rates were too small. (Fuller 1982, Cooperstein & Wambach 1984)

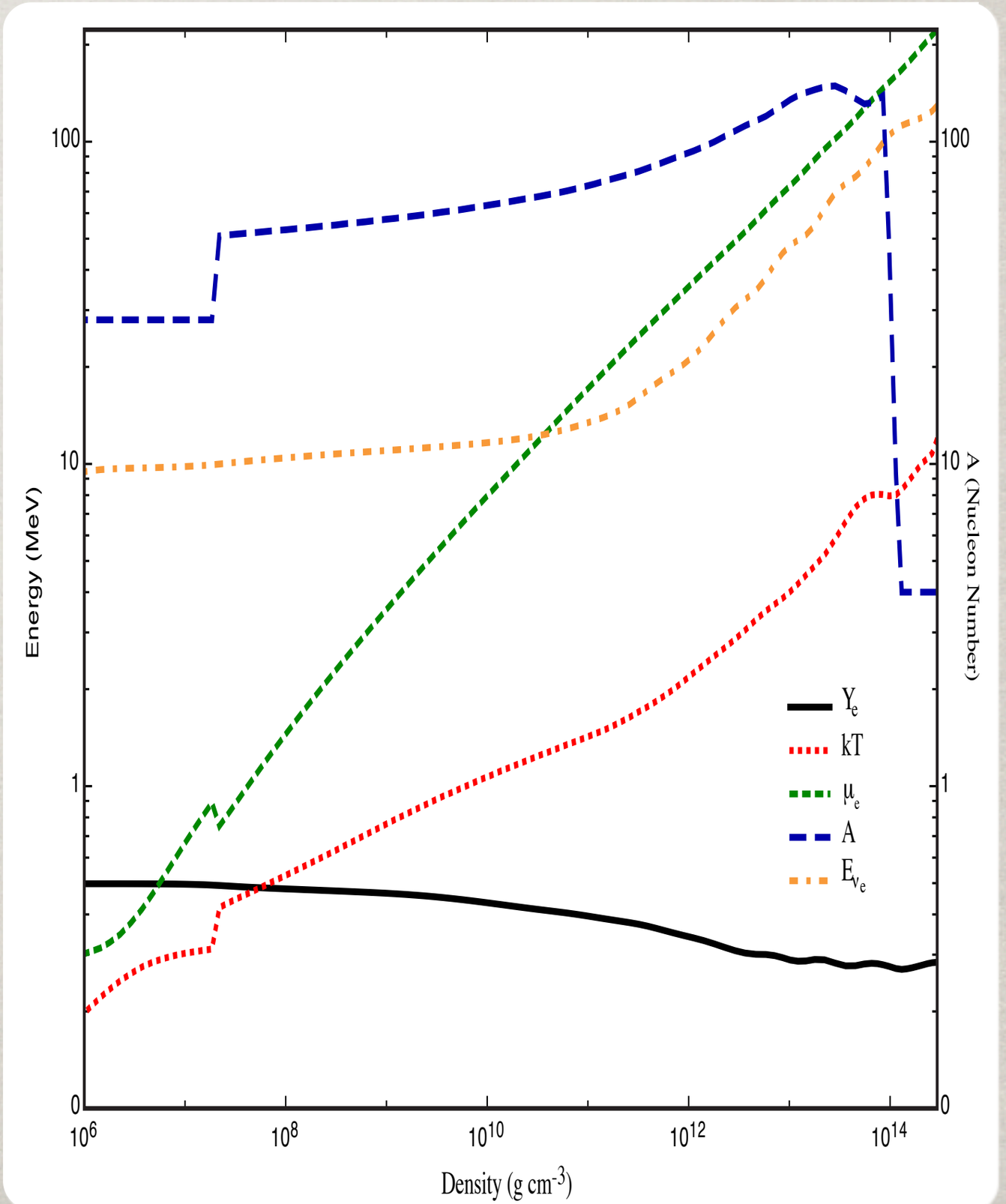

What Rates are needed?

Change in lepton abundance ($Y_l = Y_e + Y_\nu$) occurs gradually up to ~3×10^{12} g cm^{-3}.

Beyond 3×10^{12}, rate of electron capture is determined largely by blocking.

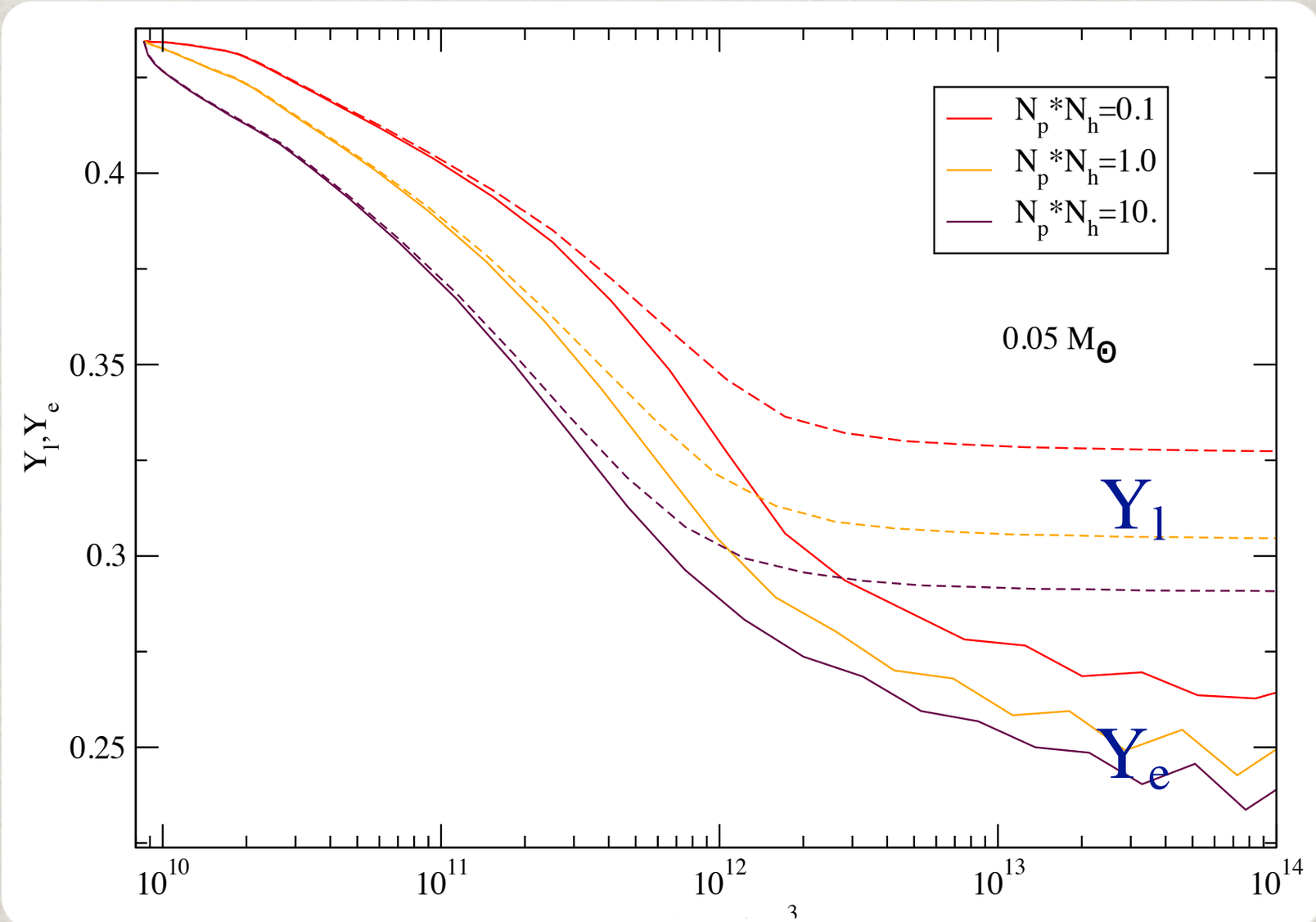

What Rates are needed?

Change in lepton abundance ($Y_l = Y_e + Y_\nu$) occurs gradually up to ~3×10^{12} g cm^{-3}.

Beyond 3×10^{12}, rate of electron capture is determined largely by blocking.

Average Nuclear Mass by 10^{12} is 100 or more with many nuclei contributing.

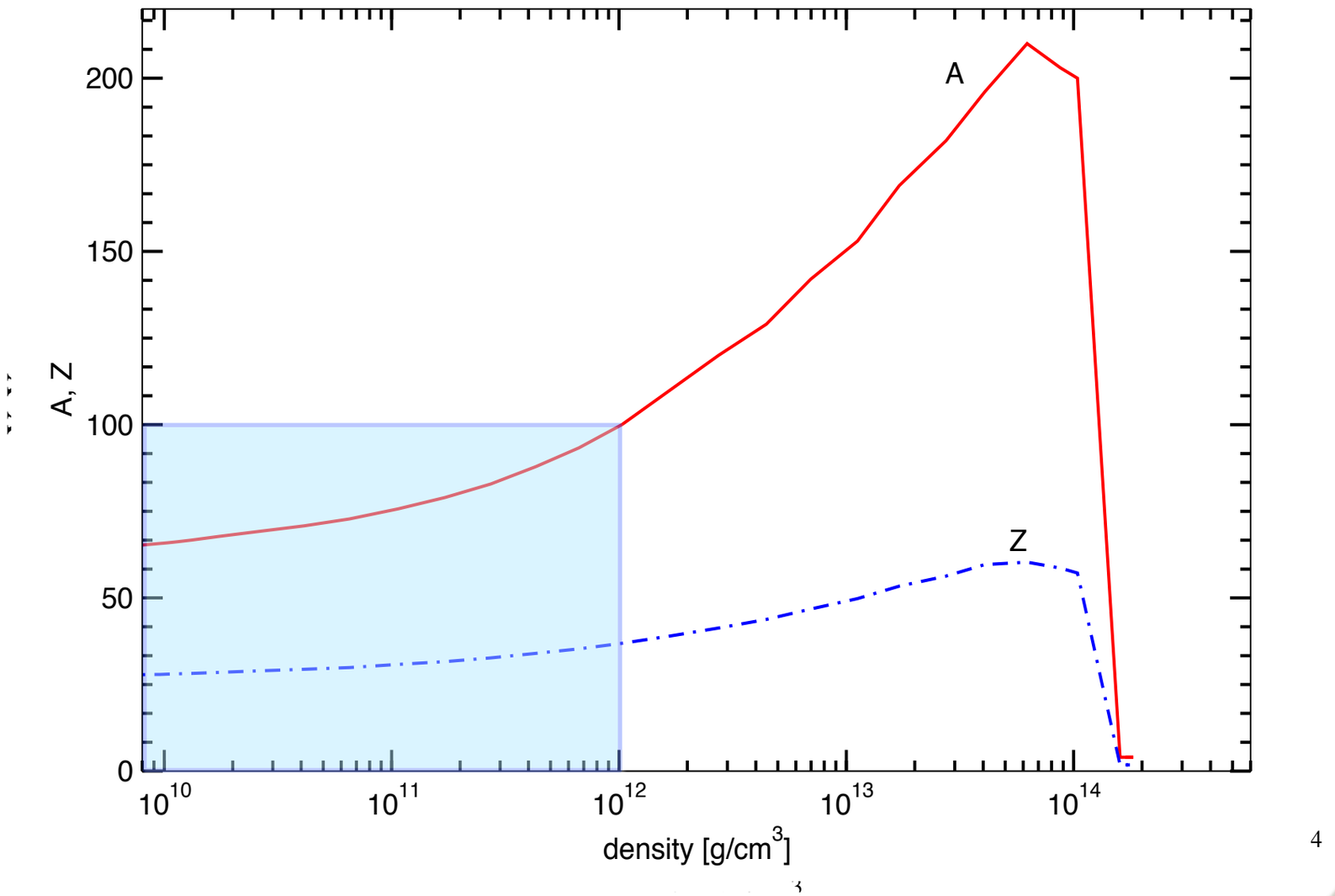

What Rates are needed?

Change in lepton abundance ($Y_l = Y_e + Y_\nu$) occurs gradually up to ~3×10^{12} g cm^{-3}.

Beyond 3×10^{12}, rate of electron capture is determined largely by blocking.

Average Nuclear Mass by 10^{12} is 100 or more with many nuclei contributing.

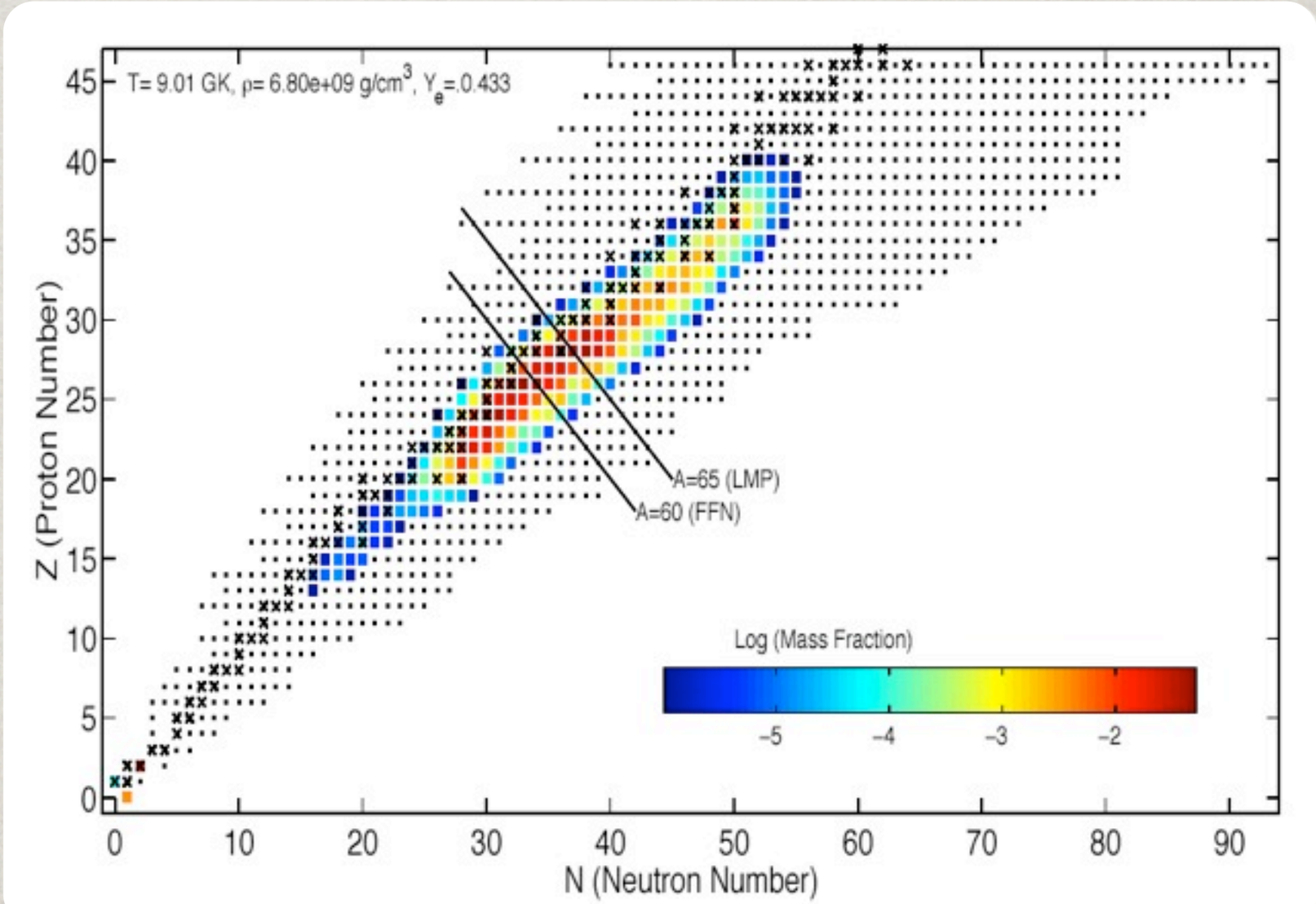

What Rates are needed?

Change in lepton abundance ($Y_l = Y_e + Y_\nu$) occurs gradually up to ~3×10^{12} g cm^{-3}.

Beyond 3×10^{12}, rate of electron capture is determined largely by blocking.

Average Nuclear Mass by 10^{12} is 100 or more with many nuclei contributing.

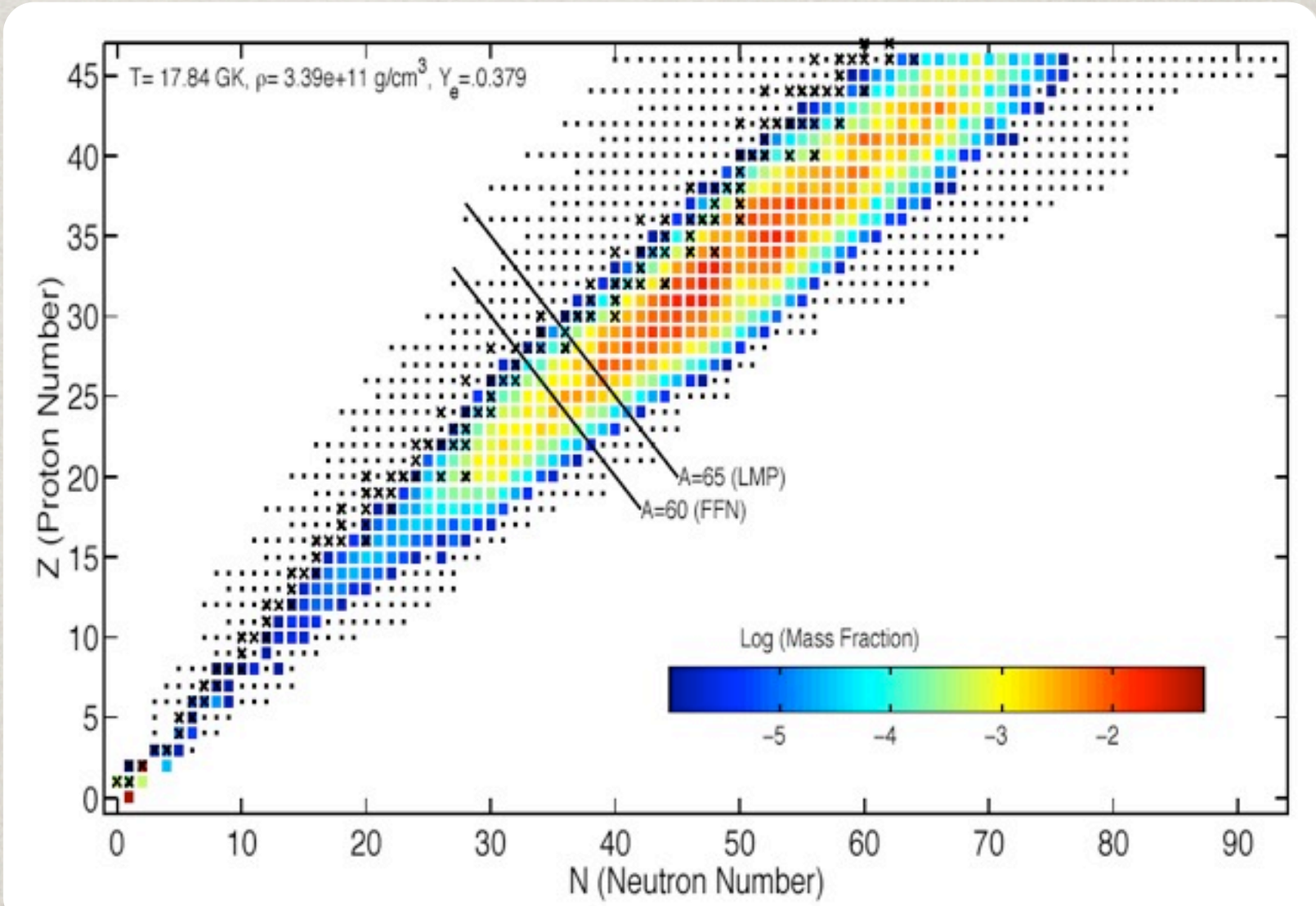

Need theory for the large number of reactions of interest and experiments to constrain this theory.

Beyond IPM

Because capture rates on heavy nuclei → 0 under IPM, captures on protons were thought to dominate.

Beyond IPM, Shell Model Diagonalization calculations could provide the answer but are limited to A<65.

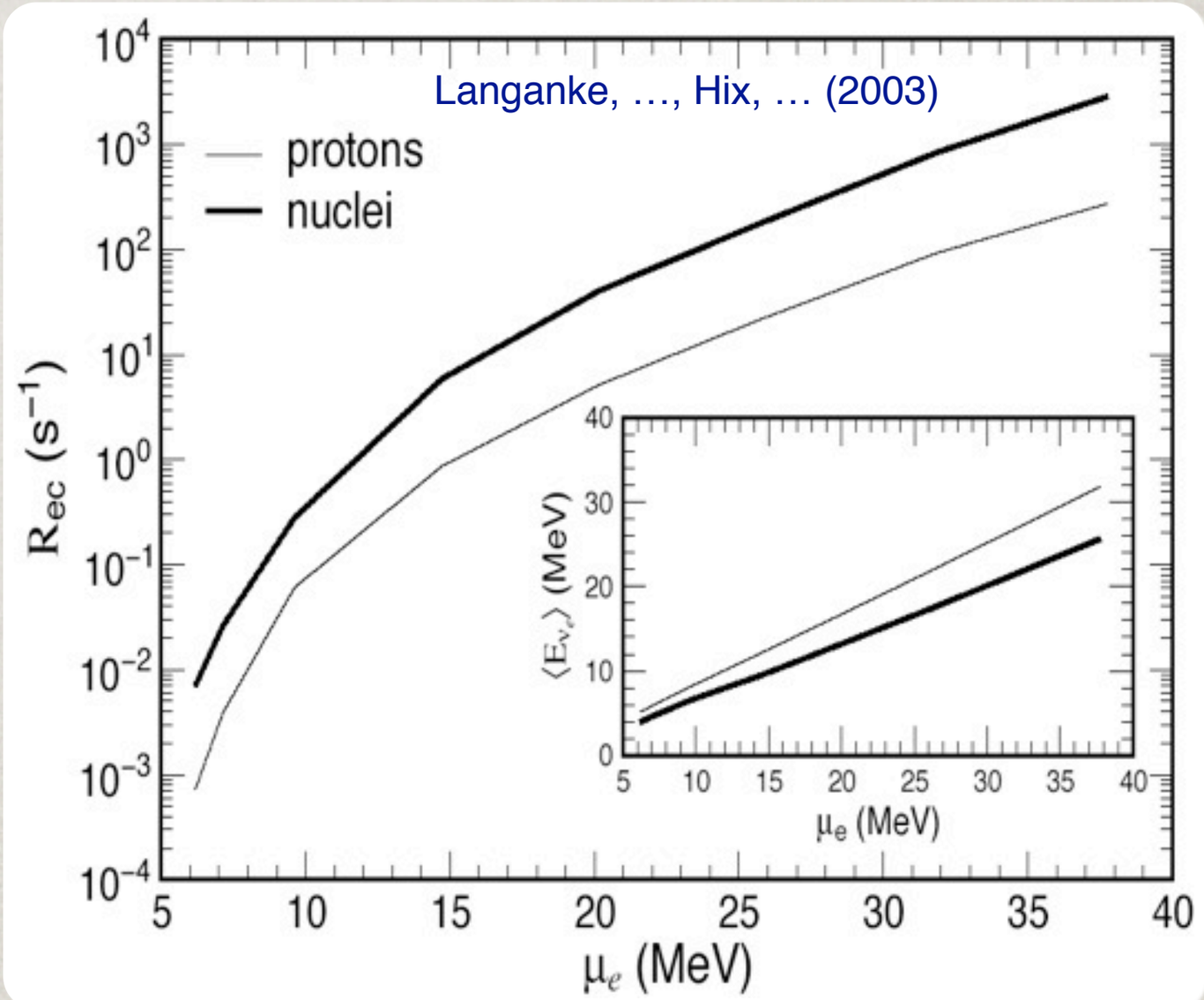

Langanke et al (2003) employed a hybrid of shell model (SMMC) and RPA to calculate a scattering of rates for A<110. Electron/neutrino capture on heavy nuclei remains important throughout collapse.

The impact of e⁻ Capture

Continued electron capture in the core reduces Y_e, which changes the initial PNS mass by 20%.

Reduced electron capture in the outer layers slows the infall, reducing the ram pressure opposing the shock reducing the long term impact in 1D.

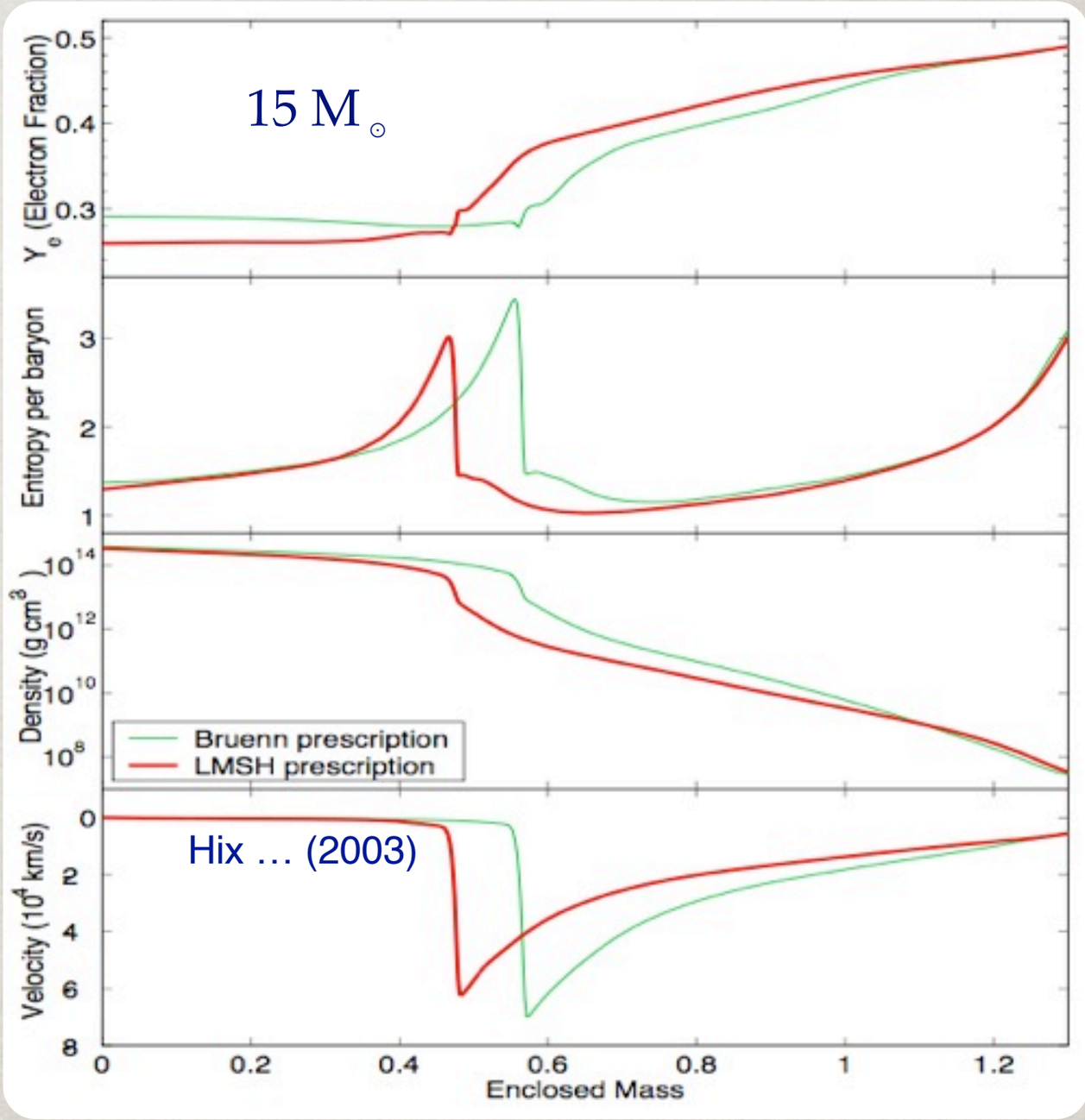

Juodagalvis, Langanke, Hix, Martínez-Pinedo, & Sampaio (2010) published an improved tabulation of nuclear electron capture for use in SN models.

Inelastic ν-Nucleus Scattering

As with electron/neutrino capture, advances in nuclear structure physics are improving our understanding of other neutrino-nucleus interactions.

While coherent, elastic ν-nucleus scattering has long been considered, inelastic ν-nucleus scattering (INNS) has often been ignored. The exception is Bruenn & Haxton (1991) which used INNS rate calculated for ^{56}Fe at T=0.

Juodogalvis, Langake, Martinez-Pinedo, Hix, Dean & Sampaio (2005) calculated INNS for 40 isotopes of Mn, Fe, Co & Ni at finite temperature using a combination of shell model and RPA. A tabulation of NSE-averaged rates has been produced for use in supernova simulations.

Dynamical Effects of INNS?

During collapse, INNS works like NES to equilibrate the neutrino distribution. However there is little effect from this addition.

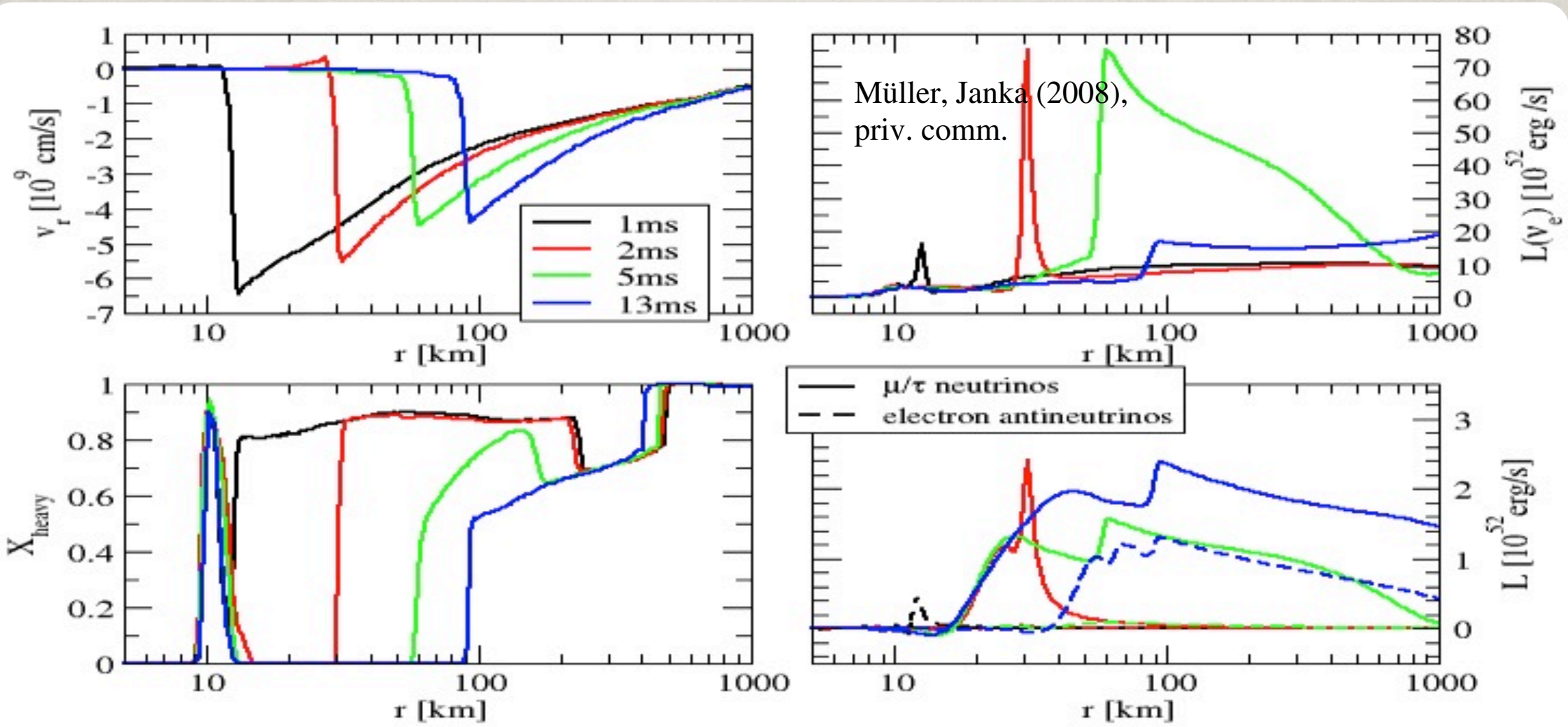

After bounce, heating rate just above shock is boosted (2-3x). However, heating of supersonically infalling matter is ineffective, so dynamics are little effected.

INNS Observable Effects

The impact of INNS is most pronounced at higher energies.

The high energy tail of ν spectra are strongly suppressed during this short interval after bounce.

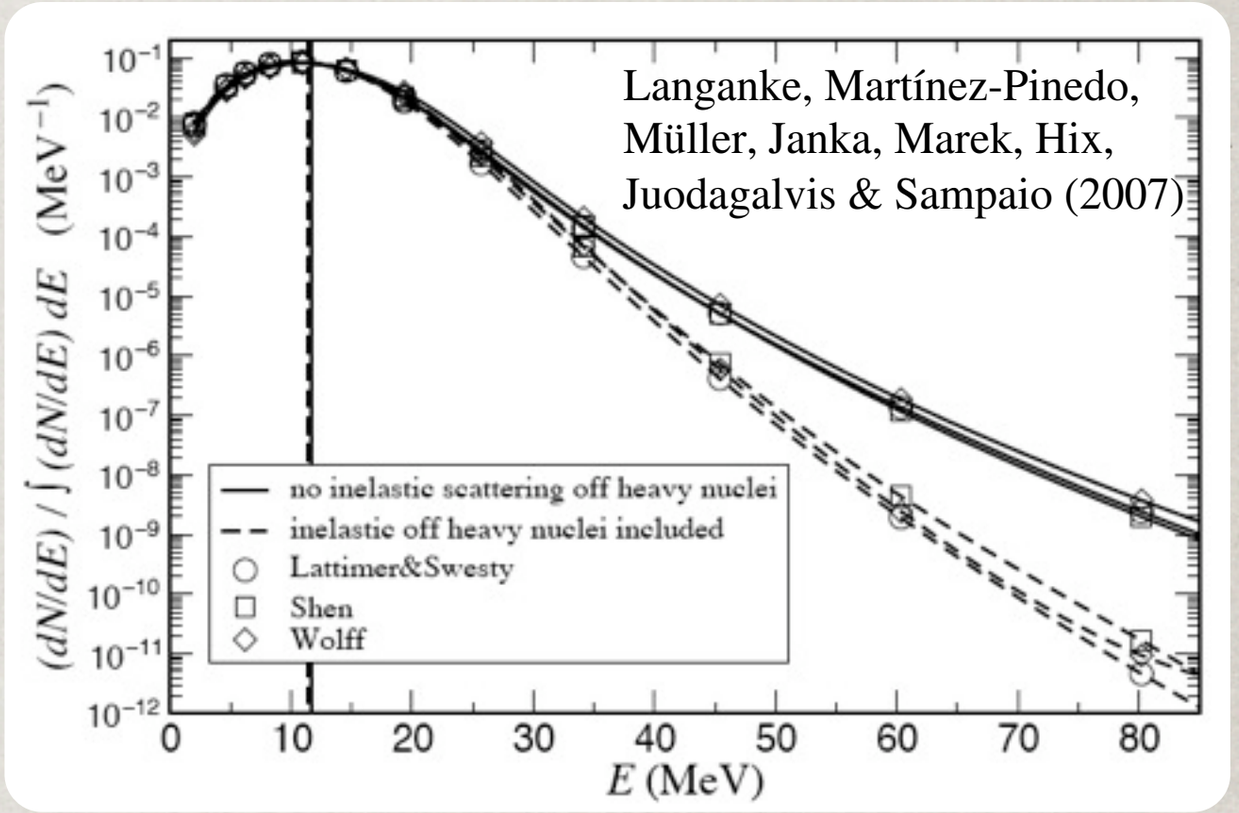

Material	$\langle\sigma\rangle$ (10^{-42} cm^2)		Reduction
	With INNS	Without INNS	
e	0.106	0.110	3%
d	4.92	5.36	8%
^{12}C	0.050	0.080	37%
^{12}C (N_{gs})	0.046	0.071	35%
^{16}O	0.0053	0.0128	58%
^{40}Ar	13.4	15.1	11%
^{56}Fe	6.2	7.5	17%
^{208}Pb	103.3	124.5	17%

Has a surprisingly large effect on potential terrestrial ν detectors, especially those with C and O which have high threshold energies.

The Equation of State

The equation of state closes the system of hydrodynamic equations by relating the pressure to the internal energy (or temperature or entropy), density and composition.

For supernovae, it includes contributions from photons, degenerate electrons & positrons, and nuclei or nuclear matter. In regions where Nuclear Statistical Equilibrium can be assumed, the supernova EOS also provides the nuclear composition.

Three commonly used SN EoS of the last 2 decades.

- LS EoS (Lattimer-Swesty 1991)
  Liquid drop model, Compressibility – 180 MeV
- STOS EOS (Shen, Toki, Oyamatsu & Sumiyoshi 1998)
  Relativistic mean field theory, Compressibility – 281 MeV
- Wilson EOS (Mayle & Wilson 1991, McAbee & Wilson 1994)
  Empirical Relation of Baron, Cooperstein & Kahana (1985), constrained by relativistic Brueckner-Hartree-Fock calculations of Muther, Prakash & Ainsworth (1987), Compressibility – 200 MeV. Includes pions at high density and pasta phase.

Impact of Equation of State

Spherically symmetric models can be used to study the effects of the EoS on the initial phase of CC supernovae.

Differences persist for more than 200 ms after bounce.

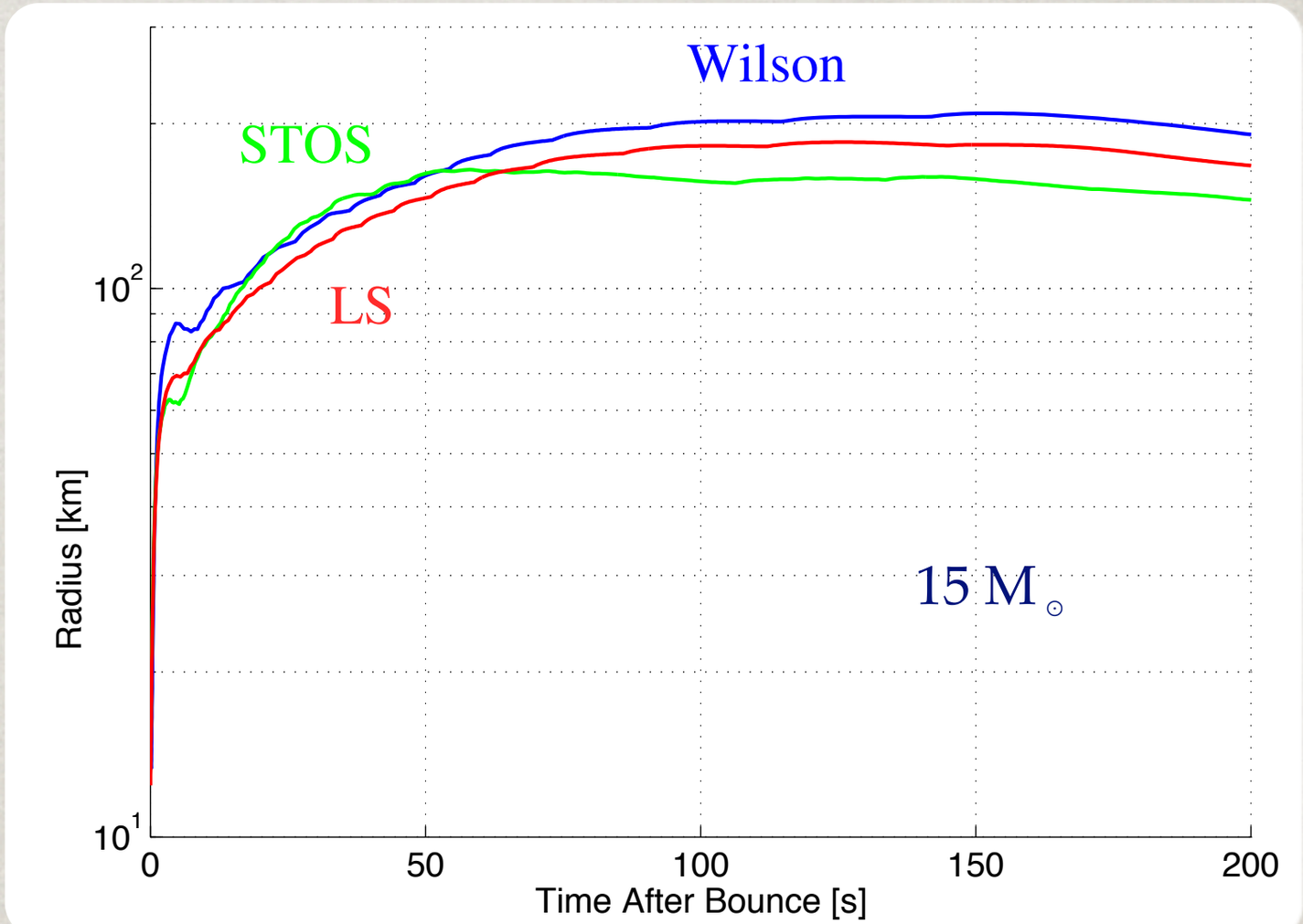

STOS: Shock launches slowly and peaks near 50 ms with smallest shock stall radius.

Wilson: Shock launches strongly, peaking near 150 ms with largest shock stall radius.

Composition

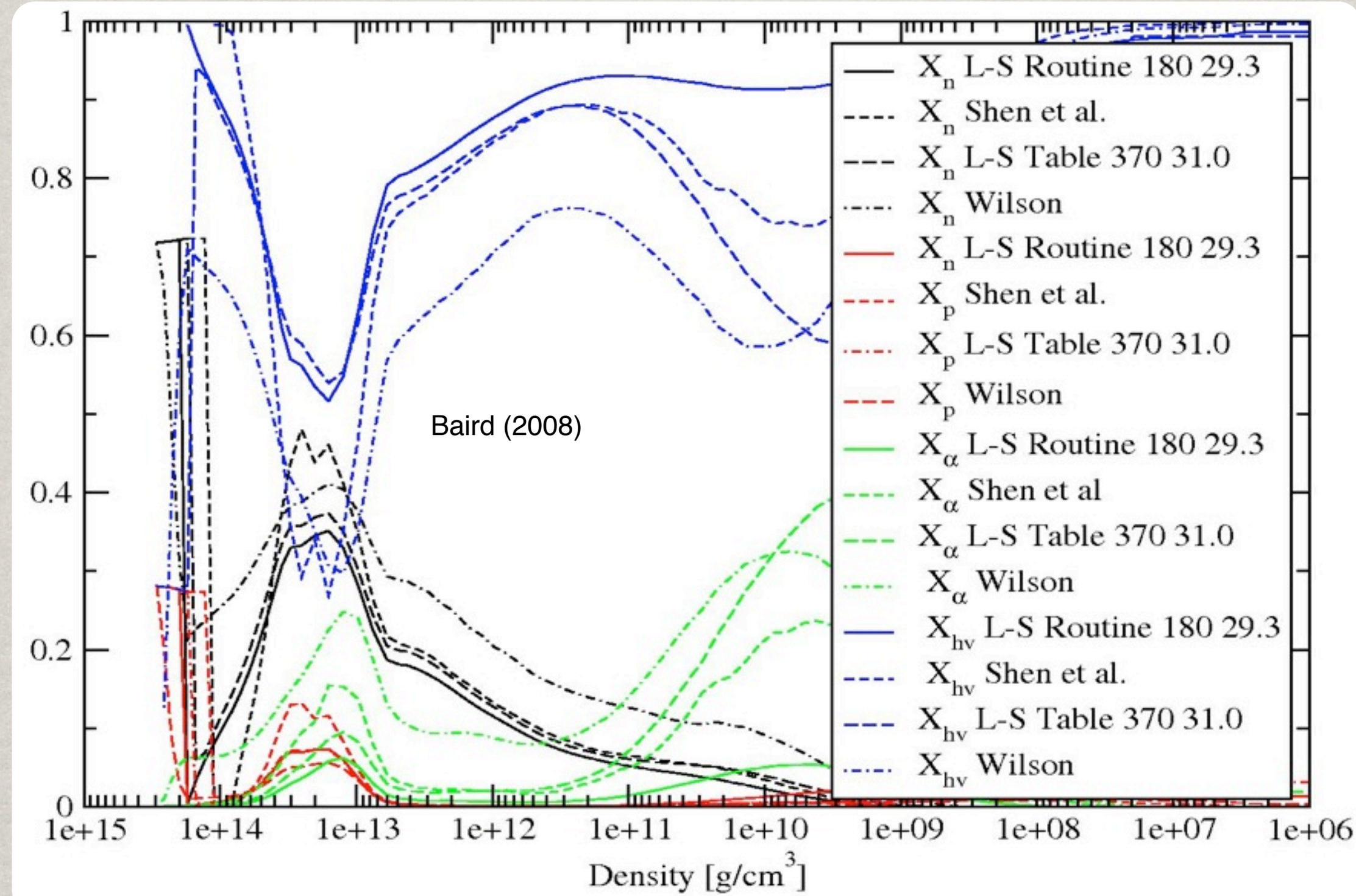

Composition of unshocked matter shows large differences.

Interplay of EOS & Nuclear Electron Capture

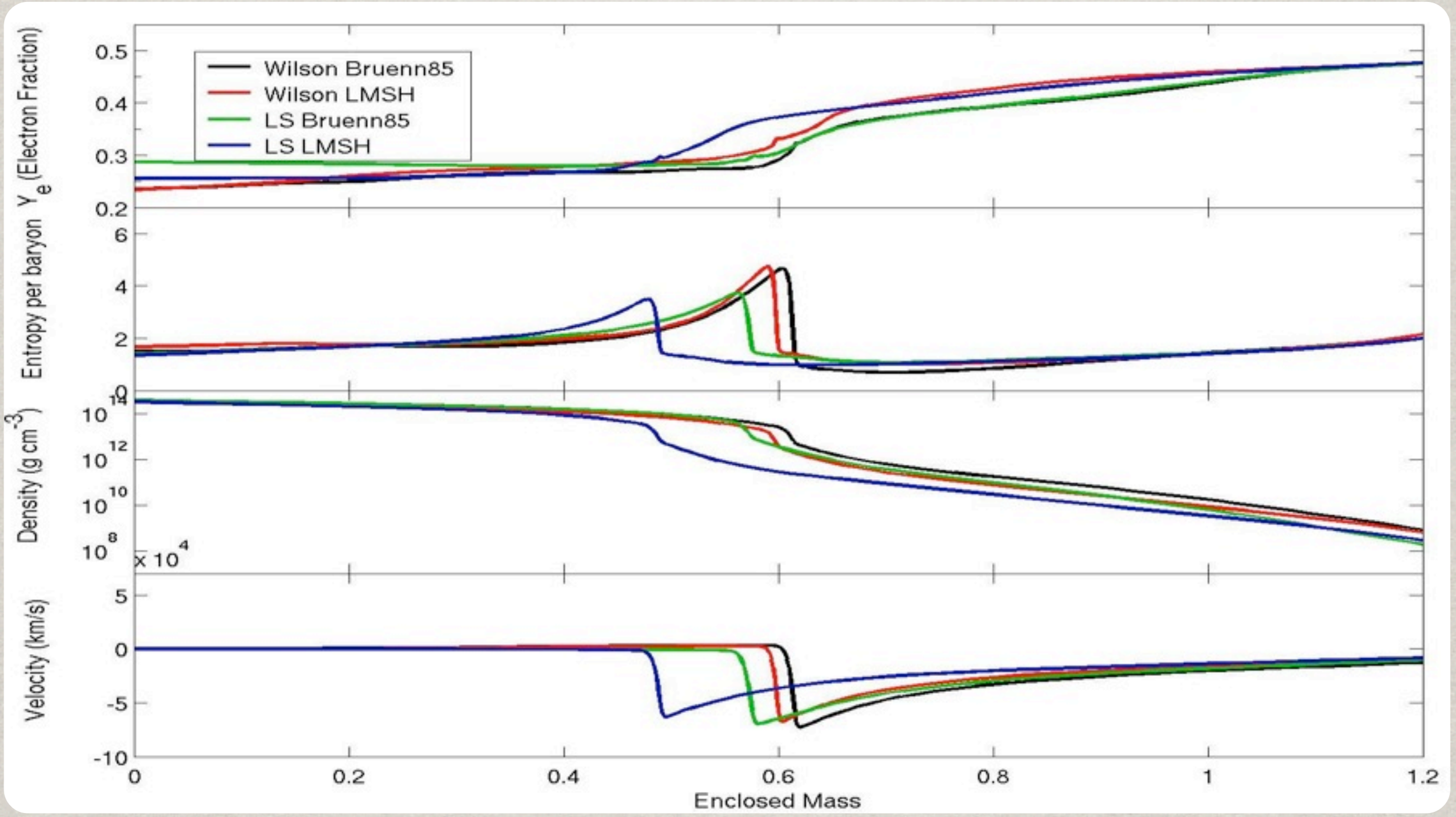

Composition provided by the EOS impacts relative strength of opacities, requiring opacities to be re-examined in light of progress on the EOS.

Exotic EOS

Aside from assemblage of neutrons and protons into ordinary nuclei or nuclear matter, other possibilities have been considered, including

Extended nuclear forms, "pasta", just above nuclear density

Kaon or Pion condensates

Quark matter or strange matter

To affect CCSN, these exotic forms must exert their influence before the explosion is re-energized (several hundred ms after bounce).

Example:

Sagert et al (2009) constructed a quark matter EOS ($B^{1/4}$=165 MeV). Transition to QM causes second shock that drives explosion.

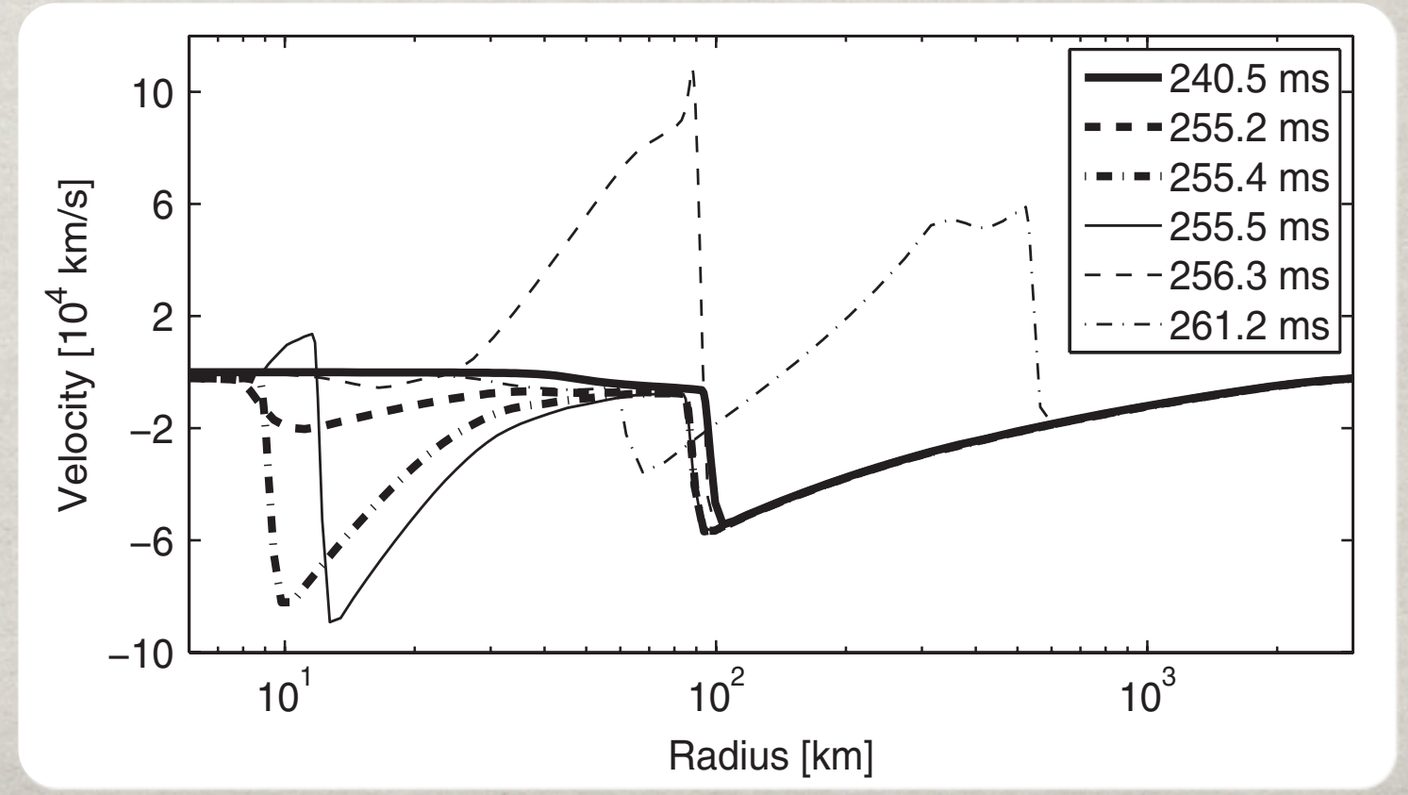

Nuclear EOS & Neutron Stars

With Neutron Stars, astrophysical observations inform us directly about microscopic physics.

Neutron Stars in binary systems allow measurement of the NS mass.

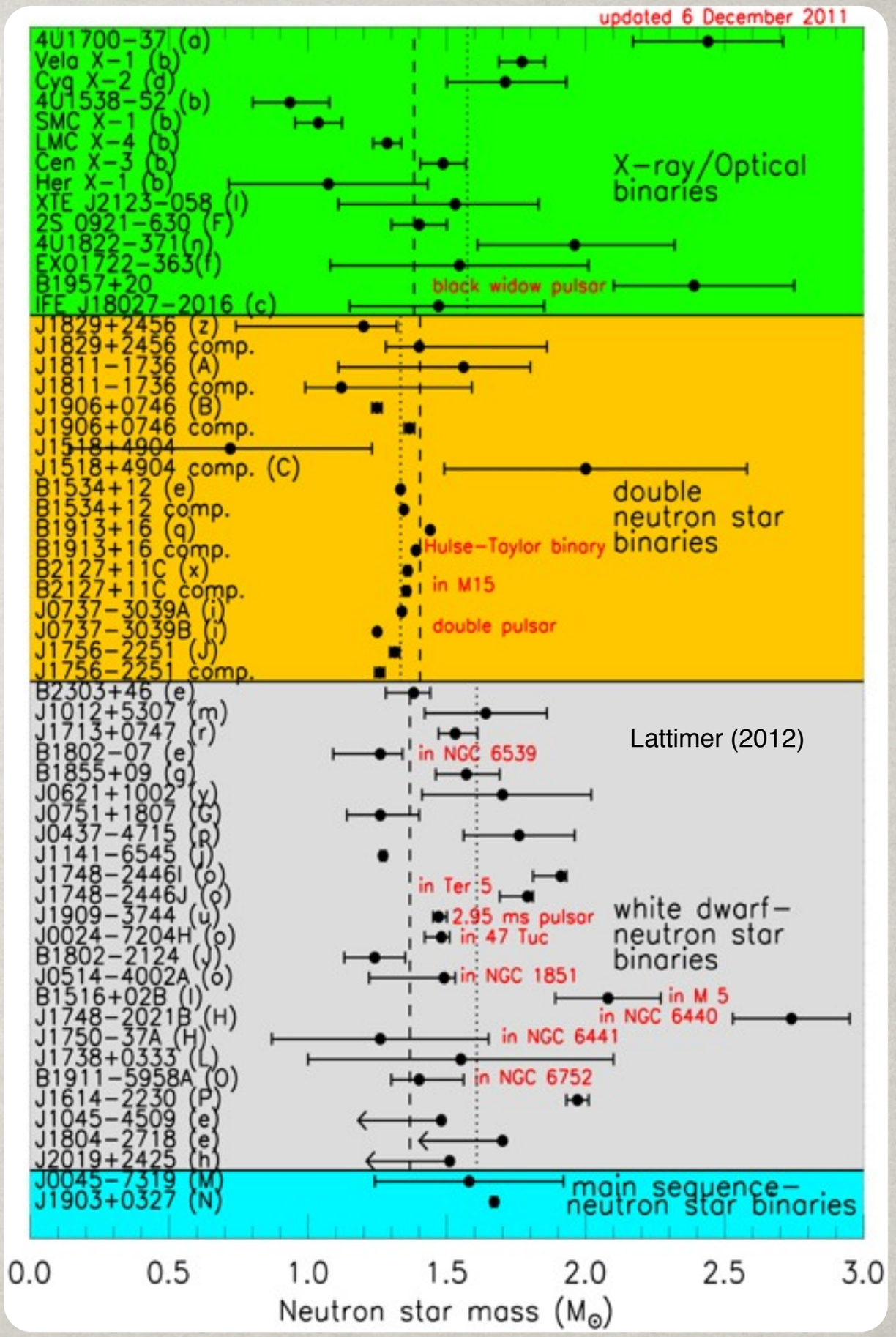

Nuclear EOS & Neutron Stars

With Neutron Stars, astrophysical observations inform us directly about microscopic physics.

Neutron Stars in binary systems allow measurement of the NS mass.

If radius can also be determined (by thermal emission, redshift, accretion rate, …), then this data can constrain the mass-radius relation for the EOS.

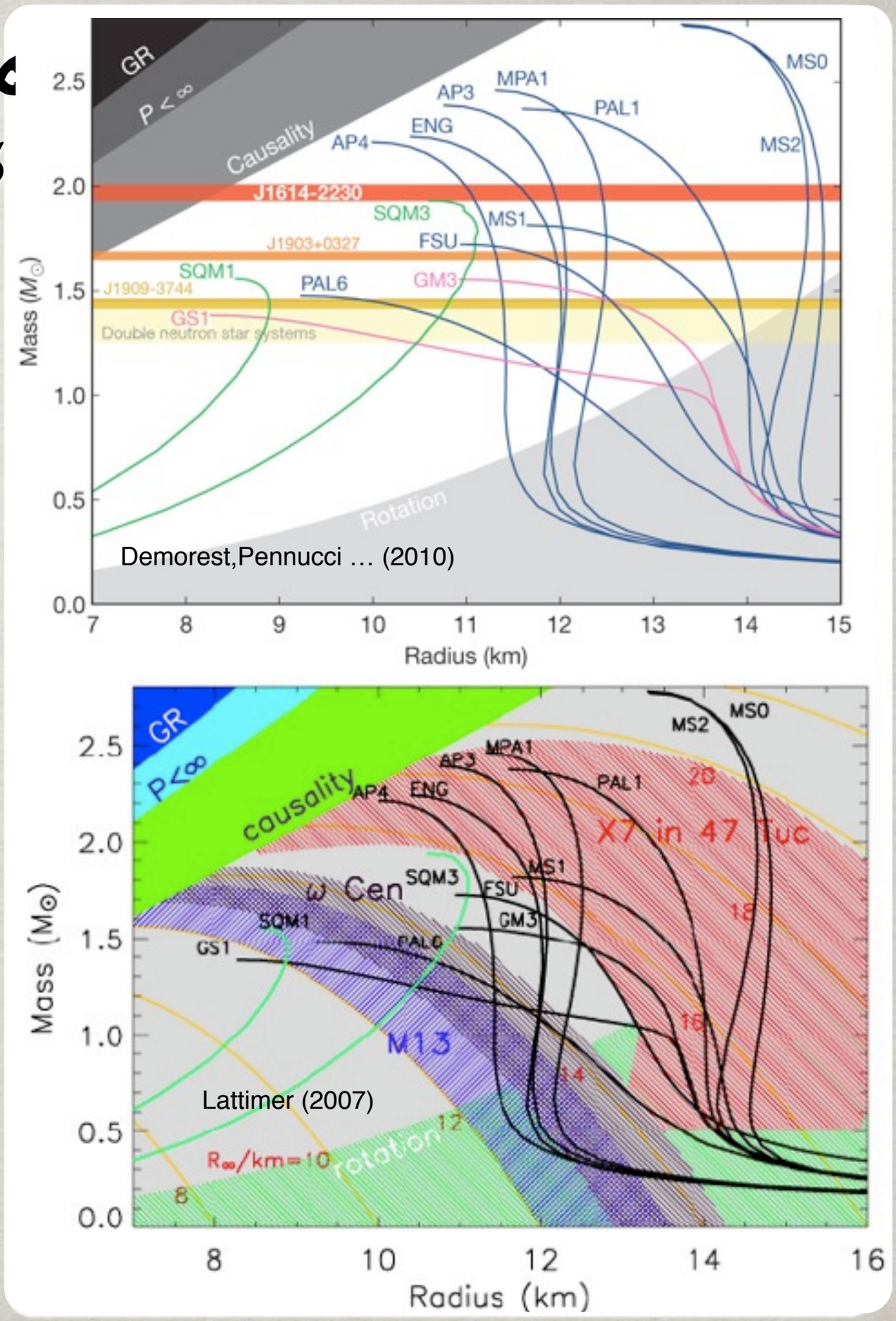

Summary

Core-Collapse Supernovae are the inevitable result of massive stellar evolution.

Self-consistent models confirm successful prolate explosions across a range of progenitors from 12-25 $M_\odot$ driven by neutrino heating and SASI. These simulations point to a successful neutrino-reheating mechanism, with the explosion delayed by 300 ms or more after bounce, at least in 2D.

Self-consistent 3D simulations, while very expensive, are possible. They are critical to teach us the value of our 2D simulations.

Nuclear physics the CCSN problem enters through nuclear matter and weak nuclear reactions.